Title
Planning and Design of Desalination Plants Effluent Systems

Author
Maalouf, Sami

Publication Date
2014

Peer reviewed|Thesis/dissertation

UNIVERSITY OF CALIFORNIA

Los Angeles

Planning and Design of Desalination Plants Effluent Systems

A dissertation submitted in partial satisfaction of the

requirements for the degree Doctor of Philosophy

in Civil Engineering

by

Sami Maalouf

2014

ABSTRACT OF THE DISSERTATION

Planning and Design of Desalination Plants Effluent Systems

By

Sami Maalouf

Doctor of Philosophy in Civil Engineering

University of California, Los Angeles, 2014

Professor William W-G. Yeh, Chair

Increasing demand for water in urban areas and agricultural zones in arid and semi-arid coastal regions has urged planners and regulators to look for alternative renewable water sources. Seawater reverse osmosis desalination (SWRO) plants have become an essential supply source for the production of freshwater in such regions. However, the disposal of hypersaline wastes from these plants in many of these regions has not been fully and properly addressed. This study aims to develop and present a strategy for the analysis and design of an optimal disposal system of wastes generated by SWRO desalination plants.

After current disposal options were evaluated, the use of multiport marine outfalls is recommended as an effective disposal system. Marine outfalls are a reliable means for

conveying wastes from process plants, to include wastewater treatment and power plants, into the coastal waters. Their proper use, however, in conjunction with SWRO desalination plants is still in its beginning stage.

A simulation-optimization approach is proposed to design a system for safe disposal of brine wastes. This disposal system is comprised of a marine outfall that is equipped with a multiport diffuser structure. A hydrodynamic model (CORMIX) is used to assess the initial dilution of hypersaline effluent discharged into coastal waters. A regression model is developed to relate the input and output parameters of the simulation model. This regression model replaces the simulation model. A mixed-integer linear programming (MILP) optimization model is then formulated to determine the design of the multiport marine outfall. The design parameters are the length, diameter and number of ports of the disposal system. Given the uncertainty of some parameter, such as current speed, wind speed and ambient temperature, a chance-constrained programming model is used to properly incorporate these stochastic parameters into the model. This simulation-optimization framework provides planners with effective tools that preserve a healthy coastal environment, meet environmental permitting requirements and restrictions, while achieving cost savings and adequate hydrodynamic performance. A case study demonstrates the applicability of the proposed methodology.

The dissertation of Sami Maalouf is approved.

Steven A. Margulis

Michael K. Stenstrom

Diego Rosso

Sami W. Asmar

William W-G. Yeh, Committee Chair

University of California, Los Angeles

2014

It rains, drop by drop
and the melted snow leaves the mountaintop
the mountains embrace the wandering fog
…but later springs bleed
water with no color
and then water leaves the streams
to embrace the tributaries
and join the river.

In poetry, water leaves the river
to embrace the tributaries
and later hide
inside the springs
but then, onto surfaces,
the springs bleed water in different colors.

–Anonymous

TABLE OF CONTENTS

LIST OF FIGURES

LIST OF TABLES

ACKNOWLEDGMENTS

As my long and meandering journey at UCLA approaches completion, I reminisce about my time at this fine university, and realize that I encountered so many special people who have enriched my personal and academic life. For this, I am forever grateful.

I am indebted to my advisor and mentor, Professor William W-G. Yeh, who has guided me throughout this project, strengthened my research skills and introduced me to the fascinating world of water systems optimization. He taught me how to ask and to answer questions adequately and was very patient for results to appear. Due to his wisdom, generosity, creativity, elegance and unparalleled kindness, my overall technical and life skills have been enhanced.

I would like to thank the other members of my doctoral committee, Sami W. Asmar, Professors Steven A. Margulis, Diego Rosso and Michael K. Stenstrom for their presence, pedagogy, valuable insight and support. I am grateful to Professor Margulis who provided me with a teaching assistantship at the early stages of my graduate studies and strengthened my understanding of hydrology and hydrometeorology. Special thanks to Sami W. Asmar for our friendship and collaboration on several projects over the last decade. His generosity and passion for science has allowed me to broaden my horizons, enabling me to work with his group at the Jet Propulsion Laboratory, Pasadena. In addition, because of his creativity and support of the arts, I was given the opportunity to participate in his music group and to share poetry at different venues in Southern California. I also extend my gratitude to Professor Diego Rosso. Our friendship and

academic collaboration has developed ever-since we started working on this research, under Professor Yeh's supervision. Professor Rosso's creativity and diverse research interests made complex topics approachable.

I would also like to extend my appreciation to all the other professors I had at UCLA– Professors Terri S. Hogue, Jennifer A. Jay, Donald R. Kendall, Keith D. Stolzenbach and Ne-Zheng Sun, for enriching my engineering knowledge and teaching me wonderful lessons about water and the environment.

I wish to acknowledge all current and former staff at the Civil and Environmental Engineering Department–especially, Maida Bassili, who kept reminding me that tenacity and perseverance will ultimately pay off. I am also thankful for my co-workers and office mates, both within and outside the university, for all that was learned and shared– particularly with Scott Boyce and Wei-Chen Cheng at UCLA, and Julio C. Herrera at MI Design, Inc.. My appreciation also goes to current and former Civil and Environmental Engineering students and visiting scholars at UCLA–Yu-Wen Chen, Barton Forman, Manuela Girotto, Ieda Hidalgo, Keith Musselman, Mahdi Navari, Adam J. Siade, Zachary P. Stanko, Tim Ushijima, Che-Chuan Wu, Bin Xu and Renato Zambon.

This research could not have been possible without the relentless encouragement and support from the following individuals and institutions: Professor Young C. Kim of CSULA who introduced me to coastal engineering, expanded my understanding of fluid mechanics and opened many doors for me to pursue academic research, Professor Nazaret Dermendjian of CSUN who welcomed me more than three years ago as an

educator and friend, and supported me enthusiastically and unconditionally in my pursuits. I am also grateful to Professor Donald G. Browne and the UCLA School of Engineering and Applied Science for providing me with a teaching assistantship via the engineering ethics program. I extend my gratitude to Robert L. Doneker of Mixzon, Inc. who provided me with access to the CORMIX model and offered valuable insight into the simulation and research processes. I wish to thank Professor Abbas Daneshvari, an art historian, philosopher and friend, who constantly reminded me to work diligently and pursue my endeavors. I also wish to thank Professor A.J. Racy of UCLA who generously welcomed me several years ago as participant at his musical ensemble which has enhanced my life, both musically and spiritually. His kind presence and wonderful musical compositions have been comforting forces throughout my UCLA journey. Special thanks to Antoine I. Harb for his friendship, support and encouragement, and for introducing me to Professor Racy's musical ensemble. I also thank Professor Adnan Darwiche of UCLA for his positive encouragement and for gifting me with his scientific and artistic knowledge.

My deep gratitude goes to my family. I thank my dear brother Omar and his family, and my sister Lamia and her family. I also thank my nephew Ghassan (Jason) who has always been a source of strength, intelligence and unconditional love. I give my deep appreciation to my youngest sister Genane who has shown a remarkable enthusiasm about this project and has always been a source of unwavering love and support. Last but not least, I thank my father Ghassan and my mother Leila for their moral support, boundless love and, above all, for teaching me many lessons in love and kindness.

VITA

1968	Born, Zahlé, Lebanon
1990	B.S., Civil Engineering California State University, Los Angeles
1990-1992	Civil Engineering Associate J.M. Montgomery Consulting Engineers, Inc. Pasadena, California
1992	M.S., Civil Engineering California State University, Los Angeles
1992-1995	Civil Engineering Associate City of Los Angeles, Department of Public Works
1995	Civil Engineer United Nations Development Programme (UNDP) Baalbek, Lebanon
1995-2000	Civil Engineering Associate City of Los Angeles, Department of Public Works
1997-2010	Lecturer (Part-time) Civil Engineering Department California State University, Los Angeles
2001-present	Civil Engineer MI Design, Inc. Encino, California
2008	Teaching Assistant (Hydrology) Civil and Environmental Engineering Department University of California, Los Angeles
2010-2012	Teaching Assistant (Engineering Ethics) School of Engineering and Applied Science University of California, Los Angeles
2011-present	Lecturer (Part-time) Civil Engineering and Construction Management California State University, Northridge

PUBLICATIONS AND PRESENTATIONS

Maalouf, S. and Kim, Y.C. (1993) Field Examination of a Distribution System Water Quality Model. *Proceedings of the ASCE Hydraulic Conference and the International Convention of Hydrology*, San Francisco, California, USA.

Maalouf, S. and Kim, Y.C. (1997) Reliability of Algorithms of Water Quality Modelling in Hydraulic Networks. *Proceedings of the 27th Congress of the International Association of Hydraulic Research*, San Francisco, California, USA.

Maalouf, S. and Kim, Y.C. (1997) Enhancement of Irrigation Systems in Developing Countries. A "Holistic" Approach. *Proceedings of the 27th Congress of the International Association of Hydraulic Research*, San Francisco, California, USA.

Maalouf, S. and Kim, Y.C. (2001) Evaluation of the Reliability of an Existing Coastal Structure. *Poster Presentation*. *Proceedings of the 29th Congress of the International Association of Hydraulic Research*, Beijing, China.

Maalouf, S. and Yeh, W.W-G. (2011) Planning and Design of Seawater Reverse Osmosis Desalination Plants Marine Outfalls. *Poster Presentation*. American Geophysical Union (AGU) Fall Meeting, San Francisco, California, USA.

Maalouf, S. and Yeh, W.W-G. (2012) Optimal Planning and Design of Seawater RO Brine Outfalls under Environmental Uncertainty. *Poster Presentation*. American Geophysical Union (AGU) Fall Meeting, San Francisco, California, USA.

Maalouf, S., Rosso, D. and Yeh, W.W-G. (2014) Optimal Planning and Design of Seawater RO Brine Outfalls under Environmental Uncertainty. *Desalination*, 333 134-145.

1. INTRODUCTION

As the world's population has drastically grown throughout the 20th century and into the current decades, existing renewable water resources are jeopardized by the rising demand for potable water. This is especially true in regions whose climates are characterized as arid and semi-arid, such as California (Green, 2007) as well as other regions (e.g., Australia, the Mediterranean Basin, Persian Gulf Countries, etc.). In addition, with rapid expansion of industries and urban centers around the globe, compounded by more frequent droughts caused by climate change, freshwater has become increasingly scarce.

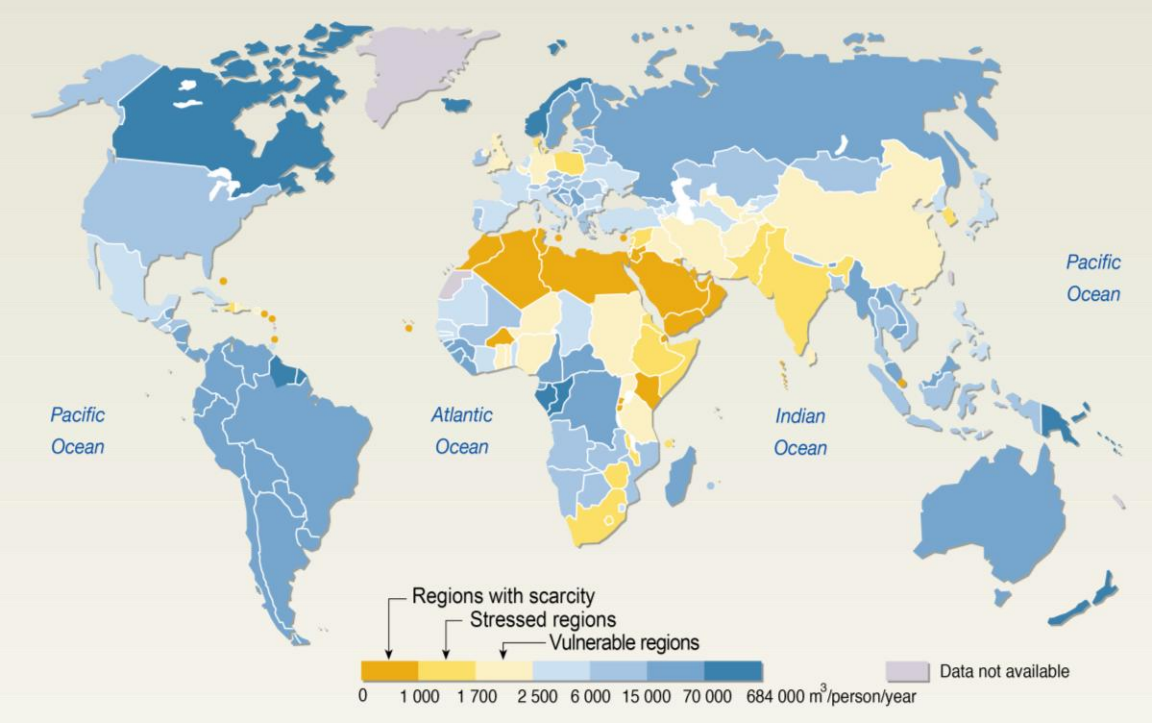

Figure 1.1. Freshwater availability in m^3 per capita per year, from data by the Food and Agriculture Organization and the United Nations Environment Programme (modified from Rekacewicz, 2008; grida.no/graphicslib/).

However, since the majority of the world's population (approximately 70%) lives within a distance of about 70 km from coastlines (El-Dessouky and Ettouney, 2002), and given the abundance of seawater (approximately 70% of the earth's surface), seawater has begun to be considered a viable source in the water supply portfolios in many of these aforementioned regions.

Seawater contains high levels of total dissolved solids (TDS). These constituents have concentrations that range between 7,000 and 50,000 mg/L (or parts per million), with sodium and chloride accounting for approximately 86% of these constituents (El-Dessouky and Ettouney, 2002; World Bank, 2004). Due to such high levels, desalting of seawater is necessary so that safe levels of drinking water are attainable. The World Health Organization, for example, states that TDS levels between 300 and 600 mg/L are considered good (World Health Organization, 2003). In addition, the US Environmental Protection Agency (USEPA) states that a TDS of 500 mg/L is a recommended safe level for potable drinking water (water.epa.gov/drink/contaminants/).

Thus, to transform seawater into potable water, TDS levels have to be reduced by orders of magnitude. This can be accomplished using desalting technologies that have traditionally included multi-stage flash (MSF) distillation, multi-effect distillation (MED), and seawater reverse osmosis (SWRO) (Bleninger and Jirka, 2010). Recent advances in SWRO membrane desalination, such as the development of pressure recovery units, have enhanced the distribution of this technology worldwide (Voutchkov, 2011). These advances, illustrated in Figure 1.2, enable SWRO desalination plants to

produce potable water more economically than thermal desalting methods (Zhu et al., 2008).

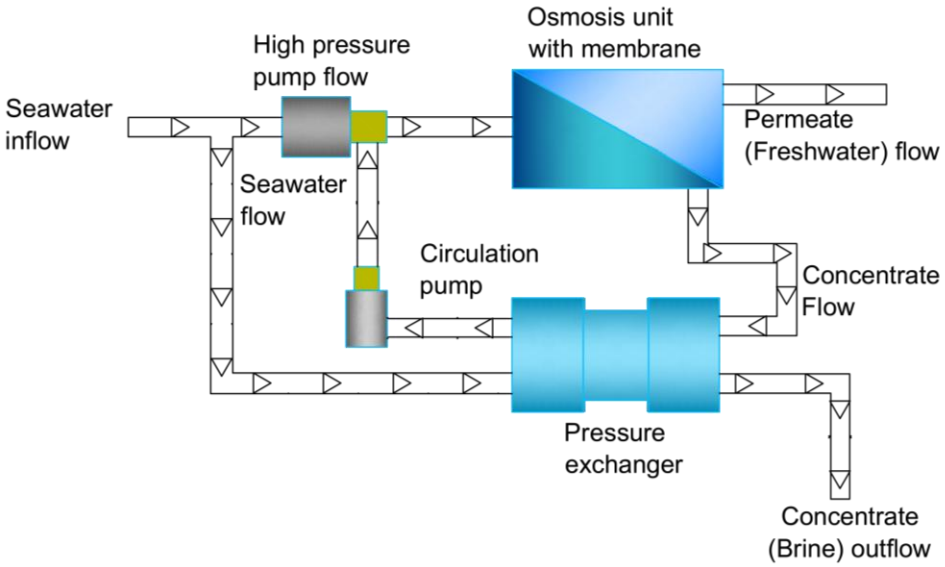

Figure 1.2. Schematic of a typical seawater reverse osmosis (SWRO) desalination plant.

The configuration illustrated in Figure 1.2, typical of current process designs, reduces TDS levels to produce potable freshwater (permeate). In the process, however, large volumes of hypersaline brine (concentrate) are also produced and subsequently redirected to coastal waters. This creates brine disposal challenges, due to elevated TDS concentration levels of about two times that of the receiving seawater body, and densities higher than the ambient seawater density (Jirka, 2008; Bleninger and Jirka, 2010). Due to rapid developments which increase threats to shorelines worldwide (Figure 1.3), it follows that SWRO technology may further degrade the coastal environment, if brine disposal challenges are not met.

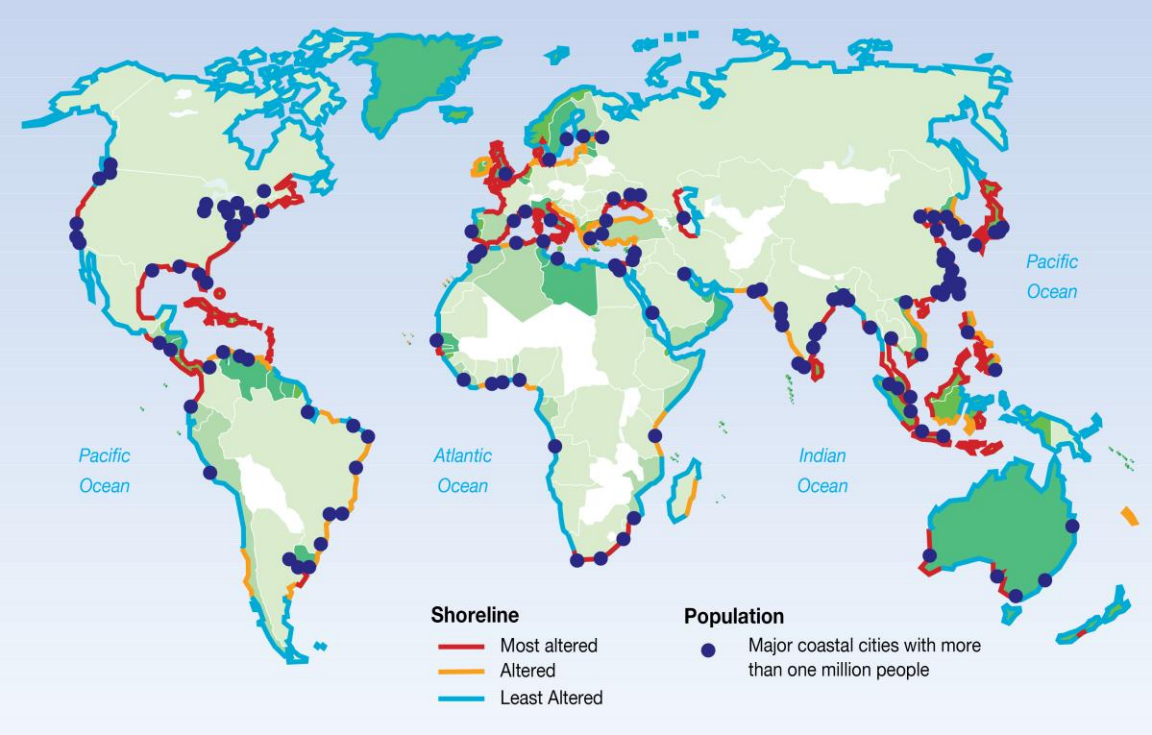

Figure 1.3. Shoreline degradation due to coastal population and developments, from data by the World Resources Institute and the United Nations Environment Programme (modified from Rekacewicz, 2002; grida.no/graphicslib/).

Some SWRO desalination plants use open channels to directly discharge brine loads into coastal waters (Bleninger and Jirka, 2010). This may adversely affect the marine environment (Lattemann and Höpner, 2008). Modern SWRO plants have been increasingly making use of more reliable means, such as marine outfalls, to discharge their brine wastes into coastal waters. Such usage can minimize the impacts on marine fauna and flora, if strict environmental regulations are adhered to.

Current environmental regulations, however, vary dramatically among nations and regions (Bleninger and Jirka, 2010; Jenkins et al., 2012). Furthermore, most of these

regulations were originally established as controls for municipal waste discharges that are usually positively buoyant (i.e., the effluent's density is less than the receiving seawater density) and may not be suitable for regulating discharges from SWRO desalination, which are negatively buoyant (i.e., the effluent's density is greater than the receiving ambient seawater density). Consequently, environmental regulatory requirements must be revisited frequently to address ongoing findings, and any variations between the planning stage and site-specific conditions after construction of SWRO plants and their outfalls.

Marine outfalls with multiport diffusers have proven to be quite efficient in maximizing initial dilution (Fischer et al., 1979; Bleninger and Jirka, 2010). Although costly to construct, they are considered to be among the most economical measures that guarantee proper disposal of waste, depending on several factors such as bathymetry and discharge capacity (Alameddine and El-Fadel, 2007; Grace, 2009; Bleninger and Jirka, 2010). An outfall system is generally designed using simulation models. These models represent the physical behavior of the outfall system by means of governing mathematical relationships (Fischer et al., 1979; Jirka, 2008; Bleninger and Jirka, 2010). In contrast, optimization models rarely have been used in outfall design. Such models are mathematical formulations that use one or more selected algorithms to minimize (or maximize) an objective function over the proper choice of decision variables, subject to a set of specified constraints. These models also have the ability to link with simulation models to ensure optimal designs (Chang et al., 2009).

The goal of this research is to develop a simulation-optimization model in order to find an optimal design for brine disposal, address dilution and regulatory constraints, and deliver the most cost-effective answer to the development of SWRO desalination multiport outfalls. A hydrodynamic simulation model (CORMIX) is used to assess the initial dilution of hypersaline effluent that is discharged into coastal waters. The response surface of CORMIX is approximated by a regression model that relates the initial dilution to various input parameters. This regression model replaces CORMIX in the mixed-integer linear programming (MILP) optimization model that is formulated to determine the design of the multiport marine outfall. The design parameters are the length, diameter and number of ports of the disposal system.

Given the uncertainty of some input variables, such as: current speed, wind speed, and ambient temperature, this study also demonstrates how these variables are incorporated into the development of the simulation-optimization framework. A chance-constrained programming model is used to properly incorporate these stochastic parameters into the model.

The simulation-optimization framework, depicted in this study, provides planners and design engineers with effective tools that meet environmental permitting requirements, while achieving adequate hydrodynamic performance and considerable cost savings. As a case example, the model is applied to a planned SWRO brine outfall along the California coastline.

2. DESALINATION – OVERVIEW AND BACKGROUND

Seawater Reverse Osmosis (SWRO) desalination has emerged as one of the technologies of choice to alleviate the problems of freshwater shortages. Since the 1990s, reverse osmosis (RO) has been adopted in most arid and semi-arid regions around the world. Frequent droughts, climate changes and seasonal shifts worldwide, in addition to population growth and depleted traditional water resources, are among a myriad of factors that have forced many coastal communities to seek reliable alternative sources of potable water. As shown in Table 2.1, the abundance of seawater (about 97% of the volume of water on earth) makes it an attractive supply source, at least for communities living in the vicinity of coastlines.

Table 2.1. Data on approximate volumes of global water resources (modified from Shiklomanov, 1993).

Water Source	Water Volume (km^3)	Freshwater (%)	Total Water (%)
Oceans, seas, bays	1.338×10^9	–	96.539
Ice caps, glaciers, permanent snow	2.406×10^7	68.700	1.7364
Groundwater, fresh	1.053×10^7	30.060	0.7598
Groundwater, saline	1.285×10^7	–	0.9272
Soil moisture	1.650×10^4	0.047	0.0012
Ground ice and permafrost	3.000×10^5	0.857	0.0216
Lakes, fresh	9.100×10^4	0.260	0.0066
Lakes, saline	8.540×10^4	–	0.0062
Atmospheric water	1.290×10^4	0.037	0.0009
Swamp water	1.147×10^4	0.030	0.0008
River flows	2.120×10^3	0.006	0.0002
Biological water	1.120×10^3	0.003	0.0001
Total freshwater	3.503×10^7	100	–
Total water reserves	1.386×10^9	–	100

Given the ubiquity of oceans and seas around the globe, and the industrial scale production of potable water via desalination, seawater has transformed into a reliable "source." Desalinated seawater seems to provide a draught-resistant and constant supply of high quality potable water (UNEP, 2008). It has proven to satisfy the shortages of water demands in some of these regions.

Aside from its rich content of nutrients, bacteria and viruses, seawater contains high concentration levels of total dissolved solids (TDS). A typical composition of seawater is shown in Table 2.2.

Table 2.2. Typical seawater constituents and their concentrations (Heitmann, 1990).

Constituent	Chemical Symbol	Concentration (mg/L)
Chloride	Cl^-	18,980
Sodium	Na^+	10,561
Magnesium	Mg^{2+}	1,272
Sulfate	SO_4^{2-}	2,649
Calcium	Ca^{2+}	400
Potassium	K^+	380
Bromide	Br^-	65
Bicarbonate	HCO_3^-	142
Other solids	–	34
Total Dissolved Solids (TDS)		34,483

While this is a typical concentration level in most oceans, TDS levels vary among different oceans and seas. Although seawater TDS concentration shown here totals 34,483 mg/L (or parts per million), these levels fluctuate considerably. This largely depends on the seasonal variations during the hydrologic cycle and geographical regions.

Seawater TDS concentrations range between 7,000 and 45,000 mg/L (and sometimes higher), as shown in Table 2.3.

Table 2.3. Seawater sources and their respective TDS concentrations (World Bank, 2004).

Source	Concentration (mg/L)
Baltic Sea	7,000
Oceans	35,000
Closed Seas	38,000
Red Sea	41,000
Arabian Gulf	45,000
Aral Sea	29,000

Water is classified in terms of different ranges of TDS concentration, as shown in Table 2.4 (World Bank, 2004). Additionally, potable water may be categorized with respect to its organoleptic properties (predominantly taste quality), in a manner shown in Table 2.5 (World Health Organization, 2003). Water with TDS of 500 mg/L is considered pure and is recommended as a safe level for drinking (USEPA).

Table 2.4. Water, classified in terms of TDS (World Bank, 2004).

Concentration (mg/L)	Classification
$TDS \leq 1{,}000$	Potable water
$1{,}000 \leq TDS \leq 5{,}000$	LSB water[†]
$5{,}000 \leq TDS \leq 15{,}000$	HSB water[‡]
$7{,}000 \leq TDS \leq 50{,}000$	Seawater

[†]LSB: Low Salinity Brackish; [‡]HSB: high Salinity Brackish.

In order to transform seawater into safe drinking water, TDS levels have to be reduced. This is achieved by using desalting technologies that have traditionally included

thermal processes such as multi-effect distillation (MED) and multi-stage flash (MSF) distillation.

Newer technologies include membrane and ion-exchange processes such as seawater reverse osmosis (SWRO) desalination, electrodialysis (ED) as well as electrodeionization (EDI) (Lattemann and Höpner, 2008a; Bleninger and Jirka, 2010; desalination.com). Some of these processes are also combined together in some instances, creating a hybrid setup to achieve optimal desalination and reduce energy consumption.

Table 2.5. Potable water organoleptic properties (World Health Organization, 2003).

Concentration (mg/L)	Classification
$TDS \leq 300$	Excellent
$300 \leq TDS \leq 600$	Good
$600 \leq TDS \leq 900$	Fair
$900 \leq TDS \leq 1{,}200$	Poor
$TDS > 1{,}200$	Unacceptable

2.1. Historical highlights

The quest for desalinating seawater (or brackish water) and transforming it to potable freshwater has challenged human beings for a long time. Early recorded accounts on desalination appear in Exodus 15:25, where Moses cast a tree into brackish (or bitter) waters. This turned the bitter water supply to a potable one and the people quenched their thirst (Einav, 2002; mechon-mamre.org/p/pt/pt0215.htm). Aside from mythic and religious accounts, a list of some milestones in the history and developments of

desalination processes is shown in Table 2.6 (UNESCO, 2008). In the US, statesman Thomas Jefferson published a report that addressed a distillation process in 1791. Figure 2.1 shows a copy of an excerpt of his document (memory.loc.gov/ammem; Jefferson, 1791 – republished in 1943 by the Journal of Chemical Education). Also in the US, UCLA researchers Sidney Loeb and Srinivasa Sourirajan reported on their development of the first asymmetric cellulose acetate membrane for desalination in 1960. This facilitated the birth of industrial scale SWRO desalination.

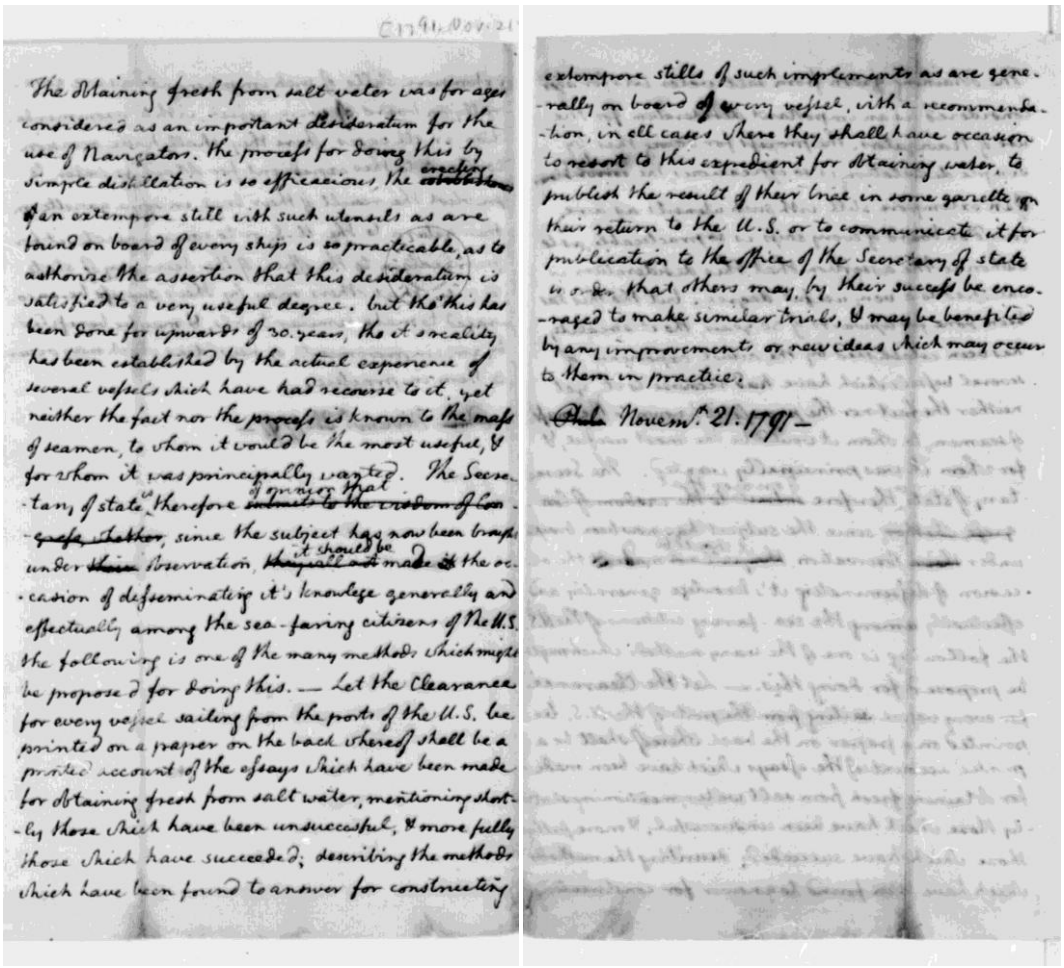

Figure 2.1. A copy of the original hand-written notes describing a desalination method by Thomas Jefferson, 1791 (Library of Congress archives).

Table 2.6. Brief desalination timeline showing some milestones leading to major advancements in various processes (modified from UNESCO, 2008).

Year	Event
320 BC	Aristotle writes about seawater distillation
70 AD	Pliny the Elder describes seawater distillation (condensation)
200 AD	Alexander of Aphrodisias describes seawater distillation
975 AD	Muwaffaq Harawī writes that distillation is a suitable method of seawater conversion to freshwater
1748	Nollet discovers the osmosis phenomenon in natural membranes
1772	James Cook begins successful use of seawater stills in his voyages
1791	Thomas Jefferson publishes "Report on the Method of Obtaining Fresh Water from Salt"
1828	Péclet discusses multi-effect evaporator
1840	Swiss firm Escher Wyss installs vapor compression distiller in British Columbia, Canada
1855	Fick creates the first synthetic cellulose nitrate membrane
1869	Schoenbein produces the first synthetic commercial polymer
1881	Seawater distiller is installed on Malta
1886	Yaryan introduces rising film vertical tube evaporators
1900	Addison Waterhouse receives US patent for multistage flash distillation process
1910	Frank Normandy publishes a book entitled "Sea Water Distillation"
1927	Sartorius Company makes membranes commercially available
1946	Kuwait Oil Company installs the country's first evaporator
1950	Hassler introduces the first concept of membrane desalination
1958	Reid and Breton show that cellulose acetate is an effective membrane material for water desalination
1960	Loeb and Sourirajan develop the first practical membranes for reverse osmosis (RO) water desalting process at UCLA
1960	Londsdale develops thin film composite type membranes
1963	Mahon developed the first capillary (Hollow Fibre) membranes
1965	The world's first commercial RO plant is built in Coalinga, California
1977	Cadotte patents thin film composite membrane

Desalination technologies grew rapidly in the 20th century as arid and semi-arid regions have sought solutions to potable water scarcity. As of 2011, more than 300

million people in 150 countries rely on desalination daily. There are 15,988 desalination plants worldwide (idadesal.org). These plants are responsible for generating approximately 66.5×10^6 m^3/day (about 17.60×10^3 MGD). Seawater is the most prevalent source of these daily volumes (Figure 2.2).

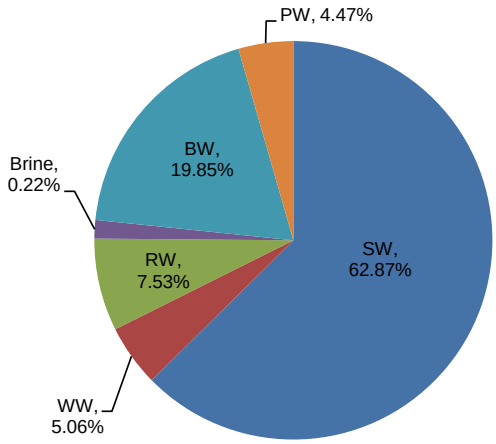

Figure 2.2. Desalination capacity worldwide (%). This breakdown is organized by feedwater category. BW: Brackish Water; PW: Pure Water; RW: River Water; SW: Seawater; WW: Wastewater (Modified from desaldata.com).

2.2. Brief description of some desalination technologies and processes

Several technologies are used to transform saline water into safe drinking water. The most prevalent technology is reverse osmosis (RO). It accounts for 60 percent of installed capacity. Multi-stage flash follows at 26 percent (Figure 2.3).

The technologies and processes shown in Figure 2.3 above are briefly described in the following subsections. Three membrane technologies will be described first (subsections *2.2.1 – 2.2.3*) and two thermal processes follow (subsections *2.2.4* and *2.2.5*).

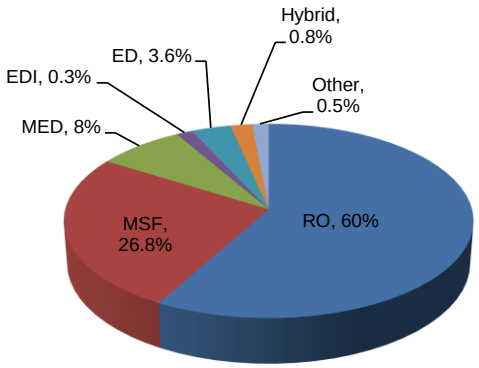

Figure 2.3. Desalination capacity worldwide (%). This breakdown is organized by the technology used. ED: electrodialysis; EDI: electrodeionization; MED: multi-effect distillation; MSF: multi-stage flash; RO: reverse osmosis (Modified from desaldata.com).

2.2.1. Reverse Osmosis

Reverse Osmosis (RO) is a membrane-based technology. Nowadays, it represents the fastest growing sector in desalination worldwide. RO desalination plants are able to produce potable water more economically than other desalting methods, due to recent advances in membrane technology. Brackish water or seawater flows through semi-permeable RO membranes under the influence of a pressure head that exceeds the osmotic pressure of the solution, as depicted in Figure 2.4.

Most RO membrane materials are aramids, polyamides, cellulose acetate and triacetate. They have either a spiral wound or hollow fiber configuration. The membranes are set in series within a pressure vessel in a typical RO process. Pressure vessels that house the RO membranes are usually set in parallel. Saline water (inflow) is pumped though these vessels under pressure. As freshwater permeates through these membranes,

the hypersaline brine solution is left behind (Heitmann, 1990; El-Dessouky and Ettouney, 2002). A typical modern SWRO process is shown in Figure 1.1 above.

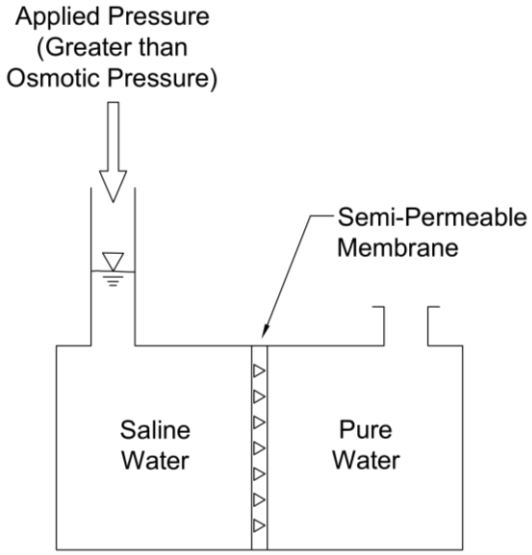

Figure 2.4. Principle of reverse osmosis (RO) (Modified from Heitmann, 1990).

Important design parameters in SWRO plants design and operation are the water recovery ratio, feed and osmotic pressures. The water recovery ratio R_w is defined as the ratio of produced freshwater (permeate) flow to the inflow. It is predicated on the number of pressure vessels and their respective membranes within the RO desalination plant. Most SWRO desalination plants are able to achieve a water recovery ratio of about 40% to 65% (Mauguin and Corsin, 2005; Voutchkov, 2011). The feed pressure is approximately two to three times greater than the osmotic pressure (lenntech.com).

2.2.2. Electrodialysis

Electrodialysis (ED) is another membrane-based technology with limited industrial

applications. The process is used to remove salt ions from water. Salt ions in this process are transported through permselective (semi-permeable) membranes, where the driving force is an electrical field that is applied across these membranes (Heitmann, 1990). A typical ED unit is comprised of a number of anion-selective and cation-selective membranes that are placed between the anode (positively charged electrode) and the cathode (negatively charged electrode). Thus, by placing multiple alternating membranes in a row and allowing positively or negatively charged ions to flow through, the salt ions can be separated from saline water. Conversely, particles that do not carry an electrical charge are not removed. (El-Dessouky and Ettouney, 2002).

2.2.3. Electrodeionization

Electrodeionization (EDI) is another membrane-based technology. It is usually used to remove residual constituents after an RO process takes place. The EDI process combines membrane separation technology with an ion-exchange medium to accomplish salt removal. A typical EDI unit has the basic components of a deionization (ion removal) system. In a manner similar to that of the ED process above, the deionization chamber consists of anion-selective and cation-selective ion exchange membranes. The spaces between these membranes are filled with electrically-active media (ion exchange resin). Unlike other ion exchange processes, where the resin is usually regenerated with acid and caustic chemicals, the electrical field in EDI "splits" water at the surface of the resin bed, producing hydrogen and hydroxide ions. These ions act as continuous regenerating agents of the ion exchange resin, without the use of chemicals. This process makes EDI more

reliable and far more economical than other ion exchange processes in terms of energy and operating costs (lenntech.com; watertechonline.com).

2.2.4. Multi-Effect Distillation

Multi-effect distillation (MED) is an old technology where the salt removal process is achieved by directing seawater to a series of chambers or effects. These effects operate at progressively lower temperatures and pressures, and vapor that is formed in one effect is used in the following effect. Initially, heat exchanger tubes are heated then cooled by spraying them with seawater.

As the flowing vapor within these tubes condense into pure water, the sprayed seawater outside the tubes begins to boil due to the absorbed heat. Vapor from the seawater is then introduced into the heat exchanger tubes in the next effect. Reusing vapor in MED reduces brine volumes and lowers the temperature as the process continues until the last effect (El-Dessouky and Ettouney, 2002; Bleninger and Jirka, 2010).

2.2.5. Multi-Stage Flash

Multi-stage flash distillation (MSF) is another thermal technology where seawater is heated up to vapor levels and directed to flow into a series of chambers (stages) of successively lower temperatures and pressures.

Seawater is heated as it flows through heat exchangers in the stages within the plant. The hot seawater is further heated by means of a heater that is referred to as brine heater.

The very hot liquid is now allowed to flow freely and flash (i.e., boil) in a series of stages. Pressure is reduced as liquid flows from one stage to another. The steam condenses and cools around the heat exchanger tubes. It also heats up the incoming seawater that flows towards the brine heater. As seawater becomes very hot, it is directed to a series of stages, as discussed above (El-Dessouky and Ettouney, 2002; Bleninger and Jirka, 2010).

2.3. Benefits and impacts of SWRO desalination plants

Compared to other desalting methods, SWRO desalination has gained popularity, because of its lower energy consumption (Jirka, 2008; Sobhani et al., 2012). Additionally, due to some attractive features that are mainly related to advancements in membrane technology, desalination is economically able to satisfy desired safe drinking water levels (Voutchkov, 2011).

Aside from their benefit as a reliable supply source of potable water, transforming an abundant supply of seawater to freshwater, SWRO desalination plants also discharge large volumes of high salinity concentrate or brine into the sea.

2.3.1. Brine volumes and concentration

High salinity brine volumes depend on the water recovery ratio R_w of the SWRO desalination plant that is defined as:

$$R_w = \frac{Q_p}{Q_i} = \frac{Q_p}{Q_p + Q_e} = 1 - \frac{Q_e}{Q_i} \tag{2.1}$$

where Q_p is defined as permeate (or produced freshwater due to the SWRO process, with $Q_p = Q_i - Q_e$). Q_i and Q_e are the influent (intake or feed) and effluent (concentrate) flow rates, respectively. The concentrate has salinity levels that are approximately double of that of ambient seawater. In addition, the concentrate contains products that include chemicals for biofouling control, antiscalants and corrosion inhibitors, among others. Some of these products are biodegradable, whereas others may be considered harmful to the marine environment (Lattemann and Höpner, 2008a, 2008b).

Brine must be discharged properly so that the ambient coastal waters' TDS concentration levels are maintained unaltered. Once R_w is determined using Equation (2.1), and assuming that the entire brine effluent (concentrate) is leaving the SWRO plant (100% rejection), we can compute the brine TDS levels as

$$C_e = C_b\left(\frac{1}{1-R_w}\right) \tag{2.2}$$

where C_e and C_b are the effluent and ambient (background) TDS concentrations, respectively. For example, if R_w is equal to 50%, the effluent TDS concentration is double the ambient concentration.

2.3.2. Seawater and SWRO brine densities

The seawater equation of state is expressed as (UNESCO, 2010):

$$\rho = \rho(\bar{S}, T, p) \tag{2.3}$$

where ρ is the density of saline water, $\bar{S}$ is salinity, T is temperature and p is pressure. Temperature is an important variable in determining density. However, temperature differences between SWRO effluent temperature and that of coastal waters are usually negligible. On the other hand, pressure effects may be eliminated in shallow coastal waters (Kämpf, 2009a), as SWRO desalination discharges mostly take place in the ocean's upper layer (depth of 0–50 m).

Unlike sea surface temperature or brine temperature that can be directly measured, salinity is not directly measured. The salinity of the medium in question has to be computed to determine ρ. Absolute salinity S_A is defined as the mass fraction of salt dissolved in seawater. It is defined as:

$$S_A = \frac{m_s}{m_w + m_s} \tag{2.4}$$

where m_s is the mass of salt and m_w is the mass of water (UNESCO, 2010). Ambient TDS concentration in grams per one kilogram (or parts per thousand) of seawater is equal to S_A.

Traditionally, salinity is defined as the total amount of solid materials in grams dissolved in one kilogram of sea water when all the carbonate has been converted to oxide, all organic matter completely oxidized and the bromine and iodine replaced by chlorine. Consequently, salinity of the ocean can be computed empirically as a function of chlorine as $S = 1.80655\, Cl^-$ (Stewart, 2008). Salinity is also computed in terms of conductivity and a modern measure to express it as a dimensionless parameter is called

Practical Salinity S_P. This is defined in terms of the Practical Salinity Scale of 1978 (UNESCO, 1983; Kämpf, 2009a, 2009b). Detailed discussion on such definitions is found elsewhere in published literature (UNESCO, 2010; Boerlage, 2011, 2012).

UNESCO (1983, 2010) offers algorithms that compute seawater and effluent densities that are between 2,000 mg/L and 42,000 mg/L (or 2 and 42 parts per thousand). For ranges where brine concentration is greater than 42,000 mg/L (or 42 parts per thousand), El-Dessouky and Ettouney (2002) provide methods to compute the effluent density. A seawater density calculator that uses these methods can be downloaded from: www.ifh.uni-karlsruhe.de/science/envflu/research/brinedis/ (Bleninger and Jirka, 2010). For example, if the ambient salinity $\overline{S}$ is equal to 35,000 mg/L (35 parts per thousand) and the ambient temperature is 25 °C, the ambient density ρ is equal to 1,023.03 kg/m^3. If the brine effluent TDS concentration is double the ambient concentration (i.e., if brine effluent $\overline{S}$ =70,000 mg/L) and given the brine temperature is the same as that of ambient seawater, brine density is equal to 1,049.56 kg/m^3.

2.4. Brine disposal, mixing zones, and simulation models

With brine TDS concentration levels approximately double of that of ambient seawater (as shown in the example of subsection *2.3.1* above), and with an associate brine density higher than ambient water density (as shown in the example of subsection *2.3.2* above), this negatively buoyant effluent rapidly sinks and spreads over the sea bed

(Figure 2.5). Subsequently, this may also lead to increased stratification effects that may in turn reduce vertical mixing. These effects may harm the benthic community adversely due to reductions in dissolved oxygen (DO) levels (Lattemann and Höpner, 2008a).

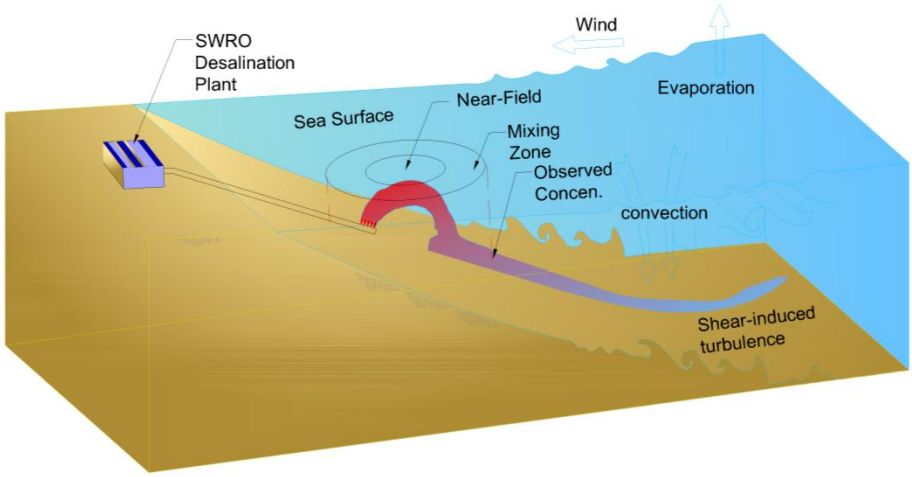

Figure 2.5. SWRO brine discharge and mixing characteristics. This configuration depicts a submerged dense effluent (concentrate) that is released to shallow coastal waters using a marine outfall with a multiport diffuser system. The concentrate rapidly sinks and spreads over the sea bed.

2.4.1. Brine disposal

Disposal of liquid brine waste into coastal waters usually is done by means of marine outfalls equipped with a single port or a multiport diffuser system. These outfalls are designed to maximize initial dilution so that environmental regulations, set by regulatory agencies, are met at the edge of a mixing zone (Fischer et al., 1979; Grace, 2009).

Figure 2.6 illustrates an example of a multiport outfall system. The system consists of the following main components: the onshore headworks (designated here as SWRO

Desalination Plant), a feeder pipe L_f and the diffuser section L_d.

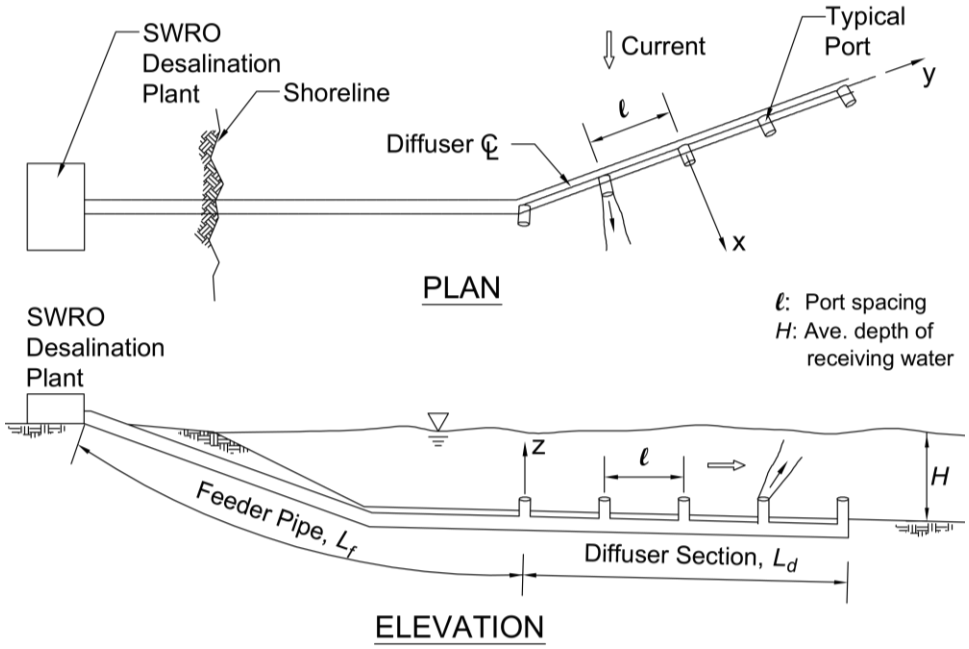

Figure 2.6. Schematic of a submerged multiport marine outfall (modified from Jirka et al., 1996; Bleninger, 2006).

The diffuser section is equipped with a number of ports that disperse brine discharge into coastal waters within the mixing zone. These ports are arranged either in a unidirectional, staged or alternating manner. Overall, marine outfalls vary considerably in terms of their construction material, installation techniques, pipeline and port diameters, as well as other design and construction related functions. The literature contains comprehensive reviews of design, construction costs and methods (Wallis, 1979; Wood et al., 1993; Grace, 2009). Online resources include mwwd.org, emisarios.unican.es, iwahq.org and www.ifh.uni-karlsruhe.de/science/envflu/research/ww-discharges/.

2.4.2. Mixing zones

The mixing zone (or zone of initial dilution) is defined as a limited 'sacrificial area or volume' within the coastal waters where the impacts to marine life are deemed minimal (Jirka et al., 2004). This negotiated area or control volume usually is limited to a region around the outfall where the initial dilution takes place. Figure 2.7 shows an example specified by the US Environmental Protection Agency (USEPA, 1991).

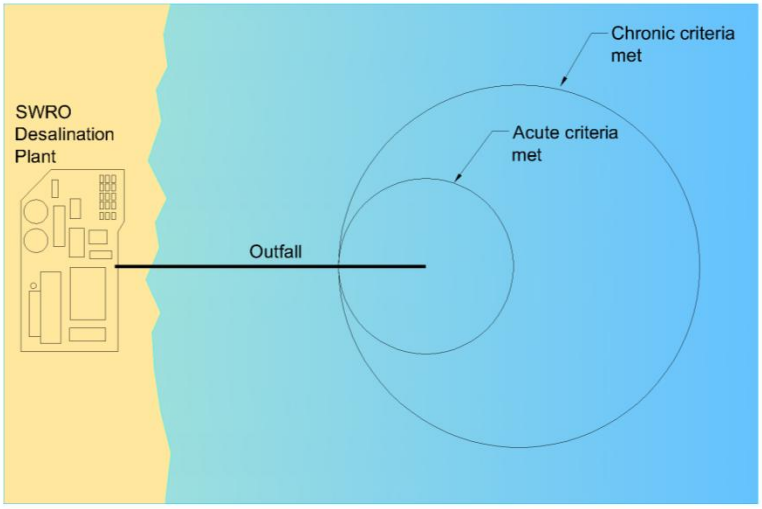

Figure 2.7. Example of a regulatory mixing zone, specified by the US Environmental Protection Agency (USEPA, 1991).

Given the conservative (non-reactive) nature of this hypersaline effluent, the mass of brine waste (i.e., constituent mass) within the mixing zone may be defined as:

$$m_c = \iiint_V C_e \, dV \tag{2.5}$$

where m_c is the constituent mass, C_e is the effluent TDS concentration and V is the volume of mixing zone.

According to USEPA regulations, the concentration within the outer zone shown in Figure 2.7 (designated here as chronic criteria met), is a multi-day average concentration of a pollutant in ambient water that should not be exceeded more than once every 3 years on the average (4 – 30 days). However, within the inner zone (designated here as acute criteria met), the one-hour average concentration in the ambient water should not exceed the criterion maximum concentration (regulatory required concentration) more than once every 3 years.

Mixing zones were originally enacted to delineate the boundaries of an allocated impact zone and initiate discussions that help planners and engineers on the one hand, and regulators on the other hand, in meeting environmental quality standards. Originally regulated to deal with positively buoyant wastewater releases into coastal waters, these administrative measures may be utilized for negatively buoyant brine discharge applications, but may need to be revisited or modified accordingly to reflect buoyancy variations (Jenkins, et al., 2012).

In the vicinity closest to the outfall's diffuser section within the mixing zone, the seawater equation of state shown above may be extended to include new brine volumes as follows:

$$\rho_{mz} = \rho(\bar{S}, T, p) + \left[m_c - \rho(\bar{S}, T, p) \times V \right] C_e \tag{2.6}$$

where ρ_{mz} is seawater density within the mixing zone closest to outfall's ports.

Local and national regulatory agencies with jurisdictions over the receiving coastal

area usually set the standards, procedures, and limitations of such zones. In the United States, for example, the USEPA has established national standards that focus on drifting organisms, migrating fish populations and routes to the growth and livelihood of such populations. Current national discharge regulations (in the US) are not specific to brine waste, but do limit chronic and acute toxicities at the mixing zone, as explained above (USEPA, 1991). Similarly, local and state regulations do not specifically address brine waste. Reports on operational SWRO desalination plants in California indicate that discharges from these plants are either released directly into coastal waters or blended with wastewater discharges prior to their release. Several additional SWRO desalination plants have been proposed in California due to rising water demand (Cooley et al., 2006; Green, 2007; Jenkins, et al., 2012). A variety of discharge methods, including direct surface discharge, use of evaporation ponds and salt-brine capillary crystallization, blending brine with other effluents, and subsurface disposal, have been proposed for these new SWRO desalination plants (Cooley et al., 2006; Sobhani et al., 2012). In addition, recent efforts to address brine discharge have led to the establishment of recommendations that may be adopted and later enforced as regulations (Jenkins, et al., 2012).

Other regulations also have been implemented, including those established by the European Union and other governing entities. The literature contains comprehensive reviews of such regulations in many countries where desalination is prevalent (Jirka et al., 2004; Bleninger and Jirka, 2010; Jenkins et al., 2012).

2.4.3. Simulation models

Unlike other treated municipal waste discharges that are usually positively buoyant, the mixing characteristics of brine disposal are directly affected by the physical nature of this dense conservative (non-reactive) effluent. In addition, blending with other discharges from nearby power plants, ambient density, temperature, and current speed of the receiving water body, as well as other factors, play an important role in the mixing process (Kikkert et al., 2007; Kämpf, 2009a; Bleninger and Jirka, 2010). While affecting the drifting organisms, migrating fish populations and routes to living and growing of such populations, brine discharges also impact the benthic flora within the mixing zone and the path of the hypersaline plume. As of 2012, many local and international efforts have been undertaken to include these impacts (Jenkins et al., 2012), clarify certain definitions and consider narratives that account for the negatively buoyant plumes—specifically from SWRO desalination plants—as they plunge into the bottom of a mixing zone (California EPA, 2011).

Jets and plumes have been studied for the last eighty years (Brown, 1935; List, 1982). Negatively buoyant jets and plumes characteristic of SWRO desalination brine discharges have been addressed thoroughly in the past four decades (Jirka, 2006). Early models and experiments included numerical simulations, design considerations (Zeitoun, et al., 1970, 1972) and disposal of brine into estuaries leading to coastal waters (Pincince and List, 1973). List (1982), Del Bene et al. (1994), Roberts et al. (1997), and Jirka (2004, 2006,

2008) provided elaborate reviews, developed models and conducted experiments that effectively address the behavior of dense and negatively buoyant discharges.

When used to release brine wastes into coastal waters, a marine outfall equipped with a multiport diffuser section dramatically reduces pollutant levels of concentrate discharges. These discharges follow mass and momentum conservation, as well as transport (advection-dispersion) principles, when their flow and mixing are assessed. The constituents in SWRO brine are, for the most part, the same as in seawater, and we may assume that these constituents are conservative (non-reactive) in nature. Consequently, their mass movements are induced by the effluent and coastal water velocities, as well as diffusion. Such movements are approximated and represented mathematically by simulation models that evaluate the fate and transport of waste discharges. These models also assess impacts on coastal water quality.

Numerous simulation models that address advection and diffusion of waste discharge into coastal waters have been developed (Palomar and Losada, 2010). Some of these models are referred to as mixing zone models, since they simulate mixing conditions and attempt to satisfy the often stringent regulations associated with the identification and enforcement of discharges into a mixing zone. Mixing zone simulations are performed using many methods, including empirical and analytical models, integral models, numerical models, physical models, random walk particle tracking (RWPT), and other models (Jirka, 2004, 2006; Palomar and Losada, 2010; Zhao et al., 2011). Overall, modeling of positively and negatively buoyant discharges has been employed effectively

to perform dilution and mixing studies (Bleninger and Jirka, 2010). Loya-Fernández et al. (2012) and Palomar et al. (2012) independently validated some of the mixing zone models by comparing measurements from SWRO discharges to predict results determined by some of these models.

The empirical, analytical, integral and numerical models are briefly described in the following subsections (*2.4.3.1 – 2.4.3.4*).

2.4.3.1. Empirical Models

Empirical models aim to establish relationships between the mixing zone, its size, dilution and other related parameters, on the one hand, and effluent and discharge parameters as they entrain the large body of receiving coastal waters, on the other hand. These models are also referred to as length-scale approaches. They are usually expressed in terms of simple equations and monograms, and they are useful tools to study the mixing behavior in the near-field primarily. Empirical models, coupled with laboratory observations, have been in use for more than 30 years (Fischer et al., 1979; Roberts et al., 1989; Jirka, 2008). They are relatively easy to implement, but are applicable to simple discharge scenarios. Their use is, therefore, limited (Stolzenbach, 2000; Zhao et al., 2011).

2.4.3.2. Analytical Models

Analytical models or "closed-form" solutions use many assumptions to simplify and later solve the rather complex governing hydrodynamic and water quality equations (McCutcheon, 1990; Smith et al., 1999; Purnama and Al-Barwani, 2005; Al-Barwani and

Purnama, 2008). Such assumptions limit the applications of these models to simple mixing cases (Martin and McCutcheon, 1998; Kämpf, 2009a). Analytical models may be also used to validate and check solutions that were determined utilizing other techniques (Riddle et al., 2001; Israelsson et al., 2006).

2.4.3.3. Integral Models

Basic mass and momentum conservation principles, and other physical laws, can be expressed by means of integral models. This is normally done through cross-sectional integration of volume momentum and buoyancy fluxes. Subject to initial conditions and some parameters that were determined by means of observation (i.e., empirically), integral models solve for a wide range of loading conditions, depending on the effluent properties and release configurations (Stolzenbach, 2000; Jirka, 2004, 2006).

2.4.3.4. Numerical Models

Numerical models employ numerical techniques such as finite difference methods (FDMs), finite element methods (FEMs), finite volume methods (FVMs), among others. Numerical models solve the equations of state that express the physical laws and include mixing parameters. Such models are often combined with other techniques and methods to produce a holistic approach that predicts the fate and transport of pollutants and assesses ocean hydrodynamics. Although these models are applicable to a wide range of mixing problems in a variety of dimensions, many limitations exist. These limitations include computational costs and other associated challenges (Zhao et al., 2011).

2.5. Simulation-optimization tools

Optimization tools have played an important role in the planning, design, operation, and performance of various processes in desalination plants. These tools have proven to be useful in improving efficiency, minimizing operation cost and increasing overall plant reliability (Abdul-Wahab and Abdo, 2007). However, the tools only have been applied to processes within plant boundaries, i.e., excluding the marine outfall and its surrounding mixing zone. Marcovecchio et al. (2005) developed an optimization model that considered a hybrid RO-MSF desalination method with an objective of determining the optimal process design and operating conditions for a given water production level. Abdul-Wahab and Abdo (2007) presented a model that helps in the troubleshooting of brine heater faults in MSF installations and enhancing their performance. Kim et al. (2009) provided a thorough review of available literature on the use of systems engineering in RO desalination plant design and operation. They also presented a mixed-integer non-linear programming (MINLP) model to minimize the total cost of a SWRO desalination plant design.

Most coastal waste disposal design endeavors have used hydrodynamic simulation models. Optimization models rarely have been employed to identify satisfactory outfall design layouts. Early efforts by Bonazountas et al. (1988) aimed to develop a multi-objective programming model that applied to three separate coastal wastewater treatment plants. Chang and Wang (1995) integrated a wastewater treatment plant and ocean outfall

subsystems into an optimization framework in Tainan County, South Taiwan, using Grey non-linear programming. In addition, Chang et al. (2009) presented a simulation-optimization approach to assess a cost-effective and reliable expansion strategy for a wastewater treatment plant in Kaohsiung, Taiwan. Alvarez-Vázquez et al. (2005, 2010) developed a general multi-objective optimal control system with applications to wastewater management. However, none of this work addressed the negatively buoyant flow characteristics of SWRO brine.

3. MODEL DEVELOPMENT

SWRO desalination discharges, as mentioned above, mostly take place in the ocean's upper layer (depth of 0–50 m). This layer is influenced by many random variables that in turn affect the mixing of these discharges with coastal waters and add to modeling complexity. These variables include currents, ambient temperature and wind variations (Sorensen, 1997; Blumberg and Georgas, 2008). Other bathymetric features, including bottom topography of the coastal ocean and its corresponding slope and friction, also play an important role in the mixing processes that take place between coastal waters and effluent discharges (Kämpf, 2009a; Bleninger and Jirka, 2010).

Atmospheric effects and wind are equally important features in generating coastal currents. Coriolis force contributes to these currents and wind drives these currents alongshore. Wind also creates downward spiral motion in shallow coastal waters (known as the Ekman spiral) as a consequence of the Coriolis effect. Coastal morphology, usually varying between one coastal area and another, impacts the speed of these currents. Thermohaline circulation, driven by density differences within the upper layer, generates currents of low velocity. Ambient high temperature may enhance the thermohaline circulation and may also increase the evaporation and salinity of coastal waters.

3.1. Governing equations

Effluent discharges into coastal waters follow mass and momentum conservation, as well as transport (advection-dispersion) principles when their flow and mixing are assessed. Some assumptions are made in this study, and are briefly described below.

3.1.1. General assumptions

This research deals with the discharge and mixing problem as a single-phase flow. Therefore, interfacial equilibrium is not considered. To simplify the modeling efforts, interactions with the air-water interface and exchanges between particles and seawater are ignored. All hydrodynamic regions of brine discharges within this study are concentrated in an open boundary system of ambient seawater. The effluent is characterized as a conservative (non-reactive) fluid. Although many reactive chemicals are included within the composition of SWRO discharges, these will be ignored as the main focus is the fate and transport of hypersaline brine and optimization of its conveying system. The brine effluent is also characterized as a continuously released incompressible Newtonian fluid from the SWRO desalination plant and its salinity and density are always higher than that of ambient seawater.

Within the outfall pipe, however, it is assumed that brine density is constant, given the system follows a turbulent regime. The flow is steady with a Reynolds number $\mathrm{Re} = \rho u D / \mu \geq 2300$, where u is the discharge velocity, D is the internal diameter of the pipe section and μ is the effluent's dynamic viscosity.

3.1.2. Mass continuity

Assuming that the control volume is infinitesimally small, the continuity equation (mass conservation) can be expressed as follows:

$$\frac{\partial \rho}{\partial t} + \nabla \cdot (\rho u) = 0 \tag{3.1}$$

where ρ is the mass density of fluid, t is the time, and ∇ is the gradient operator. Equation (3.1) is coordinate-free but can be transformed into a form that is specific to a coordinate system, such as a Cartesian, local cylindrical or spherical system (Ferziger and Perić, 2002).

3.1.3. Momentum conservation

The momentum (Navier-Stokes) equation can be written as:

$$\frac{\partial (\rho u_i)}{\partial t} + \frac{\partial (\rho u_j u_i)}{\partial x_j} + \rho 2\Omega u_i = -\frac{\partial p}{\partial x_i} - \rho g + \mu \frac{\partial^2 u_i}{\partial x_j^{\,2}} + F_{i,e} \tag{3.2}$$

in which u_i and u_j (i, j=1,2,3) are the Cartesian components of the velocity vector u, Ω is the earth rotation vector, p is the pressure, x_i and x_j are the Cartesian coordinates, g is the gravitational acceleration, and $F_{i,e}$ is a representation of the external forces, respectively.

3.1.4. Transport (advection-dispersion) equation

Effluent flow and mixing follow general turbulent transport principles, coupled with

basic hydrodynamic mass and momentum conservation laws. The transport equation can be shown as (Zhao et al., 2011):

$$\frac{\partial C}{\partial t}+\nabla\cdot\left(u\,C\right)=\nabla\cdot\left(D_m\nabla C\right)+Q-R \tag{3.3}$$

where C is the concentration of constituent, D_m is the diffusivity tensor, and Q and R are the source and sink terms, respectively.

3.1.5. Negatively buoyant jet fluxes

A typical single round port discharging brine effluent is illustrated in Figure 3.1.

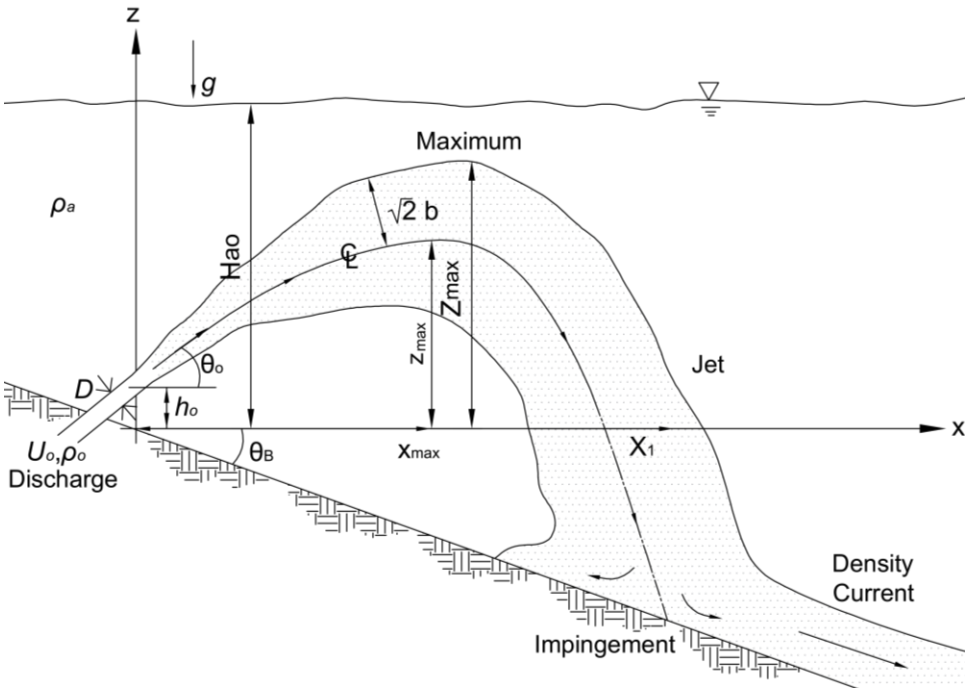

Figure 3.1. Schematic of a negatively buoyant jet discharging in the longitudinal and vertical directions (Jirka, 2008).

In this illustration, the receiving water body is assumed unstratified with a constant ambient density ρ_a. The port has a diameter D. Its height above the ocean bottom is h_o, and its inclination angle above the horizontal axis is θ_o. The discharged brine effluent forms a negatively buoyant jet in the ambient coastal waters. Originating from a single port, this jet has a discharge velocity U_o and density $\rho_o > \rho_a$. This gives the following fluxes:

$$Q_o = U_o A \tag{3.4}$$

$$Q_{co} = U_o C_e A \tag{3.5}$$

$$M_o = U_o Q_o \tag{3.6}$$

$$J_o = g'_o Q_o \tag{3.7}$$

in which Q_o is the volume (discharge) flux leaving a single round diffuser port orifice that has a cross-sectional area $A = \pi D^2/4$. Q_{co} is the mass flux and C_e is the effluent TDS concentration, defined earlier in Chapter 2. M_o and J_o are the momentum and buoyancy fluxes, respectively. $g'_o = g(\rho - \rho_o)/\rho$ is referred to as the buoyant acceleration at discharge. $g'_o < 0$ for negatively buoyant jets (Fischer et al., 1979; Jirka, 2004, 2008).

3.1.6. Initial and boundary conditions

Given the brine effluent is being discharged in an almost unbounded volume (Figure 2.5), where the boundary surface width is rather large, the initial condition may be defined as:

$$C(0,t_o) = C_o$$
$$u(0,t_o) = u_o \tag{3.8}$$
$$v(0,t_o) = v_o$$

where $t_o = 0$. C_o, u_o and v_o are the initial effluent concentration, longitudinal and vertical velocities, respectively.

The boundary condition can be expressed as:

$$x_j \to \infty : u \to 0,\ C \to 0$$
$$\left.\frac{\partial C}{\partial x_j}\right|_B = 0 \tag{3.9}$$

where $B = f(x,z)$ is a function representing the longitudinal and vertical boundary surfaces, as shown in Figure 3.1 above.

3.2. Mixing zone model structure

Hydrodynamic simulations in this study are performed using an expert system to ensure that the assumptions outlined previously are valid. A summary of input and output variables is shown in Figure 3.2.

The Cornell Mixing Zone Expert System (CORMIX) is used in this study. CORMIX is a USEPA-approved hydrodynamics model and decision support system that aids in assessing and simulating impacts of point source discharges on the coastal environment (Jirka, 2008). This expert system is comprised of three main subsystems: CORMIX1, to model submerged single-port discharges (Doneker and Jirka, 1991); CORMIX2, to model

submerged multiport discharges (Akar and Jirka, 1995); and CORMIX3, for buoyant surface discharges (Jirka, et al., 1996; Nash and Jirka, 1997). It is also able to analyze internal multiport diffuser hydrodynamic behavior (Bleninger, 2006).

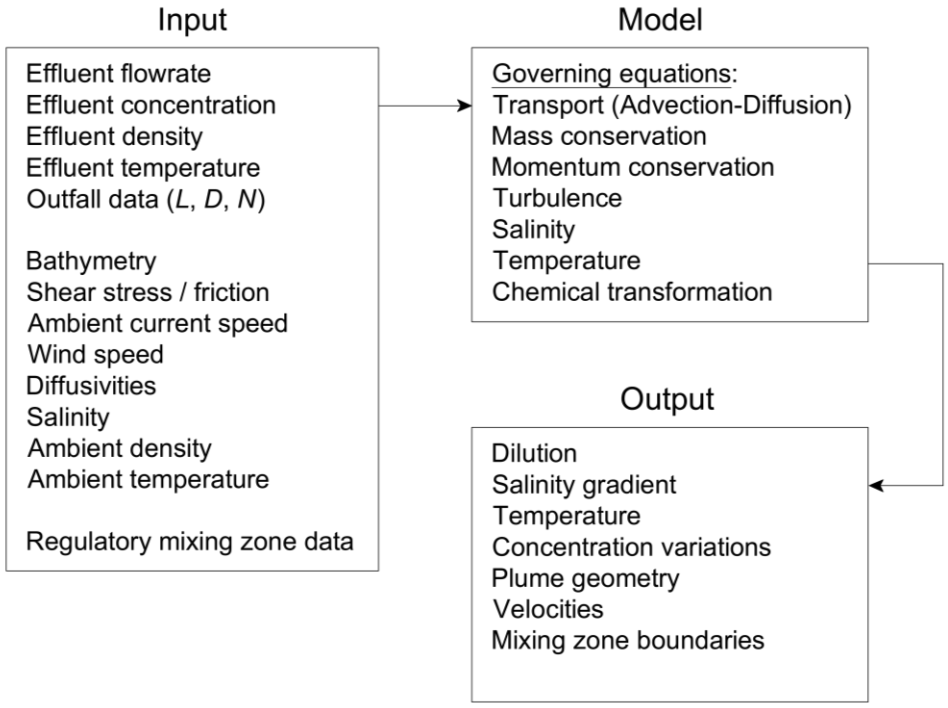

Figure 3.2. Modeling brine effluent discharges into coastal waters using an expert system.

Although CORMIX has been used predominantly for municipal wastewater applications in the past, it is also capable of performing SWRO brine flow simulations (Jirka, 2008). CORMIX uses integral equations in modeling turbulent jets (Jirka, 2004, 2006, 2008). This capability is directly applicable to the analysis of near-field mixing processes. As such, it has been recently used, calibrated and validated under many scenarios for a wide range of SWRO brine discharge cases (Loya-Fernández, et al., 2012; Palomar, et al., 2012).

At the outset, CORMIX classifies the possible flow regimes for waste discharges into several categories that are based on depth, stratification, crossflow velocity, and density of the receiving waters; the flow rate and density of the concentrate; and the type of diffusers and design patterns of their ports (nozzles). Flow classification in CORMIX determines plume boundary interaction and the physical processes that control initial mixing along the plume trajectory. Once flow has been classified, integral, length scale, and passive diffusion simulation modeling methods are used to predict the flow process in greater detail. Design features, such as the length and diameter of outfall, as well as the number of ports in the diffuser section, now can be modified to perform sensitivity analyses and verify that regulatory requirements are satisfied.

3.2.1. Effluent hydrodynamics and preliminary multiport diffuser design considerations

Brine that is released continuously from SWRO desalination plants is an incompressible Newtonian fluid that is, as noted earlier, of higher salinity (and thus higher density) than ambient seawater. A multiport diffuser section is an integral part of an optimal effluent discharge system. It must be properly designed and adequately equipped with ports (nozzles) as defined in the configuration shown in Figure 3.3. This may help avoid rapid plume sinking, improper mixing and stratification problems.

To avoid intrusion of ambient seawater into the diffuser section and ascertain that all ports operate properly, we set the port Densimetric Froude Number F_o to be at least equal to 10 (i.e., $F_o \geq 10$). It is defined as:

$$F_o = U_o \Big/ \sqrt{|g_o'| D} \tag{3.10}$$

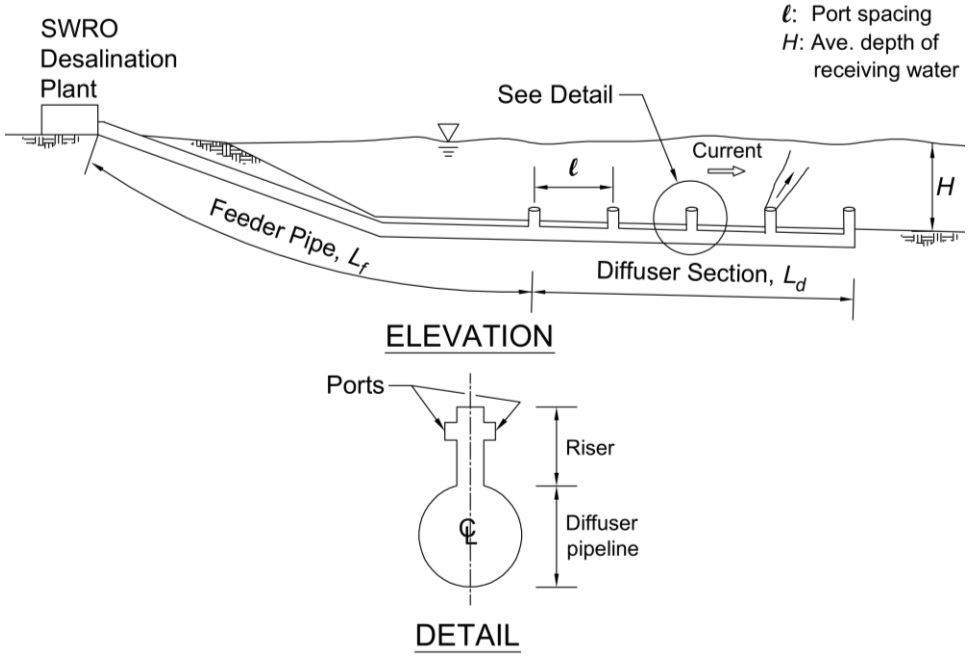

Figure 3.3. Schematic of a submerged multiport marine outfall, defining the riser and ports (nozzles) in the diffuser section (modified from Bleninger, 2006).

In a multiport diffuser environment, the discharged brine effluent forms a negatively buoyant plane (slot) jet in the ambient coastal waters. This slot has an alignment γ_o relative to the x-axis. The plane (slot) buoyant jet has an area $\bar{A} = BL_d$ and discharge velocity U_o. This gives the following fluxes:

$$\bar{Q}_o = \sum Q_{o,i} = \sum U_{o,i} A_i = U_o \bar{A} \tag{3.11}$$

$$\bar{Q}_{co} = \sum Q_{co,i} = \sum U_{o,i} C_{e,i} A_i = U_o C_e \bar{A} \tag{3.12}$$

$$\bar{M}_o = U_o^2 \bar{A} = U_o \bar{Q}_o \tag{3.13}$$

$$\bar{J}_o = U_o g_o' \bar{A} = g_o' \bar{Q}_o \tag{3.14}$$

where $\bar{Q}_o$ is the volume (discharge) flux leaving the diffuser system. $\bar{Q}_{co}$ is the mass flux. $\bar{M}_o$ and $\bar{J}_o$ are the momentum and buoyancy fluxes, respectively. These fluxes are forcing the entire plane buoyant jet (Jirka, 2006).

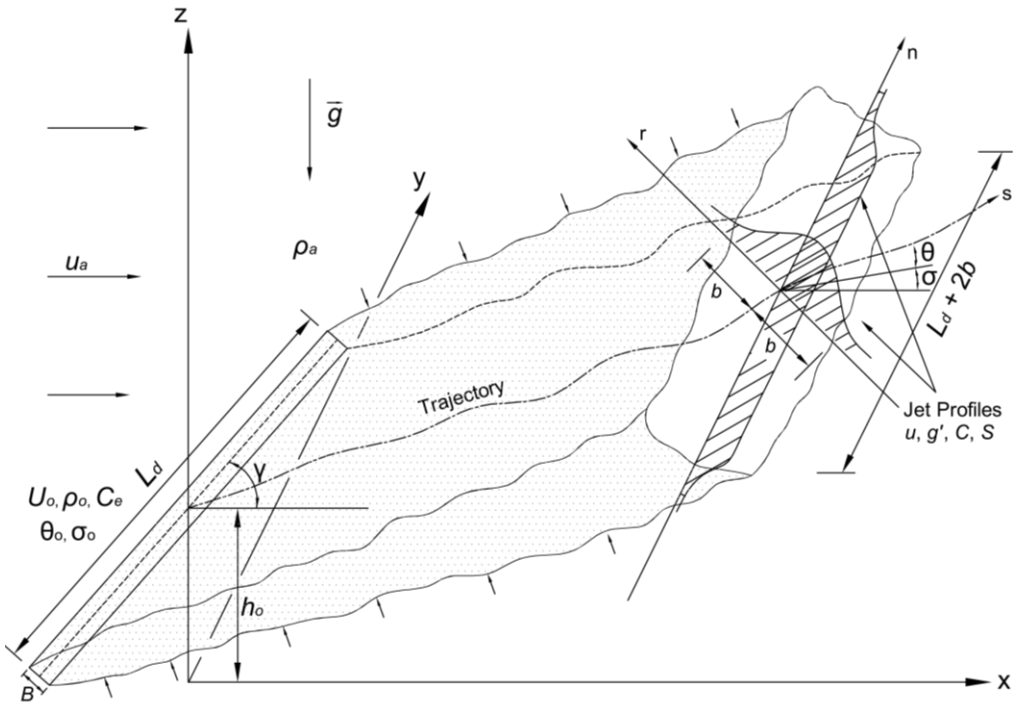

Figure 3.4. Schematic defining a plane buoyant jet with a global three-dimensional Cartesian coordinate system (x,y,z). The jet motion is represented by a local axisymmetric two-dimensional cylindrical system (r,s), although this motion exhibits a three-dimensional geometry (r,s,n) along the trajectory (modified from Jirka, 2006).

CORMIX determines the jet trajectory's spatial and temporal variations. The jet trajectory shown in Figure 3.4 is defined by a local two-dimensional cylindrical coordinate system. This system has an axial distance s and transverse distance r that is inclined with the local horizontal angle θ and a horizontal angle σ. The initial condition for the local system becomes: $s = 0 : C = C_o, u = u_o, v = v_o$. The boundary condition is:

$r \to \infty : u \to 0,\ C \to 0, \overline{u'v'} \to 0, \overline{c'v'} \to 0.$ CORMIX also solves for the local velocity u, density ρ, plume concentration C and dilution S differences along the trajectory. Detailed discussions on this topic, including complete jet properties and transition between jets and plumes, can be found elsewhere in published literature (Fischer et al., 1979; List, 1982; Akar and Jirka, 1995). Complete formulation of the integral model that solves for the jet and plume problems is also found in published literature (Jirka, 2004, 2006).

For the purpose of a preliminary design size, the required port diameter is computed by combining the brine flow rate Q_o (leaving a diffuser port), defined in Equation (3.4) above, with F_o. We have:

$$D = \left(\frac{Q_o (4/\pi)}{F_o \sqrt{|g'_o|}} \right)^{2/5} \tag{3.15}$$

3.2.2. Dilution

Negatively buoyant effluent releases (such as the concentrate from SWRO desalination plants) can achieve optimal initial dilution by means of multiport diffusers during the near-field mixing process (Fischer et al., 1979; Akar and Jirka, 1995). Dilution generally is defined as the ratio of total volume to the effluent's volume within the total volume. Within the mixing zone, dilution S begins when effluent discharges immediately leave the marine outfall and start mixing with coastal waters.

Because SWRO brine is essentially seawater with higher TDS concentration levels, dilution S is expressed as:

$$S = \frac{C_e - C_b}{C - C_b} \tag{3.16}$$

where C is the brine concentration after the initial dilution and mixing has taken place.

Rearranging the equation above yields:

$$C = \frac{C_e - C_b}{S} + C_b \tag{3.17}$$

Brine concentration C cannot exceed an upper concentration limit C_{rr}, which may be defined as the required regulatory concentration at the mixing zone's outer edge (see Figure 2.7, for an example). In other words:

$$C \le C_{rr} \tag{3.18}$$

Equation (3.16) therefore can be rearranged and written as:

$$S = \frac{C_e - C_b}{C - C_b} \ge \frac{C_e - C_b}{C_{rr} - C_b} \tag{3.19}$$

3.3. Optimization model

Optimization models, as noted in Chapter 2 above, have been used only rarely in conjunction with marine outfall designs. To our knowledge, these models never have been used in designing economically sound SWRO desalination effluent discharge systems, nor have they been employed to evaluate their performance. We present an

optimization approach with the goal of minimizing the construction cost of an outfall system, while also ensuring that all environmental requirements and regulations are met or exceeded. Although these regulations are not addressed explicitly in many countries where SWRO desalination is gaining popularity, we assume there are governmental or administrative measures that intend to prevent harmful impacts on the marine environment at the edge of a mixing zone.

Addressing other uncertain aspects in design and optimization, such as current speed, ambient temperature and wind speed, is also important.

The design of a marine outfall with a multiport diffuser structure that discharges brine wastes has an objective function of maximizing the initial dilution while meeting regulatory measures in a cost-effective manner. For this problem, the decision variables are the outfall's length, diameter and number of ports (nozzles) in the diffuser section. To meet the objective, our goal is to determine the shortest outfall length and smallest cross-sectional diameter, as well as the fewest number of deployed ports in the diffuser section. This will minimize cost.

The outfall's construction cost can be expressed in terms of the following linear function:

$$Z = \mathrm{w}_1 L + \mathrm{w}_2 D + \mathrm{w}_3 N \tag{3.20}$$

where Z is the total construction cost, L is the length of outfall pipe, and D and N are the internal port diameter and the corresponding number of ports in the diffuser section of

the outfall system, respectively. The terms w_1, w_2 and w_3 are linear cost coefficients, respectively.

For this study, it is assumed that the SWRO desalination plant has no brine storage capacity and is continuously discharging all the concentrate as soon as it is generated. Accordingly, the total brine flow rate Q_{tot} flowing out of the SWRO desalination plant and into the marine outfall is expressed as:

$$Q_{tot} = \sum_{i=1}^{n} Q_{o,i} \tag{3.21}$$

in which $Q_{o,i}$ is the flow leaving the ports and $i = 1, ..., n$ is the number of ports (nozzles).

In addition to the dilution constraints shown in Equations (3.18) and (3.19), the following constraints are imposed:

$$L_p^l \le L_p \le L_p^u, \quad \forall p \tag{3.22}$$

$$D = (D_1, D_2, \ldots, D_m) \in \mathbb{Z}^+ \tag{3.23}$$

$$N = (N_1, N_2, \ldots, N_n) \in \mathbb{Z}^+ \tag{3.24}$$

Where L_p is a decision variable representing the continuous feeder pipe section within the length of outfall. The variables L_p^l and L_p^u are the lower and upper bounds of L_p, respectively; $(D_1, D_2, \ldots, D_m)$ is a set of feasible port diameters that meets the hydrodynamic requirements outlined in Equation (3.15); $(N_1, N_2, \ldots, N_n)$ is a set of feasible number of ports in the diffuser section; m and n are the dimensions of D and N, respectively; and D and N are integers.

In Equation (3.19), the concentration C used to compute the dilution S is obtained from the hydrodynamic simulation model CORMIX. This causes great difficulty as C depends on the design parameters L, D and N as well as other uncertain input parameters. Below, we will explain how to resolve this difficulty. In addition, to ensure that the benthic communities are safe and meet environmental requirements, the outfall must maximize the dilution constraint. S is enhanced or deterred by many factors and parameters to include the diameter of outfall and diameters of ports in the diffuser section. These affect the effluent flow velocity. Other factors include the stochastic variables described above and the physical location where brine is being discharged. The dilution constraint, therefore, is a function of length and diameter of pipe and total discharge from all diffuser ports in this model, as well as variables such as current speed, ambient temperature and wind speed. It may be expressed as follows:

$$S = f(x, \xi) \tag{3.25}$$

where x is the decision variables vector and ξ is a vector representing stochastic variables. The constraint on S must always meet or exceed the lower level of regulatory dilution S_{rid}. In other words, $S \geq S_{rid}$. S_{rid} is defined as:

$$S_{rid} = \frac{C_e - C_b}{C_{rr} - C_b} \tag{3.26}$$

Chance-constrained programming (CCP) is used in this study to assess the risks associated with the presence of stochastic variables. CCP offers measures to help evaluate the reliability of the variables. This method initially was proposed by Charnes and Cooper (1959) and since has been used frequently in association with many water

resources and environmental management problems. The method is powerful, given an assumption that a stochastic constraint will hold for a prescribed reliability level.

3.3.1. Current speed

Ocean current speed is driven by wind, temperature variations and tides. Combined with the rotational effects discussed above (Coriolis force, Ekman spiral), along with the gravitational interactions between seawater masses and other bodies within our solar system (primarily the sun and moon), the ocean surface rises and falls. The effects of the moon are naturally greater than those of the sun, due to the moon's proximity to our planet (oceanservice.noaa.gov; Nash and Jirka, 1997).

The vertical rise and fall oscillation of ocean surface generates tidal currents that move in the horizontal direction. The rise and fall periods or cycles are characterized as diurnal (one high and one low tide per one lunar day), semidiurnal (two high and two low tides of approximately equal heights per one lunar day) and mixed semidiurnal (two high and two low tides of variable heights every lunar day). At full or new moon tidal current velocities are strong and are referred to as spring tidal currents. However, when the moon is at its first or third quarter phases, tidal currents are referred to as neap tidal currents and their velocities are usually weak (Nash and Jirka, 1997). Dilution processes of brine waste discharges, as they mix with coastal waters, may be affected by the variations in velocities of tidal currents.

The horizontal motion due to these oscillations is referred to as flood when it is directed towards the coastline and as ebb when this motion is directed away from land and towards the ocean. When tidal currents are alternating between ebb and flood and vice versa, slack water or slack tide occurs. Although ephemeral, this period of stagnation may range from a few seconds to several minutes, and may also cause a reduction in the dilution process of brine waste discharges as they mix with coastal waters.

Aside from alternating tidal currents, other factors such as freshwater discharges from rivers, stormwater runoff and other episodic plumes may also lengthen the period of slack tide. This may cause large pools of brine wastes to possibly take place near the ocean's bottom. Therefore, the choice of where to locate a proposed outfall system relies primarily on ambient current speed which ensures that proper mixing and dilution will take place.

Using CCP, the current speed constraint, can be expressed as:

$$\Pr\left\{\bar{w}_i \le \bar{w}_{max_i}\right\} \ge \alpha_i \tag{3.27}$$

where $\bar{w}_{max_i}$ is a reasonable upper bound for current speed that is guaranteed to be available 99% $\left(p = 0.99\right)$ of the time within a monthly current speed dataset i $(i = 1,...,12)$; and $\bar{w}_i$ is a reduced current speed, referred to here as the design current speed. It can be used to design the marine outfall system in a reliable manner, such that $\bar{w}_i < \bar{w}_{max_i}$. Finally, α_i is the monthly reliability level, where $0 \le \alpha_i \le 1$.

The deterministic equivalent to Equation (3.27) can be expressed as:

$$F_{\psi}\left(\frac{w_i - E(w_i)}{\left[Var(w_i)\right]^{0.5}}\right) \geq \alpha_i \tag{3.28}$$

where $F_{\psi}(\cdot)$ is the cumulative distribution function (cdf); $E(w_i)$ is the expected value; and $Var(w_i)$ is the variance, respectively, of a monthly current speed dataset. Let $\psi = (w_i - E(w_i))/\left[Var(w_i)\right]^{0.5}$ be a stochastic variable that can be used to deduce confidence intervals for a non-standardized stochastic variable (Kataria, et al., 2010). We now can write the above equation as:

$$F_{\psi}\left(\frac{w_i - E(w_i)}{\left[Var(w_i)\right]^{0.5}}\right) \leq 1-\alpha_i \tag{3.29}$$

Taking the inverse of Equation (3.29), we obtain:

$$w_i \leq E(w_i) + \left(F_{\psi}^{-1}(1-\alpha_i)\right)\left[Var(w_i)\right]^{0.5} \tag{3.30}$$

where $F_{\psi}^{-1}(1-\alpha_i)$ is the percent point function. Replacing w_i with $\bar{w}_i$ in the LHS of Equation (3.30), we can formulate $\bar{w}_i$ as:

$$\bar{w} = \bar{w}_{max} - \left(F_{\psi}^{-1}(\alpha)\right)\left[Var(w)\right]^{0.5} \tag{3.31}$$

To apply the findings above to an actual design problem, an example is proposed. An area representing a small coastal community in central California is chosen for this example. The ocean's upper layer current speed data, retrieved from online sources (National Data Buoy Center at www.ndbc.noaa.gov and the Central and Northern California Ocean Observing System at www.cencoos.org), reveal that within the same space or control volume (mixing zone) where similar continuous effluent discharges are

taking place, current speed exhibits high temporal variations (Figure 3.5 illustrates current speed data for the months of January and July).

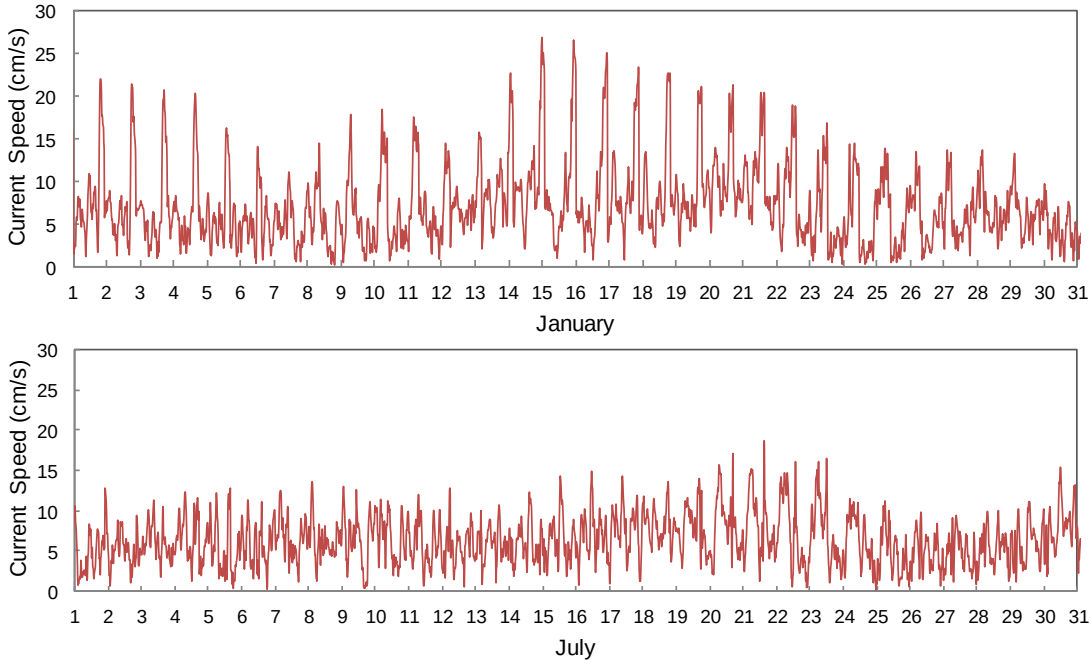

Figure 3.5. Current speed for the months of January and July, measured at locations in the vicinity of a study area representing a small coastal community in central California (data retrieved from www.ndbc.noaa.gov).

The dataset for monthly ocean current speed is summarized in Table 3.1. In addition, the data show that the underlying current speed distributions do not appear to be normal (Gaussian), but rather are positively skewed (i.e., skewed to the right). This asymmetric temporal behavior may be approximated statistically (Figure 3.6) as a two-parameter Weibull probability distribution function (pdf) (Chu, 2008).

Table 3.1. Current speed data based on historical records (open-source data from www.ndbc.noaa.gov/ and www.cencoos.org/).

Month	w_{min} (cm/s)	w_{max} (cm/s)	$E(w)$ (cm/s)	$Var(w)$ $(cm/s)^2$	$\left[Var(w)\right]^{0.5}$ (cm/s)
June	0.00	31.60	7.39	19.95	4.47
July	0.00	34.90	7.22	17.71	4.21
August	0.10	33.60	7.63	17.54	4.19
September	0.00	30.50	7.71	20.25	4.50
October	0.00	37.30	7.60	17.02	4.13
November	0.00	36.60	8.06	22.84	4.78
December	0.00	43.20	9.19	31.45	5.61
January	0.00	36.40	7.73	18.89	4.35
February	0.00	37.80	7.60	18.88	4.34
March	0.00	49.30	8.24	27.38	5.23
April	0.00	41.70	10.00	29.72	5.45
May	0.10	35.60	8.52	24.90	4.99

Given the current speed's daily and seasonal variations, the optimization problem is formulated to include the uncertainty caused by this random variable. Within the seawater body that is surrounding the outfall, a reasonable upper bound for current speed is established. This upper bound is guaranteed to be available 99% $(p = 0.99)$ of the time within a monthly current speed dataset, as shown above. The reduced monthly maximum current speed $\bar{w}_{max}$ is computed, considering normal and Weibull distributions.

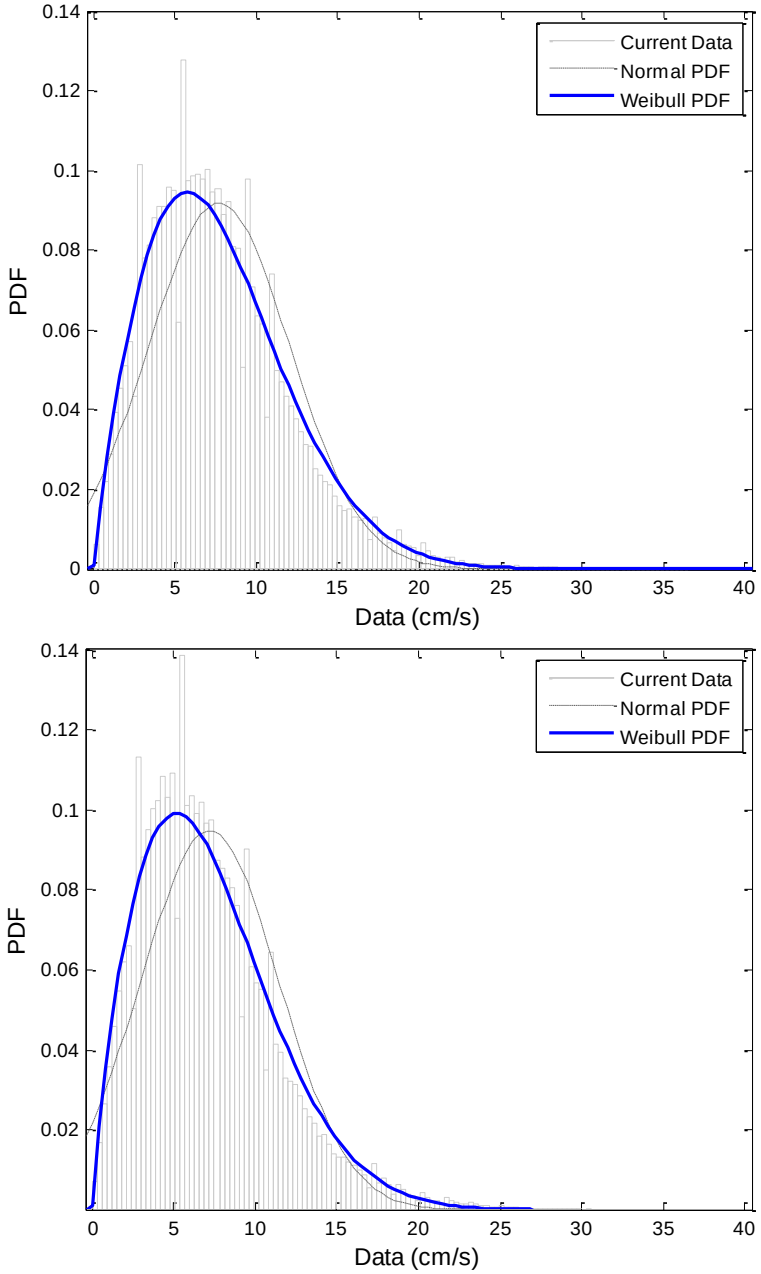

Figure 3.6. Comparisons among observational current speed data (histogram), normal and Weibull probability distribution functions for January and July.

The current speed is further reduced such that $\overline{w}_i < \overline{w}_{max_i}$, per Equation (3.31) above, considering the monthly reliability level α that varies from one month to another. Tables

3.2 and 3.3 show $\bar{w}_{max}$ and $\bar{w}_i$ results. These results will be discussed further in Chapter 4.

Table 3.2. Reduced maximum current speed, considering normal and Weibull distributions.

Month	w_{max} (cm/s)	Normal		Weibull	
		α_i	$\bar{w}_{max}$ (cm/s)	α_i	$\bar{w}_{max}$ (cm/s)
June	31.60	0.95	14.78	0.81	11.10
July	34.90	0.96	14.44	0.82	10.96
August	33.60	0.97	15.27	0.84	11.77
September	30.50	0.96	15.42	0.82	11.70
October	37.30	0.97	15.20	0.84	11.74
November	36.60	0.95	16.12	0.81	12.18
December	43.20	0.95	18.39	0.81	13.76
January	36.40	0.96	15.45	0.83	11.84
February	37.80	0.96	15.20	0.83	11.60
March	49.30	0.94	16.48	0.80	12.15
April	41.70	0.97	20.00	0.84	15.43
May	35.60	0.96	17.04	0.82	12.92

Table 3.3. Deterministic equivalent upper limit design current speed $\bar{w}$, considering Weibull distribution.

Month	α_i	$\bar{w}_{max}$ (cm/s)	$\bar{w}$ (cm/s)
June	0.81	11.10	3.38
July	0.82	10.96	3.30
August	0.84	11.77	3.48
September	0.82	11.70	3.52
October	0.84	11.74	3.47
November	0.81	12.18	3.68
December	0.81	13.76	4.21
January	0.83	11.84	3.53
February	0.83	11.60	3.47
March	0.80	12.15	3.77
April	0.84	15.43	4.56
May	0.82	12.92	3.89

Overall, using $\overline{w}_i$ ensures that the outfall design does not necessarily rely only on remote episodes of very high current speeds, as denoted above. The design is also economical as it does not only follow $w_{min} \simeq 0$, which is a stagnant and rarely occurring case.

3.3.2. Ambient temperature

Ambient temperature may enhance or deter the thermohaline circulation. High temperature may increase the evaporation and salinity of coastal waters. This impacts the outfall's optimal performance and must be assessed during planning and design. Using CCP, the ambient temperature constraint, can be expressed as:

$$\Pr\left\{\overline{T}_i \le \overline{T}_{max_i}\right\} \ge \beta_i \tag{3.32}$$

Where $\overline{T}_{max_i}$ is a reasonable upper bound for sea surface temperature (SST) that is guaranteed to be available 99% $\left(p = 0.99\right)$ of the time within a monthly SST dataset i $(i = 1,...,12)$; and $\overline{T}_i$ is a reduced SST, referred to here as the design SST. It can be used to design the marine outfall system in a reliable manner, such that $\overline{T}_i < \overline{T}_{max_i}$. Finally, β_i is the monthly reliability level, where $0 \le \beta_i \le 1$.

The deterministic equivalent to Equation (3.32) can be expressed as:

$$F_{\psi}\left(\frac{T_i - E\left(T_i\right)}{\left[Var\left(T_i\right)\right]^{0.5}}\right) \ge \beta_i \tag{3.33}$$

Where $F_{\psi}(\cdot)$ is the cumulative distribution function (cdf); $E(T_i)$ is the expected value; and $Var(T_i)$ is the variance, respectively, of a monthly SST dataset. Assuming $\psi = (T_i - E(T_i)) / [Var(T_i)]^{0.5}$ is a stochastic variable that can be used to deduce confidence intervals for a non-standardized stochastic variable, we now can write Equation (3.33) above as:

$$F_{\psi}\left(\frac{T_i - E(T_i)}{[Var(T_i)]^{0.5}}\right) \leq 1 - \beta_i \tag{3.34}$$

Taking the inverse of Equation (3.34), we obtain:

$$T_i \leq E(T_i) + \left(F_{\psi}^{-1}(1-\beta_i)\right)[Var(T_i)]^{0.5} \tag{3.35}$$

where $F_{\psi}^{-1}(1-\beta_i)$ is the percent point function. Replacing T_i with $\bar{T}_i$ in the LHS of Equation (3.30), we can formulate $\bar{T}_i$ as:

$$\bar{T} = \bar{T}_{max} - \left(F_{\psi}^{-1}(\beta)\right)[Var(T)]^{0.5} \tag{3.36}$$

An example is presented here to demonstrate the use of Equation 3.36 above. For this example, the same area along California's central coast, as the one used in the preceding subsection, is chosen. The dataset for monthly ambient sea surface temperature (SST) is retrieved from online sources (National Data Buoy Center at www.ndbc.noaa.gov, SLO Science and Ecosystem Alliance at slosea.org and the Central and Northern California Ocean Observing System at www.cencoos.org). The data reveal that temperature exhibits temporal variations. A summary of temperature data is shown in Table 3.4.

Table 3.4. Sea surface temperature data based on historical records (open-source data from www.ndbc.noaa.gov/, slosea.org and www.cencoos.org/).

Month	T_{min} (°C)	T_{max} (°C)	$E(T)$ (°C)	$Var(T)$ $(°C)^2$	$\left[Var(T)\right]^{0.5}$ (°C)
June	27.10	31.90	29.52	1.16	1.08
July	26.50	32.50	30.00	1.57	1.25
August	27.90	32.40	30.89	0.67	0.82
September	26.50	31.10	28.79	0.55	0.74
October	21.60	27.00	23.53	1.25	1.12
November	15.50	23.80	18.06	3.73	1.93
December	10.20	16.50	13.91	1.74	1.32
January	5.00	16.00	8.31	5.33	2.31
February	7.90	12.00	9.92	1.17	1.08
March	9.50	18.40	13.30	4.00	2.00
April	15.90	22.60	20.17	1.85	1.36
May	21.40	28.00	25.63	2.05	1.43

In addition, the data show that the underlying SST distributions appear to be normal (Gaussian) probability distribution function (pdf). Figure 3.7 illustrates temperature data pdf for the months of December and June.

Given the temperature's daily and seasonal variations, the optimization problem may be formulated to include the uncertainty caused by this random variable. Within the seawater body that is surrounding the outfall, a reasonable upper bound for temperature is established. This upper bound is guaranteed to be available 99% $\left(p = 0.99\right)$ of the time within a monthly temperature dataset, as shown above. The reduced monthly maximum temperature $\bar{T}_{max}$ is computed, considering normal distribution. The temperature is further reduced such that $\bar{T}_i < \bar{T}_{max_i}$, per Equation (3.36) above, considering the monthly

reliability level β that varies from one month to another. Tables 3.5 and 3.6 show $\overline{T}_{max}$ and $\overline{T}_i$ results.

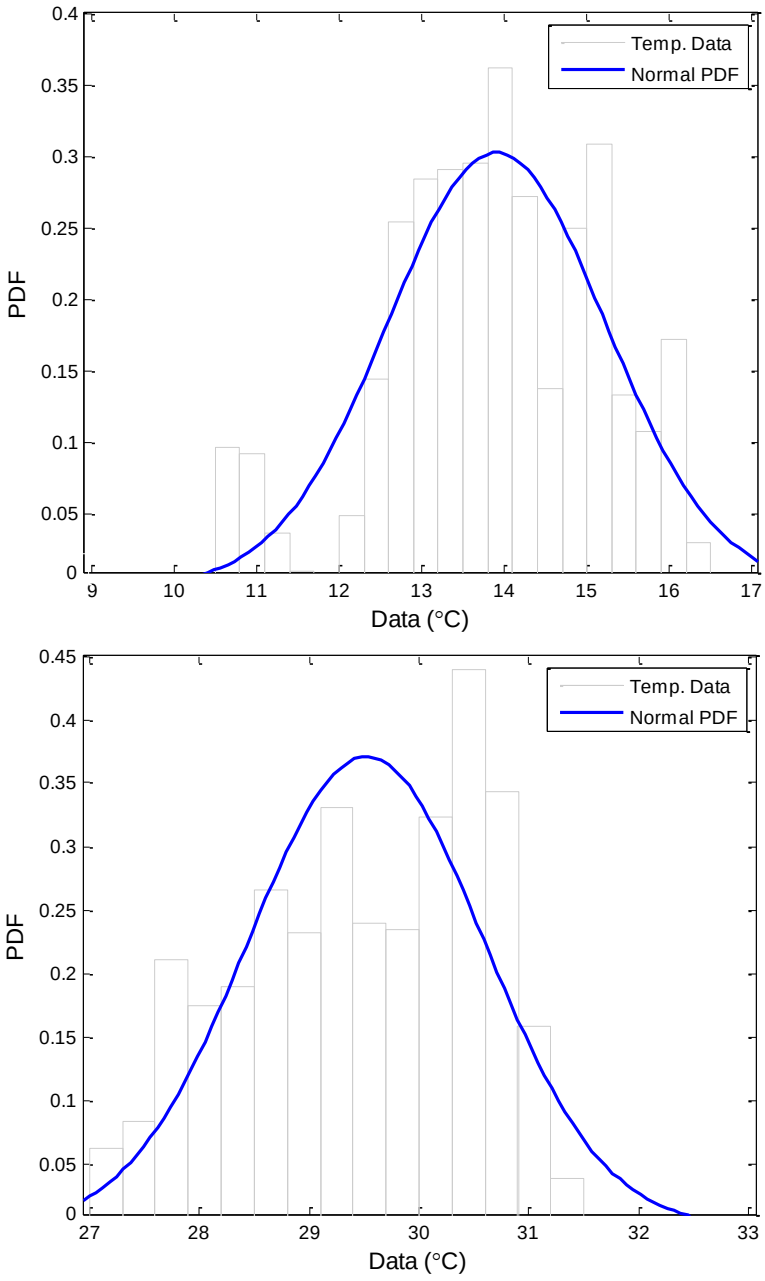

Figure 3.7. Comparisons between observational current speed data (histogram) and normal probability distribution functions for December and June.

Table 3.5. Reduced maximum temperature, considering normal distribution.

Month	T_{max} (°C)	Normal	
		β_i	$\bar{T}_{max}$ (°C)
June	31.90	0.99	31.90
July	32.50	0.98	32.50
August	32.40	0.97	32.40
September	31.10	0.99	31.10
October	27.00	0.99	27.00
November	23.80	0.99	23.80
December	16.50	0.98	16.50
January	16.00	0.93	16.00
February	12.00	0.97	12.00
March	18.40	0.99	18.40
April	22.60	0.96	22.60
May	28.00	0.95	28.00

Table 3.6. Deterministic equivalent upper limit design temperature $\bar{T}$, considering normal distribution.

Month	β_i	$\bar{T}_{max}$ (°C)	$\bar{T}$ (°C)
June	0.99	31.90	27.14
July	0.98	32.50	27.50
August	0.97	32.40	29.39
September	0.99	31.10	26.49
October	0.99	27.00	20.07
November	0.99	23.80	12.32
December	0.98	16.50	11.31
January	0.93	16.00	5.00
February	0.97	12.00	7.85
March	0.99	18.40	8.20
April	0.96	22.60	17.74
May	0.95	28.00	23.27

Using $\bar{T}_i$ properly ensures that the outfall design is not ignoring temperature variations or relying only on very high or extremely low SST. Temperature differences affect ambient density and cause increased or decreased stratification of the water column.

3.3.3. Wind speed

Surface waves and shear stresses on the sea surface are generated by sea surface winds. Due to wind speed, these waves and stresses create in turn surface currents. Surface winds are generally characterized as unsteady and non-uniform (Monahan, 2006; Bleninger, 2006). Therefore, proper wind speed parameterization is required to realize its impacts on surface currents and to adequately incorporate this stochastic variable in the outfall design endeavors.

Using CCP, the wind speed constraint, can be expressed as:

$$\Pr\left\{\bar{W}_i \le \bar{W}_{max_i}\right\} \ge \lambda_i \tag{3.37}$$

where $\bar{W}_{max_i}$ is a reasonable upper bound for wind speed that is guaranteed to be available $99\%\,(p = 0.99)$ of the time within a monthly wind speed dataset i $(i = 1,...,12)$; and $\bar{W}_i$ is a reduced wind speed, referred to here as the design wind speed. It can be used to design the marine outfall system in a reliable manner, such that $\bar{W}_i < \bar{W}_{max_i}$. Finally, λ_i is the monthly reliability level, where $0 \le \lambda_i \le 1$.

The deterministic equivalent to Equation (3.37) can be expressed as:

$$F_{\psi}\left(\frac{W_i - E(W_i)}{\left[Var(W_i)\right]^{0.5}}\right) \geq \lambda_i \tag{3.38}$$

where $F_{\psi}(\cdot)$ is the cumulative distribution function (cdf); $E(W_i)$ is the expected value; and $Var(W_i)$ is the variance, respectively, of a monthly wind speed dataset. Let $\psi = (W_i - E(W_i))/\left[Var(W_i)\right]^{0.5}$ be a stochastic variable that can be used to deduce confidence intervals for a non-standardized stochastic variable. Equation (3.38) can be expressed as:

$$F_{\psi}\left(\frac{W_i - E(W_i)}{\left[Var(W_i)\right]^{0.5}}\right) \leq 1 - \lambda_i \tag{3.39}$$

Taking the inverse of Equation (3.39), we obtain:

$$\bar{W}_i \leq E(\bar{W}_i) + \left(F_{\psi}^{-1}(1-\lambda_{ii})\right)\left[Var(\bar{W}_i)\right]^{0.5} \tag{3.40}$$

where $F_{\psi}^{-1}(1-\lambda_i)$ is the percent point function. Replacing W_i with $\bar{W}_i$ in the LHS of Equation (3.40), we can formulate $\bar{w}_i$ as:

$$\bar{W} = \bar{W}_{max} - \left(F_{\psi}^{-1}(\lambda)\right)\left[Var(W)\right]^{0.5} \tag{3.41}$$

To apply the findings above to an actual design problem, an example is proposed. The same area that represents a small coastal community in central California is chosen again for this example. The dataset for monthly sea surface wind speed is summarized in Table 3.7. The data, retrieved from online source (National Data Buoy Center at www.ndbc.noaa.gov), reveal that wind speed may exhibit some temporal variations, depending on the time of year. Figure 3.8 shows wind speed data for the months of

January and July, respectively.

Table 3.7. Sea surface wind speed data based on historical records (open-source data from www.ndbc.noaa.gov/).

Month	W_{min} (m/s)	W_{max} (m/s)	$E(W)$ (m/s)	$Var(W)$ $(m/s)^2$	$[Var(W)]^{0.5}$ (m/s)
June	0.00	15.00	5.12	11.75	3.43
July	0.10	15.10	7.04	14.65	3.83
August	0.00	13.60	5.95	9.99	3.16
September	0.00	13.80	6.78	13.29	3.65
October	0.10	18.20	7.20	15.81	3.98
November	0.10	15.70	6.16	14.98	3.87
December	0.00	15.40	4.52	12.03	3.47
January	0.00	17.80	5.09	11.85	3.44
February	0.00	15.60	5.49	10.08	3.18
March	0.00	16.20	5.82	14.79	3.85
April	0.10	15.10	7.19	16.45	4.06
May	0.30	14.40	7.66	18.55	4.31

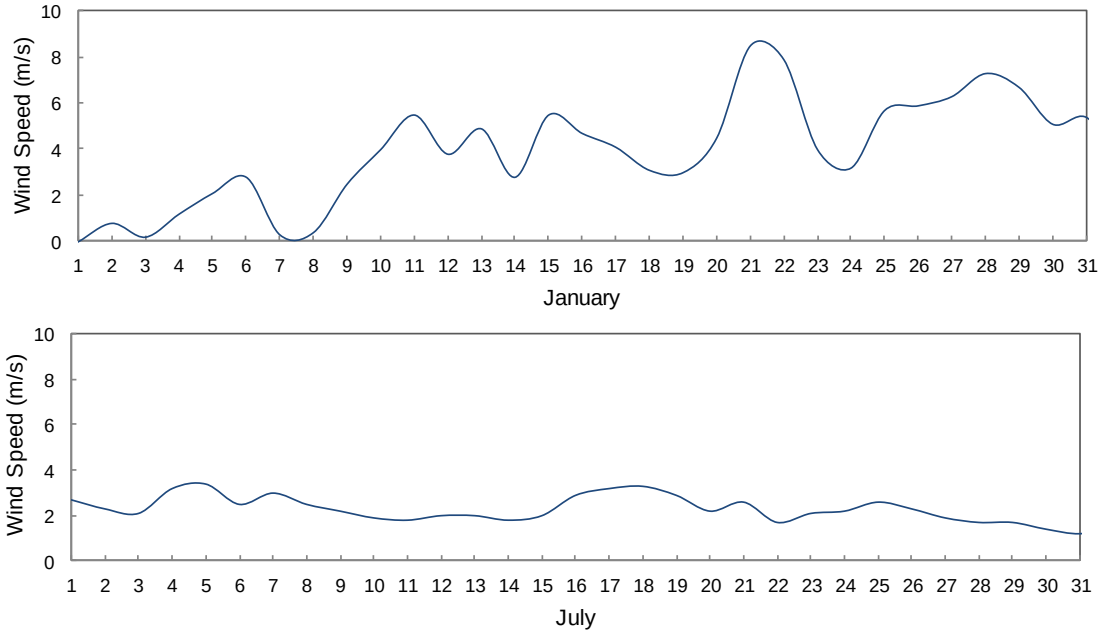

Figure 3.8. Wind speed for the months of January and July (data retrieved from www.ndbc.noaa.gov).

The data above were measured at locations in the vicinity of an area representing a small coastal community in central California. The data show that the underlying wind speed distributions do not appear to be normal (Gaussian), but rather are positively skewed (i.e., skewed to the right). This asymmetric temporal behavior may be approximated statistically as a two-parameter Weibull probability distribution function (pdf), as shown in Figure 3.9 (Monahan, 2006; Chu, 2008).

Given the wind speed's daily and seasonal variations, the optimization problem may be formulated to include the uncertainty caused by this random variable. A reasonable upper bound for wind speed is established. This upper bound is guaranteed to be available 99% $\left(p = 0.99\right)$ of the time within a monthly wind speed dataset, as shown above. The reduced monthly maximum wind speed $\overline{W}_{max}$ is computed, considering normal and Weibull distributions.

The wind speed is further reduced such that $\overline{W}_i < \overline{W}_{max_i}$, per Equation (3.41) above, considering the monthly reliability level λ that varies from one month to another. Tables 3.8 and 3.9 show $\overline{W}_{max}$ and $\overline{W}_i$ results. These results will be discussed further in Chapter 4.

Using $\overline{W}_i$ ensures that the outfall design does not necessarily rely only on remote episodes of very high wind speeds. The design will be economical as it does not only follow $W_{min} \simeq 0$, which rarely takes place.

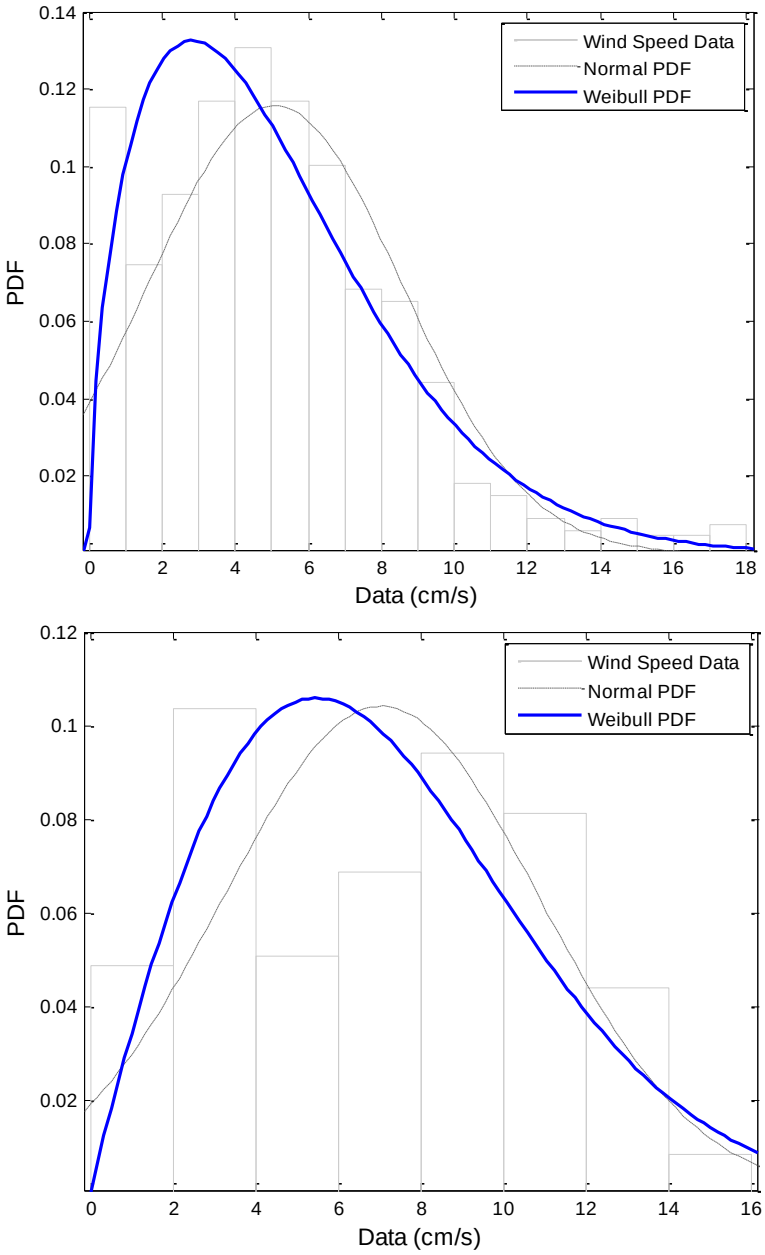

Figure 3.9. Comparisons among observational wind speed data (histogram), normal and Weibull probability distribution functions for January and July.

Table 3.8. Reduced maximum wind speed, considering normal and Weibull distributions.

Month	W_{max} (m/s)	Normal		Weibull	
		λ_i	$\bar{W}_{max}$ (m/s)	λ_i	$\bar{W}_{max}$ (m/s)
June	15.00	0.93	10.23	0.77	7.37
July	15.10	0.97	14.07	0.84	10.86
August	13.60	0.97	11.90	0.85	9.23
September	13.80	0.97	13.56	0.84	10.49
October	18.20	0.97	14.40	0.84	11.08
November	15.70	0.94	12.31	0.80	9.11
December	15.40	0.90	9.04	0.73	6.00
January	17.80	0.93	10.19	0.77	7.30
February	15.60	0.96	10.99	0.82	8.36
March	16.20	0.93	11.64	0.78	8.44
April	15.10	0.96	14.38	0.83	11.00
May	14.40	0.96	14.40	0.83	11.73

Table 3.9. Deterministic equivalent upper limit design wind speed $\bar{W}$, considering Weibull distribution.

Month	λ_i	$\bar{W}_{max}$ (m/s)	$\bar{W}$ (m/s)
June	0.81	7.37	2.35
July	0.82	10.86	3.21
August	0.84	9.23	2.71
September	0.82	10.49	3.10
October	0.84	11.08	3.29
November	0.81	9.11	2.82
December	0.81	6.00	2.08
January	0.83	7.30	2.34
February	0.83	8.36	2.51
March	0.80	8.44	2.67
April	0.84	11.00	3.28
May	0.82	11.73	3.50

3.4. Simulation–optimization framework

The simulation model CORMIX is used to run numerous design alternatives for all possible combinations of length, diameter and number of ports. This is first achieved by determining lower and upper bounds for each design parameter. These bounds must be hydrodynamically feasible and must also meet the established environmental requirements at the edge of the mixing zone and satisfy all constraints. In order to determine the lower bound, these constraints have to be initially relaxed. Next, a set $(L, D, N)^T$ of feasible length, diameter and number of ports that complies with the hydrodynamic criteria above must be found. Once this is done, the design parameters must be varied systematically, from the lower bound to the upper bound. Other important input parameters (such as the current speed, wind speed and temperature) must be adjusted, as well.

CORMIX is used to simulate the output for all possible parameter combinations $\left(L_1, D_1, N_1, \cdots, L_n, D_n, N_n\right)^T$ and other stochastic variables, such as the reduced current speed, temperature and wind speed $\left(w_1, T_1, W_1, \cdots, w_m, T_m, W_m\right)^T$, under approximately similar flow rate loading conditions.

A large number of simulations are executed and the input and output results, that satisfy all constraints, are then stored in a database. The upper bound is reached when no significant changes in the dilution output values are noticed. Once the upper limit is identified, linear regression analyses are performed using the stored input and output results from the CORMIX simulations. The following linear regression model is assumed:

$$S = \mathrm{b}_0 + \sum_{i=1}^{3} \mathrm{b}_i x_i + \sum_{j=4}^{k} \mathrm{b}_j \xi_j + \varepsilon \tag{3.42}$$

where $\mathrm{b}_0, \mathrm{b}_1, \ldots, \mathrm{b}_k$ are linear regression coefficients, $x = (L, D, N)^T$ is the decision variable vector and $\xi = \left(w, T, W \ldots\right)^T$ is a vector representing stochastic variables. This random vector $\xi \in \mathbb{R}^n$ includes wind-driven, tidal and other randomly varying currents, represented here as w. It may also include ambient temperature T and the wind speed W, among other stochastic variables. The term ε is a random error that is assumed to have a zero mean.

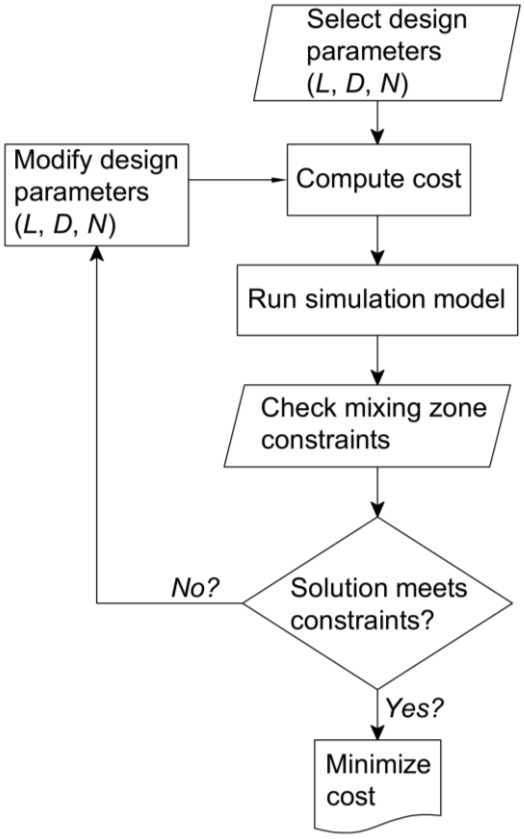

Figure 3.10. General flowchart for the simulation–optimization framework used in this study.

The following mixed-integer linear programming (MILP) optimization model is now formulated, in which CORMIX is replaced by the linear regression model shown in Equation (3.42). The model can be expressed as:

$$\min Z = \mathrm{w}_1 L + \mathrm{w}_2 D + \mathrm{w}_3 N \tag{3.43}$$

subject to:

$$L_p^l \le L_p \le L_p^u, \quad \forall p \tag{3.44}$$

$$D_m^l \le D_m \le D_m^u, \quad m \in \mathbb{Z}^+ \tag{3.45}$$

$$N_n^l \le N_n \le N_n^u, \quad n \in \mathbb{Z}^+ \tag{3.46}$$

$$S = \mathrm{b}_0 + \mathrm{b}_1 L + \mathrm{b}_2 D + \mathrm{b}_3 N + \mathrm{b}_4 w + \mathrm{b}_5 T + \mathrm{b}_6 W + \ldots + \varepsilon \tag{3.47}$$

$$S \ge S_{rid} \tag{3.48}$$

$$\Pr\left\{\bar{w}_i \le \bar{w}_{max_i}\right\} \ge \alpha_i, \quad \forall i \tag{3.49}$$

$$\Pr\left\{\bar{T}_i \le \bar{T}_{max_i}\right\} \ge \beta_i, \quad \forall i \tag{3.50}$$

$$\Pr\left\{\bar{W}_i \le \bar{W}_{max_i}\right\} \ge \lambda_i, \quad \forall i \tag{3.51}$$

$$\alpha_i \in (0,1), \quad \forall i \tag{3.52}$$

$$\beta_i \in (0,1), \quad \forall i \tag{3.53}$$

$$\lambda_i \in (0,1), \quad \forall i \tag{3.54}$$

where the minimum cost function in Equation (3.43) is the objective function; D_m^l and D_m^u are the lower and upper bounds, respectively, of the m^{th} port diameter from an integer set of feasible port diameters, as shown in Equation (3.23); N_n^l and N_n^u are the lower and

upper bounds, respectively, of the n^{th} number of ports from an integer set of feasible number of ports in the diffuser section of the outfall system, as shown in Equation (3.24); and $\bar{w}_i$, $\bar{T}_i$ and $\bar{W}_i$ are among many random variables that are assumed to follow a suitable probability distribution function (pdf) and reduced to ensure that the outfall design is conservative. The deterministic equivalent to Equation (3.49) is computed using Equations (3.28)–(3.31). The deterministic equivalent to Equation (3.50) is computed using Equations (3.33)–(3.36). The deterministic equivalent to Equation (3.51) is computed using Equations (3.38)–(3.41). The deterministic equivalents to other present stochastic variables (not demonstrated here) may be computed in a similar manner, given a pdf is defined properly.

3.5. Case study

The proposed method is demonstrated by presenting an example that is based on an actual SWRO desalination facility planned for a small community in central California. A site plan of the area is shown in Figure 3.11, depicting the approximate location where the project was planned to be constructed in the 1990s.

Although the original plans to build a SWRO desalination plant were suspended, in light of water supply deficiencies the possibility of designing and constructing the same project recently has been reconsidered. The final area of the project, however, has not yet been identified. The proposed SWRO desalination plant was originally planned to have a

design capacity of approximately 3.80 ML/d (1 MGD) of freshwater. While such capacity is relatively small compared to centralized traditional SWRO desalination plants in megacities around the world, planners currently are redefining new process plant sizes, locations and other regulatory procedures (for example, the International Water Association's work on decentralized systems). As a result, it is prudent to apply the method described to a decentralized smaller plant that fits within the framework and goals of water professionals worldwide.

The 3.80 ML/d (1 MGD) flow rate, considering an assumed recovery ratio R_w of 40% (as per discussions in subsections *2.2.1* and *2.3.1* above), requires no less than 9.50 ML/d (about 2.50 MGD) of seawater. Brine discharge subsequently will be about 5.7 ML/d (1.50 MGD). The plan calls for effluent discharge via a multiport diffuser marine outfall. Preliminary hydrodynamic computations help define the lower bound of the length of outfall pipe section *L*. This is predicated upon many factors that are site-specific (topography, bathymetry) and hydrodynamic (the highest vertical position of the upper jet boundary). Although the final location of the SWRO desalination facility and outfall has not yet been agreed upon, an upper bound is designated and it is based on environmental restrictions. Within the coastal region there exists an adjoining zone that is classified as a marine sanctuary and a kelp canopy (not shown in figure 3.11). Encroaching upon these two areas is assumed prohibited for this study. Consequently, the edge of the mixing zone must not be in close proximity to these environmentally protected regions.

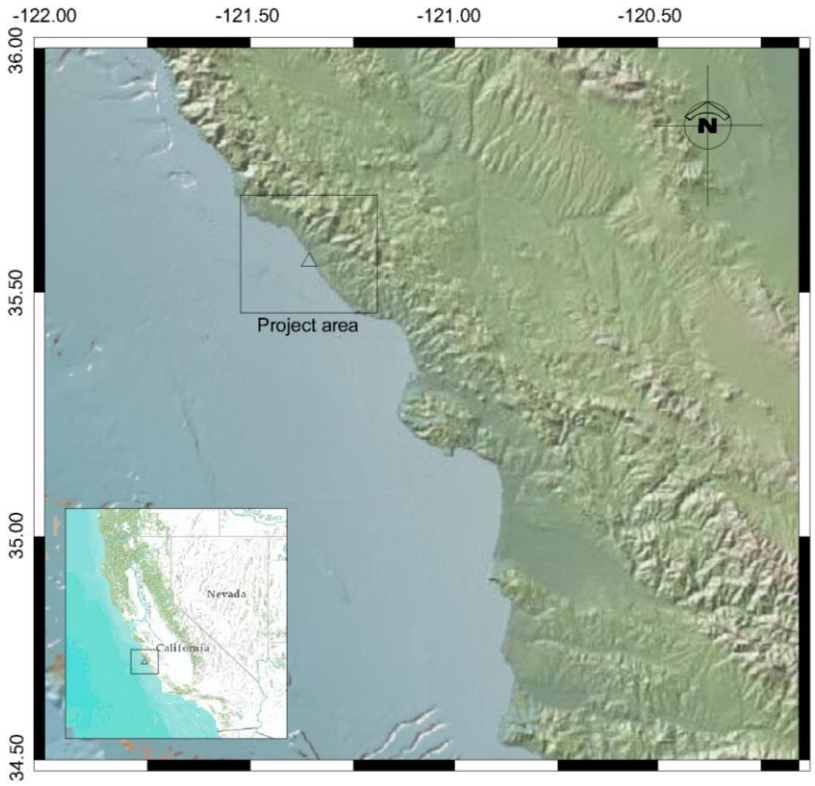

Figure 3.11. Location of a proposed SWRO desalination facility, planned for a small community in Central California. The project area is about 270km (168miles) south of San Francisco and approximately 312km (194miles) north of Los Angeles.

3.5.1. Geographical data

Topographic and bathymetric data, for preliminary assessments in this example, were retrieved using three sources: NASA World Wind (worldwind.arc.nasa.gov), Virtual Ocean (www.virtualocean.org), Google Earth (www.google.com/earth/), and ArcGIS (www.arcgis.com/). The dataset for monthly ocean current speed is summarized in Table 3.1. The raw hourly dataset is retrieved from three different stations in the vicinity of the proposed project. The stations are owned and operated by the National Data Buoy Center (NDBC, www.ndbc.noaa.gov), the Coastal Data Information Program (CDIP,

cdip.ucsd.edu) and the Monterey Bay Aquarium Research Institute (MBARI). They are located at 35.741°N 121.884°W, 36.340°N 122.102°W and 36.751°N 122.335°W, respectively. Data coverage varies from one station to another. Operation is not active at all times and some interruptions exist. Ocean current speeds (January and July) are shown in Figures 5a and 5b. Other data, such as wave height and direction, seawater salinity, temperature and other meteorological data (not shown here) are also available for the one-year time period used in this study. Such data is available, in addition to the sources above, from the Central and Northern California Ocean Observing System (CeNCOOS, www.cencoos.org). Although seawater TDS concentration levels fluctuate in the project's general area, a constant TDS concentration of 33,340 mg/L is used for this example.

3.5.2. Input parameters

Once the topographic and bathymetric information is gathered, other data are organized and initial and boundary conditions are established. Multiple simulations are performed using CORMIX, with key input parameters shown in Table 3.10.

Table 3.10. Lower and upper bounds used in analysis and design.

Variable	Unit	Lower Bound	Upper Bound
Feeder pipeline (L)	(m)	275	312
Port diameter* (D)	(mm)	32	50
Number of ports (N)	–	13	21
Current speed (w)	(cm/s)	0	Varies
Seawater temperature (T)	(°C)	7	19
Effluent flow rate	(m^3/d)	5.7×10^3	6.5×10^3
Effluent concentration	(mg/L)	54 400	54 400

* This refers to existing standard diameter sizes in the industry.

As shown in subsections *3.3.1* through *3.3.3*, that within the same space or control volume where similar continuous effluent discharges are taking place, current speed, ambient temperature and wind speed exhibit temporal variations. The ocean's upper layer current speed data and sea surface winds revealed that the underlying distributions do not appear to be normal (Gaussian) but rather are positively skewed (i.e., skewed to the right). This asymmetric behavior was approximated statistically as a two-parameter Weibull probability distribution function (pdf). On the other hand, the ambient temperature data revealed that the underlying distributions appear to be normal (Gaussian).

A significant input is the wave direction. This helps determine the definitive orientation of the outfall's diffuser section. Figure 3.12 shows the wave rose of the entire year taken into consideration (June through July). The units are degrees from true North, increasing clockwise, with North as 0 (zero) degrees and East as 90 degrees. Therefore, the waves are predominantly traveling towards the coastline from the Northwest direction (the quadrant between 270 degrees and 360 degrees), based on Figure 3.12.

CORMIX solves for brine concentration variations and assesses dilution S, starting at the lower bound. The design parameters are varied systematically, one at a time, from the lower bound to the upper bound. A total of 8,209 possible combinations are generated, combining different possibilities of decision and stochastic variables. CORMIX simulates the output using all possible parameter combinations as well as the prescribed initial and boundary conditions. Each simulation features a unique plume cumulative travel time between the marine outfall's diffuser section and the outer edge of the mixing zone.

These travel time differences among simulations depend on each design parameter combination as well as stochastic variables. Out of all combinations, 1,990 total cases comply with the prescribed dilution criteria at the outer edge of mixing zone. These cases constitute a dataset used to perform linear regression analyses as described in Equation (3.47) above.

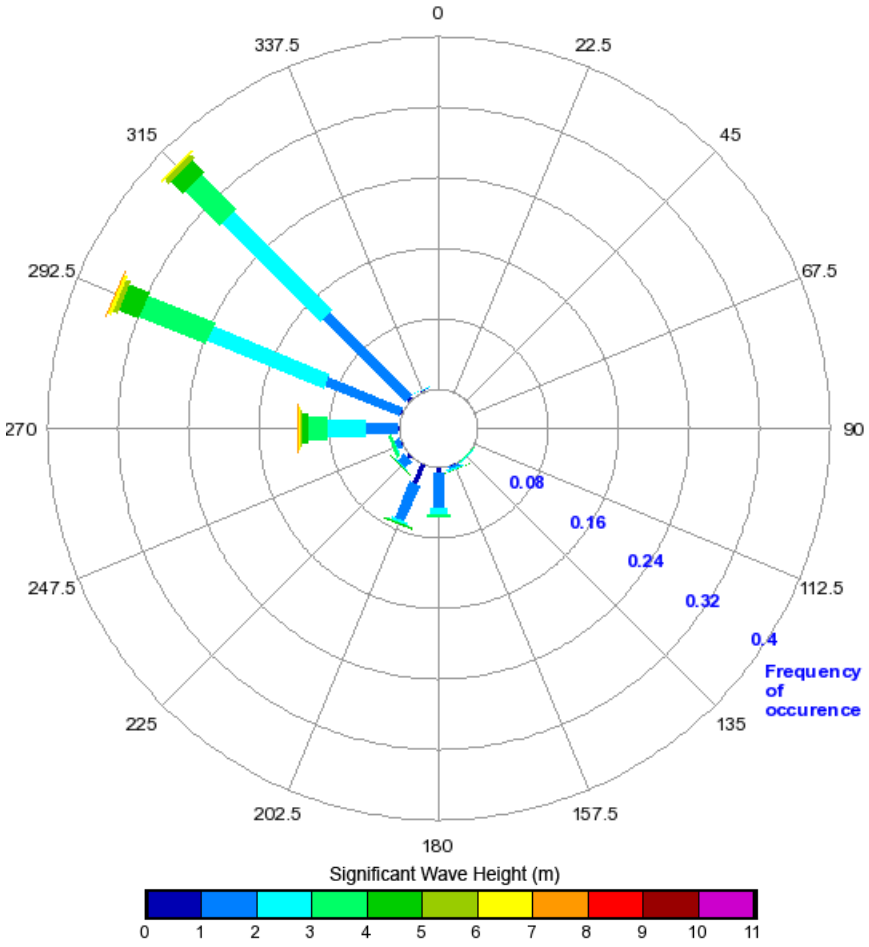

Figure 3.12. Wave rose showing dominant wave direction, frequency of occurrence and significant wave height for the entire year of study (June – July). Data were measured at a location in the vicinity of the small coastal community, discussed in this case study, in central California (retrieved from the Coastal Data Information Program at cdip.ucsd.edu).

Given these daily and seasonal variations, the optimization problem must be formulated to include the uncertainty caused by these stochastic variables. However, for this case study, only current speed is incorporated to demonstrate the use of uncertainty, while other random variables are ignored.

4. RESULTS AND DISCUSSION

In Chapter 3, Chance-constrained programming (CCP) was used to deal with the impact of uncertainty caused by the presence of one of the stochastic variables. Investigation of the current speed, ambient temperature and wind speed indicated that these random variables are sensitive to distributional assumptions. These variables are also sensitive to monthly reliability values.

To demonstrate this for the current speed variable, a set of monthly reliability values (α_i) between 0.5 and 0.99 is chosen and the corresponding design current speed $\overline{w}_i$ is computed (Figure 4.1). It is observed that the design current speed varies drastically (mean $\overline{w}_i$ values ranged between 7.4 and 0.7 cm/s), given the reliability assumptions made. While such current speed values are valid, given the historical dataset shown in Chapter 3, this range impacts the outfall design and contributes to increasing uncertainty. A more consistent method for assessing α_i was therefore essential.

A better way to deduce the monthly reliability values was presented by using the coefficient of variation of the monthly dataset (i.e., the ratio of the square root of $Var(w_i)$ to the expected value $E(w_i)$). Depending on the distributional assumptions posited to determine the cdf $F_{\psi}(\cdot)$, the values of monthly reliability α_i vary, as shown in Table 3.3. By comparing the reliability results determined from the normal and Weibull distributions, it was noticed that the normal distribution tends to give higher monthly reliability values than those computed using the Weibull distribution (Table 3.3).

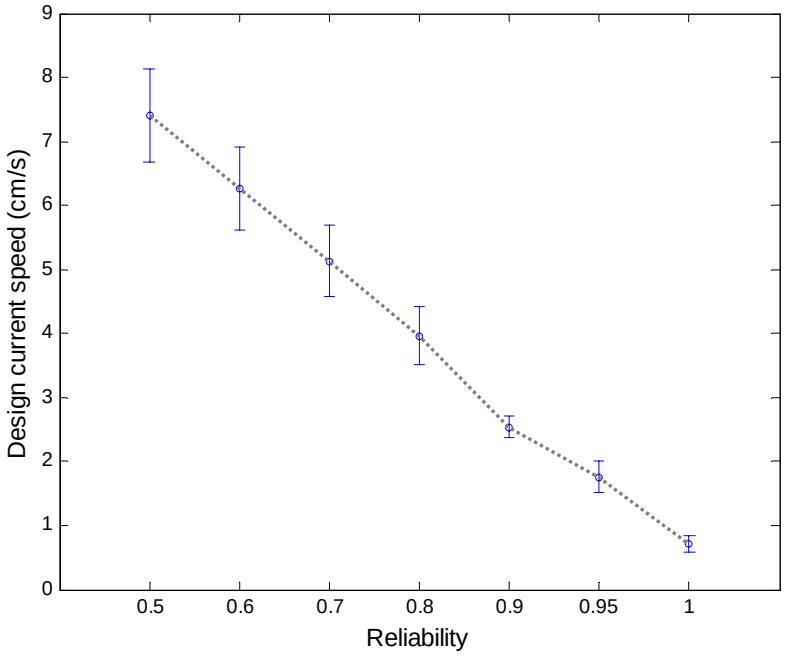

Figure 4.1. Design current speed $\overline{w}_i$ vs. reliability values taken between 0.5 and 0.99. $\overline{w}_i$ is very sensitive to such reliability variations.

Once the values of α_i were established following the method above, computing the monthly reduced maximum current speed $\overline{w}_{max}$ became possible (Table 3.2). By assuming the normal distribution, $\overline{w}_{max}$ tends to be higher. This erroneously indicated that higher current speeds were reliably present within a time period. On the other hand, the Weibull distribution assumption tends to warrant lower reliability values and, subsequently, lower current speed values. The monthly reduced maximum speed $\overline{w}_{max}$ is lower when the Weibull distribution is adopted, implying that the initial dilution S is going to be achieved under more conservative conditions (lower current speed). Due to lower monthly reliability values (using the Weibull distribution assumption), and subsequently lower current speed values, a more conservative outfall system design can

be achieved. These values were used for the case study example shown in Chapter 3.

The design current speed's deterministic equivalent $\overline{w}_i$ was then computed once the monthly reduced maximum current speed $\overline{w}_{max}$ was known. Using Equation (3.31), the monthly $\overline{w}_i$ values were calculated. These values were presented in the last column of Table 3.3 above. The design current speed was observed not to vary drastically between one month and another. Given the reliability computations made, and taking the lower of the two or more values of $\overline{w}_i$ given the same α_i, the design current speed values ranged between 3.30 and 3.77 cm/s. This range appears to be more appropriate for the design of an outfall system (Figure 4.2).

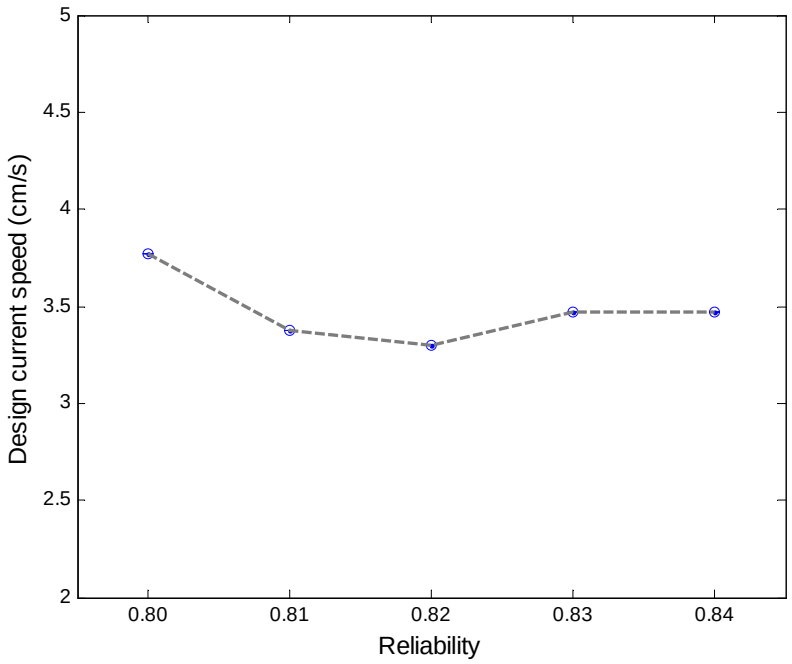

Figure 4.2. Design current speed $\overline{w}_i$ vs. reliability values that are determined using monthly current speed data. $\overline{w}_i$ varies slightly between 3.30 and 3.77 cm/s, as shown in Tables 3.2 and 3.3 above.

The outfall design is carried-out by running multiple simulations of the CORMIX model to solve for brine concentration variations and assess dilution S values, taking into consideration the deterministic equivalent current speed $\overline{w}_i$ and a cohort of decision variables (L, D, N). The output results aided in generating a response surface that was used to deduce the following linear equation (Khuri, and Mukhopadhyay, 2010):

$$S = 75.49 + 1.07L - 5.54D - 5.05N + 67.95\overline{w} \quad \left(R^2 = 0.93\right) \tag{4.1}$$

This response surface was statistically examined (Figure 4.3). It was validated by performing the analysis of variance (ANOVA) shown in Table 4.1.

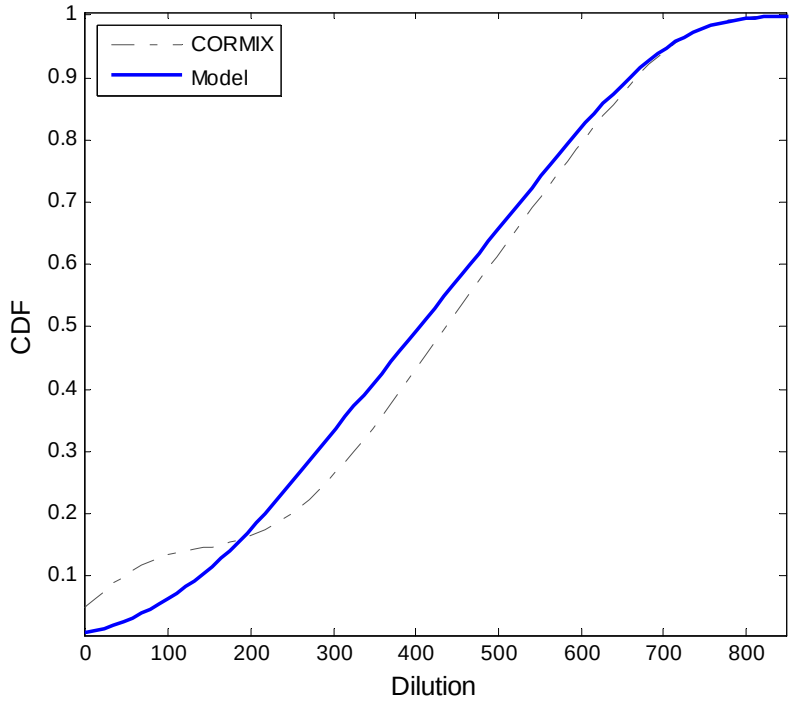

Figure 4.3. CORMIX and regression model cumulative frequencies.

Table 4.1. Analysis of variance for the model.

Reference	*DF*	*SS*	*MS*	*F*	R^2	$R^2_{adj.}$
Model	4	7.96×10^7	1.99×10^7	6.42×10^3	0.93	0.93
Error	1985	6.15×10^6	3.10×10^3			
Total	1989	8.57×10^7	1.99×10^7			

The high coefficient of determination R^2 value indicates that approximately 93% of dilution data deduced from the CORMIX simulations are within the developed response surface, represented as a linear model in Equation (3.42) of the preceding chapter. In addition, the R^2 value is identical to the adjusted coefficient of determination $R^2_{adj.}$. This indicates that non-significant terms were excluded from the linear model. Figure 4.4 presents the associated performance of dilution simulated values compared to model fits, and Table 4.2 compares dilution results computed by CORMIX to those determined by the linear model.

Overall, the model demonstrates a good fit with the CORMIX output. While it is not in full agreement with the CORMIX output at low dilution, the model demonstrates a very good fit with the CORMIX output at higher dilution values, as shown in Figure 4.4 as well as Tables 4.2 and 4.3. This is acceptable because in this case study we primarily rely on higher dilution values to achieve the objectives of meeting regulatory requirements at the mixing zone's outer edge. The model and CORMIX agree very closely at these higher dilution values. Therefore, this model may be coupled with the optimization model described in Section 3.3 above.

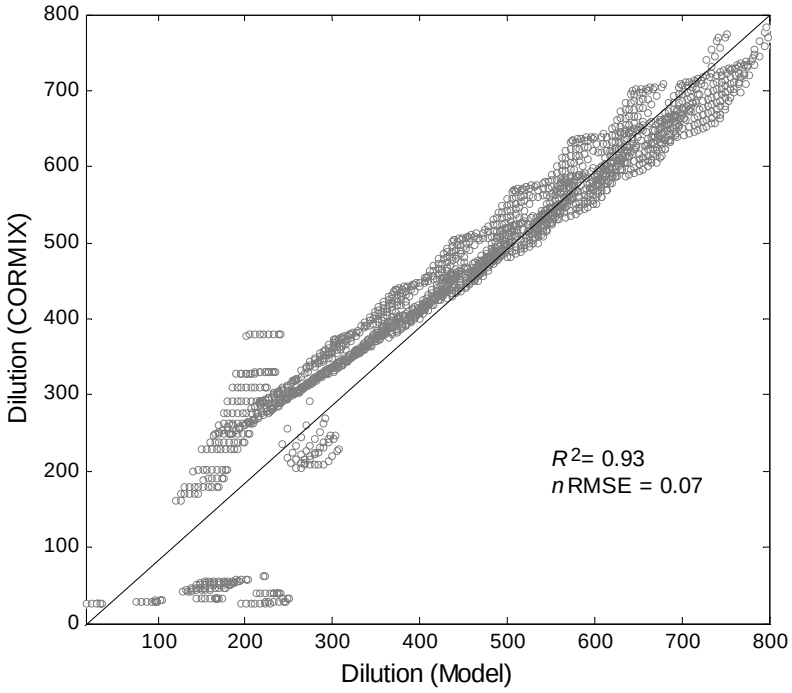

Figure 4.4. CORMIX vs. regression model and the relevant statistics for the regression equation presented in Equation (4.1).

Table 4.2. Dilution simulation values and model fits.

	S (CORMIX)	S (Model)
Min.	4	1
Max.	787	807
$E(S)$	410	410
$Var(S)$	43,095	40,001

The mixed-integer linear programming (MILP) optimization model was invoked to determine a set of optimal solutions considering the random behavior of current speed. For this case study, a criterion for the initial dilution that guarantees that S is no less than 100 at the edge of mixing zone was used. LINGO 13.0 (by LINDO Systems, Inc.

2012), an optimization solver, was used to solve the MILP problem. Table 4.3 provides a summary of the optimal length of the outfall, diameter and number of ports in the diffuser section, corresponding to different design current speed values.

Table 4.3. Optimal solutions considering randomness in current speed.

α_i	$\overline{w}$ (cm/s)	L (m)	D (mm)	N (-)
0.80	3.77	275	40	13
0.81	3.38	277	50	14
0.82	3.30	278	50	14
0.83	3.47	277	40	16
0.84	3.47	277	40	16
0.99	≈ 0	309	50	14

Once the optimization model was executed, the CORMIX simulation model was employed again to perform a post-optimization analysis and ensure that all constraints were satisfied. The results indicated that, after assessing the risks associated with the presence of the current speed's stochastic features, the proposed marine outfall should have a feeder pipeline length of no less than 275m and diffuser section length of 33m. These lengths are associated with the 13 ports that have an internal diameter of no less than 40mm. This configuration was evaluated under a reliability of 0.8 (80%) and a design current speed of 3.77 cm/s. Other results are shown in Table 4.3. CORMIX results, using the optimal solution shown in Table 4.3 and treated as input, confirmed that the dilution meets or exceeds 100 at the edge of the mixing zone. This further supports the validity of using the regression model to represent the response surface of CORMIX.

As smaller and more decentralized SWRO desalination plants are becoming more popular in many arid and semi-arid coastal areas around the world, a brine disposal approach similar to the one demonstrated here may be applied to regions other than California's coastal small communities. In addition, as higher water recovery and better separation processes in SWRO technology are on the rise and alternative means of supplying reduced energy are being explored in SWRO desalination plant operations, maximizing potable water supply, reducing energy costs and minimizing brine disposal volumes remain the primary objectives of all regulatory agencies, planners and design engineers. Consequently, it is necessary to enhance existing optimization models and approach the SWRO system from a holistic point of view. In other words, simultaneously evaluating all the above objectives is essential and will remain an area of further research.

Hypersaline brine discharge may have potential environmental impacts. As a result, a monitoring program is recommended, so that the models used can be calibrated further and field data from the receiving coastal waters and the concentrate discharge can be assimilated into simulation and optimization efforts. Such a program also should include guidelines to collect data on short- and long-term effects of the concentrate discharge on the benthic marine environment (marine plants and animals).

5. SUMMARY AND CONCLUSIONS

The work here addressed discharges arising from SWRO hypersaline brine effluent that is negatively buoyant in nature. Marine outfalls with multiport diffusers, if used properly, are very efficient in maximizing dilution levels of these negatively buoyant plumes. The study also demonstrated that optimization techniques can be applied to minimize the total costs of these outfalls. To accomplish this, CORMIX (a USEPA-approved hydrodynamics model and decision support system) was used to assess and simulate the impacts of SWRO brine discharges from the outfall into the coastal waters. CORMIX is capable of directly performing SWRO brine flow simulations and analyzing near-field mixing processes. The input and output from CORMIX were modeled with a linear regression model. This was achieved by parametrically varying all the input parameters in CORMIX to simulate the output. An optimization model was then formulated in which CORMIX was replaced by the linear regression model.

A mixed-integer linear programming (MILP) optimization model took into account the continuous nature of the outfall's pipe section as well as the discrete nature of the diameter and number of discharge ports. In addition, due to the stochastic characteristics of some variables within coastal waters—namely, current speed, ambient temperature and wind speed—the optimization model also evaluated the uncertainty of these input variables using chance-constrained programming (CCP).

Considering all these variables, our findings indicate that it is feasible to construct cost-effective marine outfalls that are efficient in maximizing dilution levels while

confirming that all environmental requirements and regulations have been met or exceeded. The model was applied to a hypothetical SWRO brine outfall along the California coastline.

A technique that reduces current speed, based on some distributional assumptions, to a reasonable maximum upper bound $\bar{w}_{max}$ that is always guaranteed (given a dataset) was presented. The value of $\bar{w}_{max}$ was further reduced to what was referred to as the design current speed, $\bar{w}$, using CCP. Similar techniques that reduced the ambient temperature and wind speed were also presented.

While it is possible to consider current speed as a realistic and constantly available (albeit variable) driver that may enhance the concentrate's initial dilution S, it is critical not to rely solely on current speed to achieve dilution. Overall, it is important to place the SWRO brine outfall in coastal zones where an abundance of ambient mixing and advective transport exists.

6. FURTHER RESEARCH

The Goal of this research was to provide planning and design tools to help construct SWRO marine outfall systems that meet environmental economic constraints. This was accomplished by presenting an integrated simulation-optimization model. The Following are suggestions for future research areas.

1. Most current environmental regulations do not have a specific policy that addresses negatively buoyant discharges directly. Therefore, it is vital to include elements within the regulatory framework that directly deal with site-specific conditions, and redefine existing mixing zone criteria.

2. Further research is required to monitor existing marine outfalls, enforce field studies and further validate simulation models, optimization models and confirm efforts that integrate these models.

3. The method presented in this study did not consider the possibilities of reusing the SWRO concentrate in other processes, such as evaporation ponds. These ponds may be employed to produce salt that can in turn be sold for commercial and culinary usages. While some studies have addressed the positive contribution of evaporation ponds in minimizing the volumes of SWRO brine discharge, further research is needed to investigate such contributions vis-à-vis optimization techniques.

4. The method presented did not consider threats from harmful algal blooms (HAB) outbreaks. These threats have been emerging around some operating large-scale SWRO

desalination plants around the world. HAB outbreaks may affect SWRO membranes, compromise the integrity of the SWRO plant and cause effluent discharge problems. Further research is needed to investigate the cause of these outbreaks and their effects on simulation-optimization models.

5. The method presented here did not take into consideration blending with other effluents (for example, blending SWRO brine with other effluents from power plants or wastewater treatment plants—a common practice in some regions). Such action alters the plume's characteristics and subsequently modifies the dilution process. While some studies have discussed the impacts of blending on dilution of SWRO brine discharge, further research is needed to investigate such impacts using optimization techniques.

6. REFERENCES

[1] Abdul-Wahab, S.A. and Abdo, J. (2007). "Optimization of Multistage Flash Desalination Process by Using a Two-level Factorial." *Applied Thermal Engineering*, 27: 413-421.

[2] Abdul-Wahab, S.A. and Al-Weshahi, M.A. (2009). "Brine Management: Substituting Chlorine with On-Site Produced Sodium Hypochlorite for Environmentally Improved Desalination Processes." *Water Resources Management*, 23: 2437-2454.

[3] Ahmed, M., Shayya, W.H., Hoey, D., and Al-Handaly, J. (2001). "Brine Disposal from Reverse Osmosis Desalination Plants in Oman and the United Arab Emirates." *Desalination*, 133: 135-47.

[4] Akar, P.J. and Jirka, G.H. (1995). "Buoyant Spreading Processes in Pollutant Transport and Mixing Part 2: Upstream Spreading in Weak Ambient Current." *J. Hydraul. Research*, 33: 87-100.

[5] Al-Agha, M. and Sh. Mortaja, R. (2004). "Desalination in the Gaza Strip: Drinking Water Supply and Environmental Imapct." *Desalination*, 173: 157-171.

[6] Alameddine, I. and El-Fadel, M. (2007). "Brine Discharge from Desalination Plants: a Modeling Approach to an Optimized Outfall design." *Desalination*, 214: 241-260.

[7] Al-Barwani, H.H. and Purnama, A. (2008). "Simulating Brine Plumes Discharged into the Seawaters." *Desalination*, 221: 608-613.

[8] Alvarez-Vázquez, L.J., García-Chan, N., Martínez, A. and Vázquez-Méndez, M.E. (2010). "Multi-Objective Pareto-Optimal Control: An Application to Wastewater Management." *Comput. Optim. Appl.*, 46(1): 135-157.

[9] Alvarez-Vázquez, L.J., Martínez, Á., Rodríguez, C. and Vázquez-Méndez, M.E. (2005). "Mathematical Model for Optimal Control in Wastewater Discharges: the Global Performance." *C.R. Biologies*, 328: 327-336.

[10] Arora, J.S. (2004). *Introduction to Optimum Design, 2nd Edition*. Academic Press, San Diego.

[11] Baensch, H.A. and Debelius, H. (1997). *Marine Atlas Volume 1*. Mergus-Verlag, Melle.

[12] Bashitialshaaer, R.A.I., Persson, K.M. and Aljaradin, M. (2011). "Estimated Future Salinity in the Arabian Gulf, the Mediterranean Sea and the Red Sea.

Consequences of Brine Discharge from Desalination." *Int. J. Academic Res.*, 3 (1), 133-140.

[13] Bawa, V.S. (1973). "On Chance Constrained Programming Problems with Joint Constraints." *Management Science*, 19(11): 1326-1331.

[14] Becker, L. and Yeh, W.W-G. (1972). "Identification of Parameters in Unsteady Open Channel Flows." *Water Resources Research*, 8(4): 956-965.

[15] Bleninger, T. (2006). "Coupled 3D Hydrodynamic Models for Submarine Outfalls: Environmental Hydraulic Design and Control of Multiport Diffusers." Doctoral thesis, Institute of Hydromechanics, University of Karlsruhe.

[16] Bleninger, T. and Jirka, G.H. (2008). "Modelling and Environmentally Sound Management of Brine Discharges from Desalination Plants." *Desalination*, 221: 585-597.

[17] Bleninger, T. and Jirka, G.H. (2010). "Environmental Planning, Prediction and Management of Brine Discharges from Desalination Plants." *R&D Reports, Project: 07-AS-003*. Middle East Desalination research Center, Muscat, Sultanate of Oman.

[18] Blumberg, A.F. and Georgas, N. (2008). "Quantifying Uncertainty in Estuarine and Coastal Ocean Circulation Modeling." *J. Hydraul. Research*, 134(4): 403-415.

[19] Boerlage, S.F.E. (2011). "Measuring Seawater and Brine salinity in Seawater Reverse Osmosis." Desalination & Water Reuse (November-December) 26-31. Retrieved January 3, 2014, from http://desalinationbiz.s3.amazonaws.com/news/images/6287.pdf

[20] Boerlage, S.F.E. (2012). "Measuring Salinity and TDS of Seawater and Brine for Process and Environmental Monitoring—Which One, When?" *Desalination and Water Treatment*, 42: 222-230.

[21] Bonazountas, M., Kallidromitous, D. and Dimou, N. (1988). In P. Zannetti (Ed.) "OUTFALL: A Sea Outfall Model." *Proc. Envirosoft88, 2nd International Conference* (pp. 95-109). Porto Carras, Greece. Computer Mechanics Institute, Southampton.

[22] Bray, B.S. (2006). "Modeling and Optimization of Seawater Intrusion Barriers in Southern California Coastal Plain." Ph.D. dissertation, University of California, Los Angeles.

[23] Brown, G.B. (1935). "On Vortex Motion in Gaseous Jets and the Origin of their Sensitivity to Sound." *Proc. Phys. Soc.*, 47: 703-732.

[24] California Ocean Plan (2009). State Water Resources Control Board, Div. Water Quality Ocean Standards Unit, Calif. EPA. Retrieved July 13, 2011, from http://www.waterboards.ca.gov/water_issues/programs/ocean/

[25] California Ocean Plan Triennial Review Workplan (2011). State Water Resources Control Board, Div. Water Quality Ocean Standards Unit, Calif. EPA. Retrieved July 13, 2011, from http://www.waterboards.ca.gov/water_issues/programs/ocean/

[26] Carmichael, J.J. and Strzepek, K.M. (2000). "A multiple-organic-pollutant Simulation/Optimization Model of Industrial and Municipal Wastewater Loading to a Riverine Environment." *Water Resources Research*, 36 (5): 1325-1332.

[27] Caron, D.A., Garneau, M., Seubert, E., Howard, M.D.A., Darjany, L., Schnetzer, A., Filteau, G., Lauri, P., Jones, B. and Trussell, S. (2010). "Harmful Algae and their Potential Impacts on Desalination Operations off Southern California." *Water Research*, 44: 385-416.

[28] Carvalho, J.L., Roberts, P.J.W. and Roldão, J. (2002). "Field Observations of Ipanema Beach Outfall." *J. Hydraul. Eng.-ASCE*, 128(2): 151-160.

[29] Casas, S.,Bonet, N., Aladjem, C., Cortina, J.L., Larrotcha, E. and Cremades, L.V. (2011). "Modelling Sodium Chloride Concentration from Seawater Reverse Osmosis Brine by Electrodialysis: Preliminary Results." *Solvent Extraction and Ion Exchange*, 29: 488-508.

[30] Cavalletti, A. and Davies, P.A. (2003). "Impact of Vertical, Turbulent, Planar, Negatively Buoyant Jet with Rigid Horizontal Bottom Boundary." *J. Hydraul. Eng.-ASCE*, 129(1): 233-241.

[31] Chang, N.B. and Hernandez, E.A. (2008). "Optimal Expansion Strategy for a Sewer System under Uncertainty." *Environ. Model. Assess.*, 13: 93-113.

[32] Chang, N.B. and Tseng, C.C., (1999). "Optimal Design of Multi-Pollutant Air Quality Monitoring Network in a Metropolitan Region Using Kaohsiung, Taiwan as an Example." *Environ. Model. Assess.*, 57(2): 121–148.

[33] Chang, N.B. and Wang, S.F. (1995). "A Grey Nonlinear Programming Approach for Planning Coastal Wastewater Treatment and Disposal Systems." *Wat. Sci. Tech*., 32(2): 19-29.

[34] Chang, N.B., Yeh, S.C. and Chang, C.H. (2009). "Optimal Expansion of a Coastal Wastewater Treatment and Ocean Outfall System under Uncertainty (II): Optimisation Analysis." *Civil Engineering and Environmental Systems*, 1-21.

[35] Charnes, A. and Cooper, W.W. (1959). "Chance-Constrained Programming." *Management Science*, 6(1): 73-79.

[36] Charnes, A. and Cooper, W.W. (1963). "Deterministic Equivalents for Optimizing and Satisficing under Chance Constraints." *Operations Research*, 11(1): 18-39.

[37] Charnes, A., Cooper, W.W., Harrald, J., Karwan, K.R. and Wallace, W.A. (1976). "A Goal Interval Programming Model for Resource Allocation in a Marine Environmental Protection Program." *J. Environ. Econ. and Management*, 3: 347-362.

[38] Chen, B. (2010). "Selection of Outlet Locations of Marine Discharge Engineering in the Maogang Economic Development Zone." *Proc. Environ. Sci.*, 2: 1727-1736.

[39] Chen, H.M. and Lo, S.L. (2009). "Prediction of the Effluent from a Domestic Wastewater Treatment Plant of CASP Using Gray Model and Neural Network." *Environ. Monit. Assess*., doi: 10.1007/s10661-009-0794-z.

[40] Cheng, R.T. and Casulli, V. (2001). "Evaluation of the UnTRIM Model for 3-D Tidal Circulation." *Proc. 7th International Conference on Estuarine and Coastal Modeling* (pp. 628-642). St. Petersburg, Florida.

[41] Cheng, W-C. (2009). "Regional Water Distribution Optimization." Ph.D. dissertation, University of California, Los Angeles.

[42] Chu, P.C. (2008). "Probability Distribution Function of the Upper Equatorial Pacific Current Speeds." *Geophysical Research Letters*, 35(L12606): 1-6.

[43] Chu, P.C. (2009). "Statistical Characteristics of the Global Surface Current Speeds Obtained From Satellite Altimetry and Scatterometer Data." *IEEE J. Sel. Top. Appl. Earth Obs. Remote Sens.*, 2: 27-32.

[44] Churchill, J.H. (1987). "Assessing Hazards due to Contaminant Discharge in Coastal Waters." *Estuarine, Coastal and Shelf Science*, 24: 225-240.

[45] Cleveland, T.G. and Yeh, W.W-G. (1990). "Sampling Network Design for Transport Parameter Identification." *J. Water Resources Planning and Management-ASCE*, 116(6): 764-783.

[46] Cooley, H., Gleick, P.H. and Wolff, G. (2006). "Desalination with a Grain of Salt-A California Perspective." Pacific Institute, Oakland, CA. Retrieved July 1, 2011, from http://www.pacinst.org/reports/desalination/

[47] Cooper, W.W., Hemphill, H., Huang, Z., Li, S., Lelas, V. and Sullivan, D.W. (1996). "Survey of Mathematical Programming Models in Air Pollution Management." *European J. Oper. Res*., 96: 1-35.

[48] Cooper, W.W., Huang, Z. and Li, S.X. (2004). "Chance-Constrained DEA." In W.W. Cooper, L.M. Seiford and J. Zhu (Eds.), *Handbook on Data Envelopment Analysis* (pp. 229-264). International Series in Operations Research & Management Science, 71. Springer, US. doi: 10.1007/1-4020-7798-X_9.

[49] Cooper, W.W., Lelas, V. and Sullivan, D.W. (2006). "Chance-Constrained Programming with Skewed Distributions of Matrix Coefficients and Applications to Environmental Regulatory Activities." In K.D. Lawrence, R.K. Klimberg (Ed.) *Applications of Management Science: In Productivity, Finance, and Operations*. (pp.265-283). Applications of Management Science, 12. Emerald Group Publishing Ltd., Bingley, UK.

[50] Darwish, M.A., Al-Najem, N.M. and Lior, N. (2009). "Towards sustainable seawater desalting in the Gulf area." *Desalination*, 235: 58–87.

[51] Das, A. (2008). "Chance Constrained Optimal Design of Trapezoidal Channels." *J. Water Resources Planning and Management-ASCE*, 134(3): 310-313.

[52] Davies, P.A. and Ahmed, I. (1996). "Laboratory Studies of a Round, Negatively Buoyant Jet Discharged Horizontally into a Rotating Homogeneous Fluid." *Fluid Dynamics Research*, 17: 237-274.

[53] Del Bene, J.V., Jirka, G.H. and Largier, J. (1994). "Ocean Brine Disposal." *Desalination*, 97: 365-372.

[54] Doneker, R.L. and Jirka, G.H. (1991). "Expert Systems for Design and Mixing Zone Analysis of Aqueous Pollutant Discharges." *J. Water Resources Planning and Management-ASCE*, 117(6): 679-697.

[55] Doneker, R.L., and Jirka, G.H. (2001). "CORMIX-GI Systems for Mixing Zone Analysis of Brine Wastewater Disposal." *Desalination*, 139: 263-274.

[56] Doneker, R.L., Sanders, T. and Ramachandran, A. (2008). "Site Scale Remote Sensing of Mixing Zone Water Quality." *Proc. 5th International Conference on Marine Waste Water Discharges and Coastal Environment*. Dubrovnik, Croatia.

[57] Duer, M.J. (1998). "Use of Variable Orifice 'Duckbill' Valves for Hydraulic and Dilution Optimization of Multiport Diffusers." *Water Science Technology*, 38(10): 277-284.

[58] Dundorf, S., MacHarg, J. and Seacord, T.F. (2007). “Optimizing Lower Energy Seawater Desalination, The Affordable Desalination Collaboration.” *Proc. International Desalination Association World Congress*. Maspalomas, Canary Islands.

[59] Durham, B., Yoxtheimer, D., Alloway, C. and Diaz, C. (2003). “Innovative Water Resource Solutions for Islands.” *Desalination*, 156: 155-161.

[60] Einav, R. and Lokiec, F. (2003). “Environmental Aspects of a Desalination Plant in Ashkelon.” *Desalination*, 156: 79-85.

[61] Einav, R., Harussi, K. and Perry, D. (2002). “The Footprint of the Desalination Processes on the Environment.” *Desalination*, 152: 141-154.

[62] El Saliby, I., Okour, Y., Kandasamy, J. and Kim, S. (2009). "Desalination Plants in Australia, Review and Facts." *Desalination*, 247: 1-14.

[63] El-Dessouky, H.T. and Ettouney, H.M. (2002). *Fundamentals of Salt Water Desalination.* Elsevier Science B.V., Amsterdam.

[64] Ellis, J.H., McBean, E.A. and Farquhar, G.J. (1985). "Chance-Constrained/Stochastic Linear Programming Model for Acid Rain Abatement-I. Complete Colinearity and Noncolinearity." *Atmospheric Environment*, 19(6): 925-937.

[65] El-Naas, M.H., Al-Marzouqi, A.H. and Chaala, O. (2010). "A Combined Approach for the Management of Desalination Reject Brine and Capture of CO_2." *Desalination*, 251: 70–74.

[66] Emch, P. and Yeh, W.W-G. (1998). “Management Model for Conjunctive Use of Coastal Surface Water and Groundwater.” *J. Water Resources Planning and Management-ASCE*, 124(3): 129-139.

[67] Energy Recovery, Inc. (2011). Product Innovation. *ERI*. Retrieved May 12, 2011, from http://www.energyrecovery.com/index.cfm/0/0/36-PX-Device-Product-Overview

[68] Eroglu, V., Sarikaya, H.Z. and Aydin, A.F. (2001). “Planning of Wastewater Treatment and Disposal Systems of Istanbul Metropolitan Area.” *Water Science and Technology*, 44(2-3): 31-38.

[69] Etemad-Shahidi, A. and Azimi, A.H. (2007). “Simulation of Thermal Discharges Using Two Mixing Zone Models.” *J. Coastal Research*, 50: 663-667.

[70] Etemad-Shahidi, A., and Azimi, A.H. (2003). “Testing the CORMIX2 and VISJET Models to Predict the Dilution of San Francisco Outfall.” *Proc. Diffuse Pollution Conference* (pp. 129-133). Dublin, Ireland.

[71] Fernández-Torquemada, Y., González-Correa, J.M., Loya, A., Ferrero, L.M., Díaz-Valdés, M. and Sánchez-Lizaso, J.L. (2009). “Dispersion of Brine Discharge from Seawater Reverse Osmosis Desalination Plants.” *Desalination and Water Treatment*, 5: 137-145.

[72] Fernández-Torquemada, Y., Sánchez-Lizaso, J.L. and González-Correa, J.M. (2005). “Preliminary Results of the Monitoring of the Brine Discharge Produced by the SWRO Desalination Plant of Alicante (SE Spain).” *Desalination*, 182: 395-402.

[73] Ferziger, J.H. and Perić, M. (2002). *Computational Methods for Fluid Dynamics*. Springer-Verlag, Berlin Heidelberg.

[74] Fischer, H.B. (1980). “Mixing Processes on the Atlantic Continental Shelf, Cape Cod to Cape Hatteras.” *Limnol. Ocennogr.*, 25(l): 114-125.

[75] Fischer, H.B., List, E.J., Koh, R.C.Y., Imberger, J. and Brooks, N.H. (1979). *Mixing in Inland and Coastal Waters.* Academic Press, New York.

[76] Fogel, D.B. (2006). "Nils Barricelli - Artificial Life, Coevolution, Self-adaptation." *Comp. Intel. Mag.-IEEE*, 1(1): 41-45, doi: 10.1109/MCI.2006.1597062.

[77] Freire, A., Juanes, J., Revilla, J., Guinda, X., García, A., Álvarez, C. and Nikolov, K. (2010). In G.C. Christodoulou and A.I . Stamou (Ed.) "Methodology for the implementation of the WFD combined approach: Environmental Mixing Zones for outfall discharges into coastal waters." *Proc. 6th International Symposium on Environmental Hydraulics* (pp. 577-582). Athens, Greece. CRC Press, doi:10.1201/b10553-93.

[78] Fritzmann, C., Löwenberg, J., Wintgens, T. and Melin, T. (2007). “State-of-the-Art of Reverse Osmosis Desalination.” *Desalination*, 216: 1-76.

[79] Gill, A.E. (1982). *Atmosphere-Ocean Dynamics*. Academic Press, San Diego.

[80] Glater, J. and Cohen, Y. (2003). *Brine Disposal from Land Based Membrane Desalination Plants: A Critical Assessment*. (MWD Contract No. 400-00-013). Retrieved March 15, 2010, from http://polysep.ucla.edu/

[81] Goldberg, D.E. (1989). *Genetic Algorithms in Search, Optimization, and Machine Learning*. Addison-Wesley, Reading, MA.

[82] Gottberg, A.V., Pang, A. and Talavera, J.L. (2005). *Optimizing Water Recovery and Energy Consumption for Seawater RO Systems*. GE Water and Process Technologies. Retrieved February 22, 2010, from http://knowledgecentral.gewater.com/kcpguest/documents/Technical%20Papers_Cust/Americas/English/TP1021EN.pdf

[83] Grace, R. (2009). *Marine Outfall Construction: Background, Techniques, and Case Studies.* ASCE Press, Reston, VA.

[84] Graves, M. and Choffel, K. (2004). *Economic Siting Factors for Seawater Desalination Projects along the Texas Gulf-Coast*. HDR Engineering, Inc.. Retrieved January 22, 2010, from http://www.twdb.state.tx.us/innovativewater/desal/

[85] Green, D. (2007). *Managing Water: Avoiding Crisis in California.* University of California Press, Berkeley.

[86] Hashim, A. and Hajjaj, M. (2005). "Impact of Desalination Plants Fluid Effluents on the Integrity of Seawater, with the Arabian Gulf in Perspective." *Desalination*, 182: 373-93.

[87] Heitmann, H-G. (Ed.). (1990). *Saline Water Processing*. VCH Verlagsgesellschaft, Weinheim.

[88] Hernandez-Torres, J.M., Hernandez-Mascarell, A., Navarro-Hernandez, M., Monerris, M.M., Molina, R. and Cortes, J.M. (2009). *Monitoring and Decision Support Systems for Impacts Minimization of Desalination Plant Outfall in Marine Ecosystems*. ASDECO. Retrieved February 17, 2011, from http://www.proyectoasdeco.com/

[89] Hossain, M. S., Chowdhury, S.R. and Chowdhury, M.A.T. (2007). "Integration of Remote Sensing, GIS and Participatory Approach for Coastal Island Resource Use Zoning in Bangladesh." *Songklanakarin J. Social Sci. & Humanities*, 13(3): 413-433.

[90] Huang, G.H., Baetz, B.W. and Patry, G.G. (1995). "Grey Fuzzy Integer Programming: An Application to Regional Waste Management Planning Under Uncertainty." *Socio-Econ Plann. Science*, 29(1): 17-38.

[91] Huang, Y.P., Kao, L.J. and Sandnes, F.E. (2008). "Identifying Insightful Salinity and Temperature Variations in Ocean Data." *Proc. 8th International Conference on Computer and Information Technology* (pp. 191-196). Sydney, Australia. IEEE Press.

[92] Hunt, C.D., Rust, S.W. and Sinnott, L. (2007). "Application of Statistical Modeling to Optimize a Coastal Water Quality Monitoring Program." *Environ. Monit. Assess.*, 137: 505-522.

[93] Israelsson, P.H., Kim, Y.D. and Adams, E.E. (2006). "A Comparison of Three Lagrangian Approaches for Extending Near Field Mixing Calculations." *Environ. Model. and Softw.*, 21(12): 1631-1649.

[94] James, L.D. (2002). "Modelling Pollution Dispersion, the Ecosystem and Water Quality in Coastal Waters: a Review." *Environ. Model. and Softw.*, 17(4): 363-385.

[95] Jenkins, S., Paduan, J., Roberts, P.J.W., Schlenk, D. and Weis, J. (2012). "Management of Brine Discharges to Coastal Waters Recommendations of a Science Advisory Panel." *Technical Report 694*. Southern California Coastal Water Research Project, Costa Mesa, CA.

[96] Ji, J.H. and Chang, N.B. (2005). "Risk Assessment for Optimal Freshwater Inflow in Response to Sustainability Indicators in Semi-arid Coastal Bay." *Stoch. Environ. Res. Risk Assess.*, 19: 111-124.

[97] Jirka, G.H. (2004). "Integral Model for Turbulent Buoyant Jets in Unbounded Stratified Flows. Part 1: Single Round Jet." *Environ. Fluid Mech.*, 4: 1-56.

[98] Jirka, G.H. (2006). "Integral Model for Turbulent Buoyant Jets in Unbounded Stratified Flows Part 2: Plane Jet Dynamics Resulting from Multiport Diffuser Jets." *Environ. Fluid Mech.*, 6: 43-100.

[99] Jirka, G.H. (2008). "Improved Discharge Configurations for Brine Effluents from Desalination Plants." *J. Hydraul. Eng.-ASCE*, 134(1): 116-120.

[100] Jirka, G.H. and Akar, P.J. (1991). "Hydrodynamic Classification of Submerged Multiport Diffuser Discharges." *J. Hydraul. Eng.-ASCE*, 117(9): 1113-1128.

[101] Jirka, G.H., Bleninger, T., Burrows, R. & Larsen, T. (2004). "Environmental Quality Standards in the EC-Water Framework Directive: consequences for water pollution control for point sources." *European Water Association*, 1: 1-20.

[102] Jirka, G.H., Doneker, R.L. and Hinton, S.W. (1996). *User's Manual for CORMIX: A Hydrodynamic Mixing Zone Model and Decision Support System for Pollutant Discharges into Surface Waters*. (Cooperative Agreement No. CX824847-01-0). Retrieved March 15, 2010, from http://water.epa.gov/scitech/datait/models/

[103] Kämpf, J. (2009a). Impacts of Blending on Dilution of Negatively Buoyant Brine Discharge in a Shallow Tidal Sea. *Marine Pollution Bulletin*, 58: 1032-1038.

[104] Kämpf, J. (2009b). *Ocean Modelling for Beginners*. Springer-Verlag, Berlin Heidelberg.

[105] Kämpf, J., Brokensha, C. and Bolton, T. (2009). “Hindcasts of the Fate of Desalination Brine in Large Inverse Estuaries: Spencer Gulf and Gulf St. Vincent, South Australia.” *Desalination and Water Treatment*, 2: 325-333.

[106] Karmakar, S. and Mujumdar, P.P. (2006). “Grey fuzzy optimization model for water quality management of a river system.” *Advances in Water Resources*, 29: 1088-1105.

[107] Kataria, M., Elofsson, K. and Hasler, B. (2010). "Distributional Assumptions in Chance-Constrained Programming Models of Stochastic Water Pollution." *Environ. Model. Assess*., 15(4): 273-281.

[108] Khuri, A.I. and Mukhopadhyay, S. (2010). "Response Surface Methodology." *Computational Statistics*, 2: 128-149.

[109] Kikkert, G.A., Davidson, M.J. and Nokes, R.I. (2007). “Characterising Strongly Advected Discharges in the Initial Dilution Zone.” *Environ. Fluid Mech.*, 7(1): 23-41.

[110] Kim, S.J., Lee, Y.G., Cho, K.H., Kim, Y.M., Choi, S., Kim, I.S., Yang, D.R. and Kim, J.H. (2009). “Site-Specific Raw Seawater Quality Impact Study on SWRO Process for Optimizing Operation of the Pressurized Step.” *Desalination*, 238: 140-157.

[111] Kim, Y.M., Kim, S.J., Kim, Y.S., Lee, S., Kim, I.S. and Kim, J.H. (2009). “Overview of Systems Engineering Approaches for a Large-Scale Seawater Desalination Plant with a Reverse Osmosis Network.” *Desalination*, 238: 312-332.

[112] Kim, Y.M., Lee, Y.S., Lee, Y.G., Kim, S.J., Yang, D.R., Kim, I.S. and Kim J.H. (2009). “Development of a Package Model for Process Simulation and Cost Estimation of Seawater Reverse Osmosis Desalination Plant.” *Desalination*, 247: 326-335.

[113] Klinger, B.A. (2011). *Density of Seawater*. George Mason University, Fairfax, VA. Retrieved July 22, 2011, from http://mason.gmu.edu/~bklinger/seawater.pdf

[114] Ladewig, B. and Asquith, B. (2012). *Desalination Concentrate Management.* Springer, Heidelberg.

[115] Lamei, A., Van der Zaaga, P. and Von Münch, E. (2008). "Basic Cost Equations to Estimate Unit Production Costs for RO Desalination and Long-Distance Piping

to Supply Water to Tourism-Dominated Arid Coastal Regions of Egypt." *Desalination* 225, 1-12.

[116] Lattemann, S. and Höpner, T. (2008a). "Environmental Impact and Impact Assessment of Seawater Desalination." *Desalination*, 220: 1-15.

[117] Lattemann, S. and Höpner, T. (2008b). "Impacts of Seawater Desalination Plants on the Marine Environment of the Gulf." In A.H. Abuzinada, H.-J. Barth, F. Krupp, B. Böer and T.Z. Al Abdessalaam (Eds.), *Protecting The Gulf's Marine Ecosystems From Pollution* (pp. 191-205). Birkhäuser Verlag, Basel, Switzerland.

[118] Lee, Y.G., Lee, Y.S., Jeon, J.J., Lee, S., Yang, D.R., Kim, I.S. and Kim, J.H. (2009). "Artificial Neural Network Model for Optimizing Operation of a Seawater Reverse Osmosis Desalination Plant." *Desalination*, 247: 180-189.

[119] List, E.J. (1982). "Turbulent Jets and Plumes." *Ann. Rev. Fluid Mech.*, 14: 189-212.

[120] Liu, B. (2009). *Theory and Practice of Uncertain Programming*. Springer-Verlag, Berlin Heidelberg.

[121] Liu, W.C, Kuo, J.T., Young, C.C. and Wu, M.C. (2007). "Evaluation of Marine Outfall with Three-Dimensional Hydrodynamic and Water Quality Modeling." *Environ. Model. Assess.*, 12: 201-211.

[122] Loáiciga, H.A., Yeh, W.W-G. and Ortega-Guerrero, M.A. (2006). "Probability Density Functions in the Analysis of Hydraulic Conductivity Data." *J. Hydrologic Eng.-ASCE*, 11(5): 442-450.

[123] Loucks, D.P. (1970). "Some Comments on Linear Decision Rules and Chance Constraints." *Water Resources Research*, 6(2): 668-671.

[124] Loucks, D.P. and Dorfman, P.J. (1975). "An Evaluation of Some Linear Decision Rules in Chance-Constrained Models for Reservoir Planning and Operation." *Water Resources Research*, 2(6): 777-782.

[125] Louie, P.W.F., Yeh, W.W-G. and Hsu, N-S. (1984). "Multiobjective Water Resources Management Planning." *J. Water Resources Planning and Management-ASCE*, 110(1): 39-56.

[126] Loya-Fernández, Á., Ferrero-Vicente, L.M., Marco-Méndez, C., Martínez-García, E., Zubcoff, J. and Sánchez-Lizaso, J.L. (2012). "Comparing Four Mixing Zone Models with Brine Discharge Measurements from a Reverse Osmosis Desalination Plant in Spain." *Desalination*, 286: 217-224.

[127] Lu, Y.Y., Hu, Y.D., Xu, D.M. and Wu, L.Y. (2006). “Optimum Design of Reverse Osmosis Seawater Desalination System Considering Membrane Cleaning and Replacing.” *J. Membrane Science*, 282: 7-13.

[128] Ludwig, H. (2004). “Hybrid Systems in Seawater Desalination - Practical Design Aspects, Present Status and Development Perspectives.” *Desalination*, 164: 1-18.

[129] Lung, W-S. (1995)."Mixing-Zone Modeling for Toxic Waste-Load Allocations." *J. Hydraul. Eng.-ASCE*, 121(11): 839-842.

[130] MacWilliams, M.L. and Cheng, R.T. (2006). “Three-Dimensional Hydrodynamic Modeling of San Pablo Bay on an Unstructured Grid.” *Proc.7th Int. Conf. on Hydroscience and Engineering* (pp. 1-16). Philadelphia, Pennsylvania.

[131] Malaeb, L. and Ayoub, G.M. (2011). "Reverse osmosis Technology for Water Treatment: State of the Art Review." *Desalination*, 267: 1-8.

[132] Malcangio, D. and Petrillo, A.F. (2009). "Modeling of Brine Outfall at the Planning Stage of Desalination Plants." *Desalination*, 254: 114-125.

[133] Malek, A., Hawlader, M.N.A. and Ho, J.C. (1996). “Design and Economics of RO Seawater Desalination.” *Desalination*, 105: 245-261.

[134] Malfeito, J.J., Díaz-Caneja, J., Fariñas, M., Fernández-Torquemada, Y., González-Correa, J.M., Carrtalá-Giménez, A. and Sánchez-Lizaso, J.L. (2005). “Brine Discharge from the Javea Desalination Plant.” *Desalination*, 185: 87-94.

[135] Manolakos, D., Sh. Mohamed, E., Karagiannis, I. and Papadakis, G. (2008). “Technical and Economic Comparison between PV-RO System and RO-Solar Rankine System. Case Study: Thirasia Island.” *Desalination*, 221: 37-46.

[136] Marcovecchio, M., Mussati, S.F., Aguirre, P.A. and Scenna, N.J. (2005). "Optimization of Hybrid Desalination Processes Including Multi Stage Flash and Reverse Osmosis Systems." *Desalination*, 182: 111-122.

[137] Martin, J.L. and McCutcheon, S.C. (1998). *Hydrodynamics and Transport for Water Quality Modeling*. Lewis Publishers, New York.

[138] Mauguin, G. and Corsin, P. (2005). “Concentrate and Other Waste Disposal from SWRO Plants: Characterization and Reduction of the Environmental Impact.” *Desalination*, 182: 355-364.

[139] Mays, L.W. and Tung, Y.K. (2002). *Hydrosystems Engineering and Management*. Water Resources Publications, LLC, Highlands Ranch.

[140] McCutcheon, S.C. (1990). *Water Quality Modeling: Transport and Surface Exchange in Rivers*. CRC Press, Inc., Boca Raton, Florida.

[141] McKinney, D.C. and Loucks, D.P. (1992). "Network Design for Predicting Groundwater Contamination." *Water Resources Research*, 28(1): 133-147.

[142] Mezher, T., Fath, H., Abbas, Z. and Arslan, K. (2011). "Techno-Economic Assessment and Environmental Impacts of Desalination Technologies." *Desalination*, 266: 263-273.

[143] Mirfenderesk, H., Hughes, L. and Tomlinson, R. (2007). "Verification of a Three Dimensional Advection Dispersion Model Using Dye Release Experiment." *Proc. 16th Australasian Fluid Mechanics Conference* (pp. 233-240). Gold Coast, Australia.

[144] Monahan, A.H. (2006). "The Probability Distribution of Sea Surface Wind Speeds. Part I: Theory and SeaWinds Observations." *Journal of Climate*, 19: 497-520.

[145] Montgomery, D.C. (2001). *Design and Analysis of Experiments*. John Wiley & Sons, New York.

[146] Moura, A., Rijo, R., Silva, P. and Crespo, S. (2010). "A Multi-Objective Genetic Algorithm Applied to Autonomous Underwater Vehicles for Sewage Outfall Plume Dispersion Observations." *Applied Soft Computing*, 10: 1119-1126.

[147] Mukhtasor, Lye, L.M. and Sharp, J.J. (2002). "Methods of Compliance Evaluation for Ocean Outfall Design and Analysis." *Environmental Management*, 30(4): 536-546.

[148] Mukhtasor, Sharp, J.J and Lye, L.M. (1999). "Uncertainty Analysis of Ocean Outfalls." *Can. J. Civ. Eng.*, 26: 434-444.

[149] Nash, J. D., and Jirka, G. H. (1997). "Buoyant discharges in reversing ambient currents: Experimental investigation and prediction." *Technical Report No. CBWP-MANTA-TR-97-2*, Maryland Dept. of Natural Resources.

[150] Ning, S.K. and Chang, N.B. (2002). "Multi-Objective, Decision-Based Assessment of a Water Quality Monitoring Network in a River System." *J. Environmental Monitoring*, 4: 121-126.

[151] Oh, H.J., Hwang, T.M. and Lee, S. (2009). "A Simplified Simulation Model of RO Systems for Seawater Desalination." *Desalination*, 238: 128-139.

[152] Olson, D.L. and Swenseth, S.R. (1987). "A Linear Approximation for Chance-Constrained Programming." *J. Oper. Res. Soc*., 38(3): 261-267.

[153] Onta, P.R., Gupta, A.D. and Harboe, R. (1991). "Multistep Planning Model for Conjunctive Use of Surface and Groundwater Resources." *J. Water Resources Planning and Management-ASCE*, 117(6): 662-678.

[154] Ostojic-Skomrlj, N. and Margeta, J. (1996). "Long Term Investment Planning for Coastal Pollution Control Infrastructure." *Water Science and Technology*, 32(9-10): 273-282.

[155] Palomar, P., and Losada, L.J. (2010). "Desalination in Spain: Recent developments and Recommendations." *Desalination*, 255: 97-106.

[156] Palomar, P., Lara, J.L. and Losada, I.J. (2012). "Near Field Brine Discharge Modeling Part 2: Validation of Commercial Tools." *Desalination*, 290: 28-42.

[157] Pankratz, T. (2004). "An Overview of Seawater Intake Facilities for Seawater Desalination." The Future of Desalination in Texas Vol 2: Biennial Report on Water Desalination, Texas Water Development Board.

[158] Passone, S., Das, D.B., Nassehil, V. and Bikangaga, J.H. (2003). "Design of Discharge Policies for Multiple Effluent Sources and Returning Pollutants Scenarios in a Branching Estuary." *Estuarine Coastal and Shelf Science*, 56: 227-237.

[159] Peñate, B. and García-Rodríguez, L. (2012). "Current Trends and Future Prospects in the Design of Seawater Reverse Osmosis Desalination Technology." *Desalination*, 284: 1-8.

[160] Pincince, A.B. and List, E.J. (1973). "Disposal of Brine into an Estuary." *J. Water Pollution Control Fed*., 45(11): 2335-2344.

[161] Poojari, C.A. and Varghese, B. (2008). "Genetic Algorithm Based Technique for Solving Chance Constrained Problems." *European J. Oper. Res*., 185(3): 1128-1154.

[162] Purnama, A. and Al-Barwani, H.H. (2005). "Near-Shore Outfall Plumes on Eroding Beaches." *Global J. Pure and Applied Math.*, 1(2): 163-172.

[163] Qutob, M.A. (2004). "Environmental Impacts of Water Desalination Along the Coastal Region of Israel and the Palestinian Authority." *Proc. Water for Life in the Middle East, 2nd Israeli-Palestinian International Conference*. Retrieved October 28, 2009, from http://www.ipcri.org/files/water/water-papers.html

[164] Ramos, P.A., Neves, M.V. and Pereira, F.L. (2007). "Mapping and Initial Dilution Estimation of an Ocean Outfall Plume Using an Autonomous Underwater Vehicle." *Continental Shelf Research*, 27: 583–593.

[165] Ramp, S.R., Davis, R.E., Leonard, N.E., Shulman, L., Chao, Y., Robinson, A.R., Marsden, J., Lermusiaux, P.F.J., Fratantoni, D.M., Paduan, J.D., Chavez, F.P., Bahr, F.L., Liang, S., Leslie, W. and Li, Z. (2009). "Preparing to Predict: The Second Autonomous Ocean Sampling Network (AOSN-II) Experiment in the Monterey Bay." *Deep Sea Research II*, 56: 68-86.

[166] Raventos, N., Macpherson, E. and Garcia-Rubies, A. (2006). "Effect of Brine Discharge from a Desalination Plant on Macrobenthic Communities in the NW Mediterranean." *Marine Environmental Research*, 62: 1-14.

[167] Ravizky, A. and Nadav, N. (2007). "Salt Production by the Evaporation of SWRO Brine in Eilat: a Success Story." *Desalination*, 205: 374-379.

[168] Riddle, A.M., Beling, E.M. and Murray-Smith, R.J. (2001). "Modeling the Uncertainties in Predicting Produced Water Concentrations in the North Sea." *Environ. Model. and Softw.*, 16(7): 659-668.

[169] Roberts, D.A., Johnson, E.L. and Knott, N.A. (2010). "Impacts of Desalination Plant Discharges on the Marine Environment: A Critical Review of Published Studies." *Water Research*, 44: 5117-5128.

[170] Roberts, P.J.W., Ferrier, A. and Daviero, G. (1997). "Mixing in Inclined Dense Jets." *J. Hydraul. Eng.-ASCE*, 123(8): 693-699.

[171] Roberts, P.J.W., Snyder, W.H. and Baumgartner, D.J. (1989). "Ocean Outfalls. I. Submerged Wastefield Formation." *J. Hydraul. Eng.-ASCE*, 115(1): 1-25.

[172] Safrai, I. and Zask, A. (2006). "Environmental Regulations for discharging Desalination Brine to the Sea and its Possible Impacts." *Innovations and Applications of Seawater and Marginal Water Desalination, 8th Annual Conference*. Haifa, Israel.

[173] Safrai, I. and Zask, A. (2008). "Reverse Osmosis Desalination Plants - Marine Environmentalist Regulator Point of View." *Desalination*, 220: 72-84.

[174] Saif, Y., Elkamel, A. and Pritzker, M. (2008). "Global Optimization of Reverse Osmosis Network for Wastewater Treatment and Minimization." *Ind. Eng. Chem. Res.*, 47: 3060-3070.

[175] Sandery, P.A. and Kämpf, J. (2007). “Transport Timescales for Identifying Seasonal Variation in Bass Strait, South-Eastern Australia.” *Estuarine, Coastal and Shelf Science* 74: 684-696.

[176] Sankaranarayanan, S., Shankar, N.J. and Cheong, H.F. (1998). “Three-Dimensional Finite Difference Model for Transport of Conservative Pollutants.” *Ocean Engng*. 25(6): 425-442.

[177] Santos, C., Catarino, J., Marques, E., Figueiredo, Z., Trancoso, A., Marecos, H. and Neves, R. (2002). “Monitoring Sea Water Around the Disposal Area of Guia Submarine Outfall.” *Proc. 2nd International Conference on Marine Waste Water Discharges*. Istanbul, Turkey. Retrieved February 17, 2011, from http://www.iahr.org/e-library/MWWD2002/

[178] Schnurbusch, S.A. (2000). "A Mixing Zone Guidance Document Prepared for the Oregon Department of Environmental Quality." M.S. thesis, Portland State University.

[179] Schwenk, T. (2004). *Sensitive Chaos.* Rudolf Steiner Press, Forest Row, East Sussex.

[180] Shiklomanov, I. (1993). "World Fresh Water Resources.” In P.H. Gleick (Ed.) *Water in Crisis: A Guide to the World’s Fresh Water Resources*. (pp.13-24). Oxford University Press, New York.

[181] Shu-Ii Yang, S-I., Hsu, N-S., Louie, P.W.F. and Yeh, W.W-G. (1996). "Water Distribution Network Reliability: Stochastic Simulation." *J. Infrastructure Sys.-ASCE*, 2(2): 65-72.

[182] Smith, D.G. (Ed.). (1981). *The Cambridge Encyclopedia of Earth Sciences*. Crown Publishers, Inc. / Cambridge University Press, New York.

[183] Smith, R. and Purnama, A. (1999). “Two Outfalls in an Estuary: Optimal Wasteload Allocation.” *Journal of Engineering Mathematics*, 35: 273-283.

[184] Smith, R.N., Chao, Y., Li, P.P., Caron, D.A., Jones, B.H. and Sukhatme, G. (2010). “Planning and Implementing Trajectories for Autonomous Underwater Vehicles to Track Evolving Ocean Processes based on Predictions from a Regional Ocean Model.” *The International Journal of Robotics Research*, 29: 1475-1497.

[185] Sobhani, R., Abahusayn, M., Gabelich, C.J. and Rosso, D. (2012). “Process Applicability and Energy Analysis of Brackish Groundwater Desalination with Zero Liquid Discharge in Inland Areas of the Arabian Peninsula.” *Desalination*, 291: 106-116.

[186] Sorensen, R.M. (1997). *Basic Coastal Engineering.* Chapman & Hall, New York.

[187] Stewart, R.H. (2008). Introduction to Physical Oceanography. Texas A&M Univ. Retrieved July 13, 2011, from http://oceanworld.tamu.edu/

[188] Stolzenbach, K.D. (2000). *Mixing Zones*. *Physics of Environmental Transport,* Lecture Notes, University of California, Los Angeles.

[189] Storn, R. and Price, K. (1997). "Differential Evolution - A Simple and Efficient Adaptive Scheme for Global Optimization over Continuous Spaces." *Journal of Global Optimization*, 11: 341-359.

[190] Subramani, A., Badruzzaman, M., Oppenheimer, J. and Jacangelo, J.G. (2011). "Energy Minimization Strategies and Renewable Energy Utilization for Desalination: A Review." *Water Research*, 45 5): 1907-1920.

[191] Svensson, M. (2005). "Desalination and the Environment: Options and Considerations for Brine Disposal in Inland and Coastal Locations." SLU, for Yara International and Aqualyng. Retrieved December 8, 2009, from http://ex-epsilon.slu.se:8080/archive/00000805/01/exjobb_05_02.pdf

[192] Tan, C-C., Tung, C-P., Chen, C-H. and Yeh, W.W-G. (2008). "An Integrated Optimization Algorithm for Parameter Structure Identification in Groundwater Modeling." *Advances in Water Resources*, 31: 545-560.

[193] Tanuwidjaja, D. and Hoek, E.M.V. (2006). "High-Efficiency Seawater Desalination Via NF/RO Multi-Pass Arrays." *Proc. 2006 AIChE Annual Meeting*. San Francisco, California.

[194] Thomas, J-S. and Durham, B. (2003). "Integrated Water Resource Management: Looking at the Whole Picture." *Desalination*, 156: 2l-28.

[195] Tsai, F.T-C., Sun, N-Z., Yeh, W.W-G. (2003). "A Combinatorial Optimization Scheme for Parameter Structure Identification in Ground-Water Modeling." *Ground Water*, 41(2): 156-169.

[196] Tsanis, I.K. and Wu, J. (2000). Application and Verification of a Three-Dimensional Hydrodynamic Model to Hamilton Harbour, Canada." *Global Nest: the Int. J.*, 2(1): 77-89.

[197] Tseng, C.C. and Chang, N.B. (2001). "Assessing Relocation Strategies of Urban Air Quality Monitoring Stations by GA-based Compromise Programming." *Environment International*, 26: 523–541.

[198] UNESCO (1983). *Technical Papers in Marine Science 44*. *Algorithms for Computation of Fundamental Properties of Seawater*. Retrieved February 15, 2011, from http://unesdoc.unesco.org/images/0005/000598/059832eb.pdf

[199] UNESCO (2010). *Manuals and Guides 51*. *The international Thermodynamic Equation of seawater: Calculation and Use of Thermodynamic Properties*. Retrieved July 22, 2011, from http://unesdoc.unesco.org/images/0018/001881/188170e.pdf

[200] United Nations (2010). World Population prospects. *UN Department of Economic and Social Affairs*. Retrieved May 12, 2011, from http://www.un.org/esa/population/

[201] USEPA (1991). *Technical Support Document for Water Quality-Based Toxics Control*. (Publ. No.: 505/2-90-001). Retrieved August 11, 2010, from http://www.epa.gov/npdes/pubs/owm0264.pdf

[202] Vargas-Guzmán, J.A. (2012). "Heavy Tailed Probability Distributions for Non-Gaussian Simulations with Higher-Order Cumulant Parameters Predicted from Sample Data." *Stoch Environ Res. Risk Assess*., 26(6): 765-776.

[203] Vavra, C. and Petriciolet, A.B. (2004). "Efficient Wastewater Treatment Process for Brine Water." *Membrane Technology*, 2004(4): 5-8.

[204] Vince, F., Marechal, F., Aoustin, E. and Bréant, P. (2008). "Multi-Objective Optimization of RO Desalination Plants." *Desalination*, 222: 96-118.

[205] Voutchkov, N. (2011). "Overview of Seawater Concentrate Disposal Alternatives." *Desalination*, 273: 205-219.

[206] Wallis, I.G. (1979). "Ocean Outfall Construction Costs." *J. WPCF*, 51(5): 951-957.

[207] Webster, M., Scott, J., Sokolov, A. and Stone, P. (2006). In Joint Program on the Science and Policy of Global Change "Estimating the Probability Distributions from Complex Models with Bifurcations: The Case of Ocean Circulation Collapse." Report Number 133. MIT, Boston.

[208] Wilf, M. and Klinko, K. (2001). "Optimization of Seawater RO Systems Design." *Desalination*, 138: 299-306.

[209] Wood, I.R., Bell, R.G. and Wilkinson, D.L. (1993). *Ocean Disposal of Wastewater.* World Scientific, Singapore.

[210] World Bank (2004). *Seawater and Brackish Water Desalination in the Middle East, North Africa and Central Asia: A Review of Key Issues and Experience in Six Countries*. (Publ. No.: 33515). Retrieved March 15, 2010, from http://siteresources.worldbank.org/INTWSS/Resources/Desal_mainreport-Final2.pdf

[211] World Health Organization (2003). *Total Dissolved Solids in Drinking-Water: Background Document for Development of WHO Guidelines for Drinking-Water Quality*. (Publ. No.: WSH/03.04/16). Retrieved May 8, 2011, from http://www.who.int/water_sanitation_health/dwq/chemicals/tds.pdf

[212] Yannopoulos, P.C. (2006). "An Improved Integral Model for Plane and Round Turbulent Buoyant Jets." *J. Fluid Mech.*, 547: 267-296.

[213] Yeh, S.C., Chang, N.B., Chang, C.H., Chai, H. and Huang, J. (2009). "Optimal Expansion of a Coastal Wastewater Treatment and Ocean Outfall System under Uncertainty (I): Simulation Analysis." *Civil Engineering and Environmental Systems*, 1-20.

[214] Yeh, W.W-G. (1986). "Review of Parameter Identification Procedures in Groundwater Hydrology: The Inverse Problem," *Water Resources Research*, 22(1): 95-108.

[215] Yeh, W.W-G. (1992). "Systems Analysis in Ground-Water Planning and Management." *J. Water Resources Planning and Management-ASCE*, 118(3): 224-237.

[216] Younos, T. (2005). "Permits and Regulatory Requirements." *J. Contemp. Water Res. & Educ*., 132(1): 19-26.

[217] Zeitoun, M.A., McHilhenny, W.E., Reid, R.O., Wong, C-M., Savage, W.F., Rinne, W.W. and Gransee, C.L. (1970). "Conceptual Designs of Outfall Systems for Desalting Plants." *Res. and Devel. Progress Rep. No. 550*, Office of Saline Water, U.S. Dept. of Interior, Washington, D.C..

[218] Zeitoun, M.A., Reid, R.O., McHilhenny, W.E. and Mitchell, T.M. (1972). "Model Studies of Outfall Systems for Desalination Plants. Part III. Numerical simulations and design considerations." *Res. and Devel. Progress Rep. No. 804*, Office of Saline Water, U.S. Dept. of Interior, Washington, D.C..

[219] Zhang, X.Y. and Adams, E.E. (1999). "Prediction of Near Field Plume Characteristics Using Far Field Circulation Model." *J. Hydraul. Eng.-ASCE*, 125(3): 233-241.

[220] Zhao, L., Chen, Z. and Lee, K. (2011). "Modelling the Dispersion of Wastewater Discharges from Offshore Outfalls: a Review." *Environ. Rev.*, 19: 107-120.

[221] Zhao, Y.W., Qin, Y., Chen, B., Zhao, X., Li, Y., Yin, X.A. and Chen, G.Q. (2009). "GIS-Based Optimization for the Locations of Sewage Treatment Plants and Sewage Outfalls – A Case Study of Nansha District in Guangzhou City, China." *Comm. in Nonlinear Science and Numerical Simulation*, 14(4): 1746-1757.

[222] Zhu, A., Christofides, P.D. and Cohen, Y. (2008). "Effect of Thermodynamic Restriction on Energy Cost Optimization of RO Membrane Water Desalination." *Ind. Eng. Chem. Res.*, 48: 6010-6021.